DEPARTMENT OF TRANSPORTATION

Evaluation of Proprietary Rejuvenators

Muhammed Kutay
Department of Civil and Environmental Engineering
Michigan State University

June 2025

Research Project
Final Report 2025-39

LOCAL ROAD RESEARCH BOARD

To get this document in an alternative format or language, please call 651-366-4720 (711 or 1-800-627-3529 for MN Relay). You can also email your request to ADArequest.dot@state.mn.us. Please make your request at least two weeks before you need the document.

Technical Report Documentation Page

1. Report No.	2.	3. Recipients Accession No.
MN 2025-39		

4. Title and Subtitle	5. Report Date
Evaluation of Proprietary Rejuvenators	June 2025
	6.

7. Author(s)	8. Performing Organization Report No.
Tanzila Islam, Poornachandra Vaddy, M. Emin Kutay, Syed Waqar Haider, Bora Cetin	

9. Performing Organization Name and Address	10. Project/Task/Work Unit No.
Department of Civil and Environmental Engineering Michigan State University 428 S. Shaw Lane, 3546 Engineering Building, East Lansing, MI 48824	11. Contract (C) or Grant (G) No. (c) 1036336 (wo) 4

12. Sponsoring Organization Name and Address	13. Type of Report and Period Covered
Minnesota Department of Transportation Office of Research & Innovation 395 John Ireland Boulevard, MS 330 St. Paul, Minnesota 55155-1899	Final Report 14. Sponsoring Agency Code

15. Supplementary Notes

http://mdl.mndot.gov/

16. Abstract (Limit: 250 words)

The scope of this study included a thorough evaluation of the short-term and long-term performance of Spray-on Rejuvenators (SORs) to assess their effectiveness in extending asphalt pavement life. Laboratory testing on cores extracted from field included a modified Bending Beam Rheometer (BBR) to measure creep stiffness at different temperatures (20°C, 4°C, and -10°C) at multiple aging conditions. Results showed that SORs had the greatest impact at 20°C, while differences between treated and control sections were less significant at lower temperatures. In the MnROAD28 section, most SORs reduced creep stiffness after one year, with some remaining effective for two years. By the third year, only Reclamite, ARA1 Ti, CRF, and RPE-R showed lower creep stiffness than control. In the MnROAD34 section, microcracks initially increased stiffness due to a bridging effect, but softening effects became dominant over time.

Field studies assessed permeability, surface friction, albedo, and mean texture depth (MTD). SOR applications reduced pavement marking reflectivity and increased Albedo over time. MTD remained relatively constant for most sections, except for CRF and GSB-88, where the MTD values increased due to fine sand/gravel applications, but later decreased. Friction measurements showed minor reductions immediately after application, but most SORs regained or exceeded initial values after one year. Both field and lab results also indicated that SORs had minimal impact on permeability, rutting and skid resistance. The findings suggest SORs slow pavement aging, though their effectiveness diminishes over time, requiring reapplication within two to three years.

17. Document Analysis/Descriptors	18. Availability Statement
Asphalt pavements, Rejuvenators, Preservation, Binders, Stiffness	

19. Security Class (this report)	20. Security Class (this page)	21. No. of Pages	22. Price
Unclassified	Unclassified	107	

Evaluation of Proprietary Rejuvenators

Final Report

Prepared by:

Tanzila Islam, MSc

Poornachandra Vaddy

M. Emin Kutay, PhD, PE

Syed Waqar Haider, PhD, PE

Bora Cetin, PhD

Department of Civil and Environmental Engineering
Michigan State University

June 2025

Published by:

Minnesota Department of Transportation
Office of Research & Innovation
395 John Ireland Boulevard, MS 330
St. Paul, Minnesota 55155-1899

Acknowledgements

The authors sincerely acknowledge the Local Road Research Board and the Minnesota Department of Transportation (MnDOT) for their financial support, which made this research possible. Special thanks are extended to Dr. Michael Vrtis and his colleagues at MnROAD for their invaluable assistance in facilitating the application of Spray-on Rejuvenators (SORs) and providing the field cores for laboratory evaluations.

The authors also express their gratitude to the members of the Technical Advisory Panel (TAP) for their guidance and valuable feedback throughout the study: Michael Vrtis, Marcus Bekele, JinYeene Neumann, Mike Lanotte, Paul Nolan, Josh Peterson, Nick Preisler, Joel Ulring, and Julie Swiler.

Additionally, appreciation is extended to Benjamin Worel, Joseph Podolsky, Craig Nolden, Jacob Calvert, Jeffrey Tabery for their support in field data collection. Their efforts in gathering and organizing field data were instrumental in ensuring the accuracy and reliability of this study.

This study would not have been possible without the voluntary participation of the products included in the study and their willingness to advance the knowledge base on the use of SOR, especially regarding long-term performance. The cooperation of the city of St. Michael, MN was vital to the study. Steve Bot provided insight into the SOR experience and allowed the products to be evaluated at a larger scale than MnROAD could accommodate.

Table of Contents

Appendix C Skid resistance results

Appendix D Dynamic friction test results of rejuvenated test sections at test speeds of 20 and 60 kph

List of Figures

List of Tables

Executive Summary

In this study, the short-term and long-term performance of 12 different Spray-on Rejuvenators (SORs) were evaluated to investigate their effectiveness. These SORs were categorized into Group A (without sand/gravel) and Group B (with sand/gravel applied after treatment). The scope of the work included various laboratory and field tests conducted over a 36-month period on two test sections at the MnROAD research facility (called MnROAD28 and MnROAD34), and a local street in St. Michael, MN. The primary objective was to assess the impact of SORs on pavement stiffness, aging resistance, permeability, rutting resistance, skid resistance, and surface characteristics.

Laboratory tests such as the Bending Beam Rheometer (BBR), Hamburg Wheel Tracking (HWT), British Pendulum Test (BPT), and permeability tests were conducted to analyze SOR-treated asphalt mixtures over different aging periods. A modified Bending Beam Rheometer (BBR) was developed in this study to measure creep stiffness of asphalt mixture beams at 20°C, 4°C, and -10°C under different aging conditions. Results showed that SORs had the most significant impact at 20°C. At lower temperatures, differences between treated and control sections were less pronounced. In the MnROAD28 section, most SORs exhibited reduced stiffness up to one year, with Reclamite, ARA1 Ti, CRF, and RPE-R maintaining effectiveness for up to three years. Short-term results (0-year field-aged) showed a significant reduction in creep stiffness for several SORs, indicating immediate softening effects. After 12 months, all SOR-treated test sections exhibited lower creep stiffness than control sections, confirming their role in retarding aging. At 24 and 36 months, most SORs continued to show beneficial effects, though some products lost their effectiveness, suggesting the need for reapplication. In contrast, the MnROAD34 section exhibited an interesting phenomenon where the stiffnesses increased after SOR application. In MnROAD34 cores, small micro-cracks were visible on the surface, possibly caused by construction-related issues. The increase in stiffness after application of SORs was attributed to “bridging effect” where SORs created bridges over micro-cracks, causing a slight increase in stiffness when tested in bending (i.e., BBR test). However, over time, the softening effect became dominant in MnROAD34 sections as well. The effectiveness of SORs varied based on the asphalt binder type also, with PG 58S-28 (MnROAD28) and PG 58H-34 (MnROAD34) exhibiting different stiffness reduction rates. Some SORs were more effective with the PG58H-34 binder by preserving flexibility without excessive-softening, while others showed better performance with the PG58S-28 binder.

To assess rutting resistance, Hamburg Wheel Tracking (HWT) tests were conducted at 45°C up to 20,000 passes. Results confirmed that the application of SORs did not significantly affect the rutting resistance of the asphalt mixtures. British Pendulum Test (BPT) results indicated that most Group A SORs lowered the skid resistance. Some Group B SORs initially exhibited a reduction in skid resistance, but values generally recovered or exceeded initial levels after one year. Permeability tests were conducted on the top 20 mm of field cores using a flexible wall permeameter. Results showed minimal changes in most SOR-treated sections. Field permeability tests also indicated minimal changes in most SOR-treated sections. However, Reclamite and Replenify led to a consistent reduction in permeability. After 24 months, permeability increased in most cases, indicating that the effectiveness of some SORs diminished over time.

Furthermore, a ranking method was proposed, where SORs were ranked based on their overall performance from laboratory tests. Results indicated that Reclamite, RPE-R, CRF, and ARA1 Ti consistently exhibited the most effective performances across multiple criteria, maintaining efficacy in softening the asphalt binder and reducing creep stiffness while also exhibiting minimal negative impacts on skid resistance and permeability. Other SORs showed varying degrees of performance, with some products requiring more frequent reapplication to sustain their benefits.

Field evaluations included measurements of pavement marking reflectivity, albedo, mean texture depth, permeability, and skid resistance before and after SOR applications. Data collection was performed at multiple intervals: before application, and after 1-month, 12-month, 24-month, and 36 months after the SOR application. Albedo measurements showed minimal change for Group A SORs, while some Group B SORs exhibited increased albedo due to bright fine sand or gravel applications. Over time, albedo increased in most test sections, likely due to asphalt aging. However, SOR applications adversely affected pavement marking reflectivity, with some products causing reductions exceeding 30%. Post-application reflectivity should be verified against agency requirements to ensure roadway visibility and safety.

The mean texture depth (MTD) of the control sections showed variation, possibly due to the testing or spatial variability. Most SOR-treated cells exhibited no significant changes, except for CRF and GSB-88. MTD in the case of these SORs initially increased due to fine sand/gravel but later decreased, suggesting that fine particles might have swept away over time. Dynamic Friction Test (DFT) results also showed minor reductions in the SOR-treated sections immediately after application. However, for Group B SORs, most regained or exceeded initial friction values after one year of application. Variations in friction coefficients were also influenced by the presence and displacement of fine sand/gravel in some treatments.

From the whole study for three years, it can be recommended that SORs should be reapplied every two to three years for sustained effectiveness, depending on environmental conditions and traffic loads. SORs also should be selected based on pavement age, binder type, and expected traffic conditions. Binder compatibility should be considered also to optimize the SOR selection. Regular monitoring of pavement surface properties (i.e., surface friction, reflectivity) is recommended to ensure long-term effectiveness and safety. A field maintenance program incorporating periodic skid resistance testing might be established as well.

Overall, SORs effectively slow the aging process of asphalt pavements, though their performance varies by product and diminishes over time. While they offer a sustainable strategy for pavement preservation, their long-term effectiveness depends on appropriate selection, periodic reapplication, and careful monitoring of surface properties. Future research should explore the long-term impact of multi-cycle applications and optimize reapplication strategies for different environmental and traffic conditions.

Chapter 1: Introduction

1.1 Background

The aging of asphalt pavement is a natural and inevitable process that occurs throughout its lifespan. This aging is primarily due to oxidation, which causes chemical changes in the asphalt binder, increasing stiffness and brittleness. As a result, aged asphalt pavements become more susceptible to cracking, moisture-induced damage, and surface distress (Sirin et al, 2018; Vallegra, 1981). The deterioration of pavement performance over time increases maintenance costs and shortens service life, making effective preservation strategies essential. To mitigate the effects of aging and extend pavement durability, rejuvenators are applied to restore the essential components of the asphalt binder. Rejuvenators available in the market are classified into two main categories based on their composition: petroleum-based and bio-based rejuvenators. Petroleum-based rejuvenators consist of components derived from petroleum, while bio-based rejuvenators are fully or partially made from agricultural or plant materials. The selection of rejuvenators depends on various factors, including the condition of the pavement, environmental factors, and performance requirements. However, this study did not consider some other factors like cost, aesthetics, or environmental impacts such as embodied energy, carbon emissions, or Environmental Product Declarations (EPDs), which might also influence product selection.

There are two primary methods of rejuvenator application: in-mix rejuvenation and spray-on rejuvenation. In-mix rejuvenation involves blending the rejuvenator directly into the asphalt mixture during production, whereas spray-on rejuvenation is applied to the surface of in-service pavement sections as a preventive maintenance treatment (Boyer, 2000, Lee et al, 2013; Pan et al, 2018; Mokhtari et al, 2017). Spray-on rejuvenation is a widely used strategy by roadway owners across the United States for preserving pavement conditions and delaying major rehabilitation efforts. This study specifically focuses on evaluating the effectiveness of spray-on rejuvenators, which will be referred to as SORs throughout this report for clarity and simplicity.

Previous studies have shown that the long-term performance of the SORs depends on chemical composition, application rate, and interaction with pavement materials. Given the wide range of available SORs, selecting the most suitable option can be challenging for roadway agencies. This study aims to evaluate the short-term and long-term effects of SORs on pavement performance, focusing on their impact on creep stiffness, surface properties, friction, permeability, and durability. By assessing multiple SORs through laboratory and field investigations, this report will provide insights into their effectiveness and contribute to developing guidelines for their application in pavement preservation programs.

1.2 Scope of the study

As part of this research, three groups of test sections at two locations were selected. The first location was on the Minnesota Road Research Facility (MnROAD) Low Volume Road where two groups of tests sections were constructed. At MnROAD, twelve different types of rejuvenators were applied on two

different substrates, one with PG 58S-28 and the other with PG 58H-34 binder. The third group of test section was at the 15th street, St. Michael, MN, with a single HMA substrate throughout the test section. Note that the MnROAD test sections with PG 58S-28 and PG 58H-34 binders are denoted in this report as MnROAD28 and MnROAD34, respectively. In addition to the rejuvenated test cells, two to three test cells at each test section are allocated as controls. These control test sections were further used in evaluating the effectiveness of each rejuvenator as each product's performance is compared to the control condition.

The laboratory testing program focused on short-term and long-term effects, assessing properties such as creep stiffness, permeability, abrasion resistance, friction, and rutting resistance within 1–2 months of application. Further evaluations included Bending Beam Rheometer (BBR) testing to measure creep stiffness at different aging stages: immediately after application, and at one-year, two-year, three-year, and laboratory-aged conditions. It is important to note that the products included in this study were voluntarily submitted by manufacturers or local suppliers in response to a general call for spray-applied rejuvenators to help document field performance. As a result, not all selected products were necessarily tailored to the specific conditions of the test sections. For example, CRF is typically designed for more heavily distressed pavements, which might not fully align with the relatively new surfaces used in this study.

In addition to laboratory testing, field performance was monitored for up to three years after the construction of SOR-treated test sections. Field data included reflectivity, albedo, dynamic friction coefficient, permeability, and mean texture depth, measured before application and at intervals of 1 month, 12 months, 24 months, and 36 months post-application.

1.3 Objectives of the study

This study aims to evaluate the performance and key characteristics of spray-on rejuvenators (SORs) through both laboratory and field investigations. The primary objective of applying SORs is to reduce the stiffness and brittleness of asphalt mixture surfaces, which naturally increase over time due to aging. Therefore, it is essential to assess the stiffness of SOR-treated asphalt surfaces at different aging intervals while ensuring that these treatments do not compromise pavement's resistance to damage and safety. The study examines both short-term and long-term effects of SORs on pavement durability and aging resistance.

Field testing was conducted at the MnROAD Low Volume Road (LVR) test sections, which are representative of rural county roads. These sections experienced minimal salt usage and limited plowing compared to high-volume roads. The road layout included traffic on the inside lane, while the outside lane remained closed to traffic, allowing a direct comparison of the effects of traffic on SOR performance. Most test sections were surrounded by open cornfields, which did not create any shading on the pavement. However, the sections containing BioRestor and control cells were located near tree-lined areas and experienced intermittent shading throughout the day. Overall, shading was minimal across all MnROAD sections, ensuring comparable exposure conditions. Therefore, any conclusions regarding pavement aging should be compared to the data from MnROAD sections. So, shading and

slope variations across the sections were also considered, as they might influence environmental exposure and treatment effectiveness.

Chapter 2: Literature Review

2.1 Background

Roadway agencies use various pavement preservation techniques to extend the service life of asphalt pavements, with spray-on rejuvenators (SORs) becoming preferred for their simple application process and affordability. These treatments are intended to help mitigate the effects of oxidative aging, seal minor cracks, and reduce permeability, and improve surface characteristics. Over the years, various research studies have been conducted to assess the effectiveness of different rejuvenators, including asphalt emulsions, cutbacks, and maltene-based products. Studies have demonstrated that SORs can penetrate the surface layer and soften the aged binder, though their effectiveness varies based on penetration depth, aging conditions, and binder compatibility. Some concerns, such as reduced skid resistance and short-term friction loss, have also been reported, highlighting the need for careful selection and application. With numerous proprietary rejuvenators available on the market, ongoing research continues to upgrade their evaluation methods to ensure optimal performance and long-term pavement durability.

2.2 Introduction to rejuvenators

Roadway agencies use several pavement preservation techniques, including micro-surfacing, chip seals, asphalt emulsion fog seals, and Spray-on Rejuvenators (SORs). Among these, SORs are gaining popularity due to their affordability and ease of application (Quintus & Raghunathan, 2017). These liquid treatments are sprayed onto pavement surfaces to achieve several objectives, as listed below (Boyer, 2000; Lee et al, 2013; Chiu & Lee, 2006):

- Reverse the adverse effects of oxidative aging in asphalt binders
- Seal cracks to slow down crack growth
- Reduce permeability to protect underlying layers
- Improve surface aesthetics and, in some cases, enhance friction

Asphalt binders primarily consist of asphaltenes (A) and maltenes (M). Asphaltenes are solid, high-molecular-weight compounds that contribute to stiffness. While maltenes are the lighter, oil-like parts that help keep the binder flexible. Maltenes are the soluble fraction of the binder and comprise four components: polar compounds (PC), first acidaffins (A1), second acidaffins (A2), and saturates (S) (Boyer, 2000). Over time, due to oxidation, nitrogen bases and acidaffins convert into asphaltenes (stiffer compounds), disrupting the balance between these components. This change causes the binder to become stiffer and more brittle, reducing the pavement's ability to resist cracking (Boyer, 2000; Rostler & White, 1970). This aging effect is more pronounced in surface layers due to exposure to sunlight, air, and moisture. Certain spray-on rejuvenators are rich with maltene components, and once they penetrate into the asphalt pavement, they restore the balance between the maltene and asphaltenes (Blanchette et al, 2020). The rejuvenator undergoes physical and chemical reactions with the aged

asphalt binder. It revitalizes it by balancing the asphaltenes to maltenes ratio to the original state, thereby improving the longevity of the asphalt pavement systems (Lee et al, 2013; Chiu & Lee, 2006).

Throughout several years, many Departments of Transportation (DOTs) have been using rejuvenators as they have been showing promising results in terms of revitalization of asphalt pavements, increase in pavement indexes, increase in service life, etc. According to Gayle and King (2008), majority of the states in the US have been using rejuvenators for maintaining the asphalt pavement sections. Figure 2.1 shows the results of a survey that was conducted in 2008 regarding rejuvenator usage in the US. While many studies highlight the benefits of rejuvenators, others have raised concerns about their potential drawbacks, such as reduced skid resistance and rutting resistance (Chiu & Lee, 2006; Kebede, 2016). Therefore, evaluation of both the advantages and limitations of spray-on rejuvenators (SORs) is necessary.

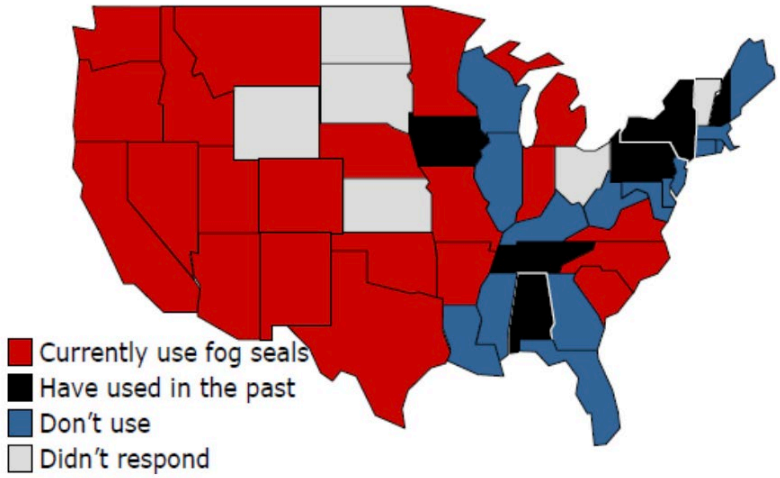

Figure 2.1 Rejuvenator's usage status of different states in US (*11*)

2.3 State-of-the-practice

Several research studies have been conducted over the years to investigate the effectiveness of spray-on rejuvenators in restoring asphalt pavement properties. Although this study offers new perspectives through both laboratory and field evaluations, it is important to recognize that spray-on rejuvenation is an established technology that has been in use for several years. A study by Rostler and White (1970) evaluated five rejuvenating products across four categories: asphalt solutions, asphalt emulsions, emulsions of asphalt components, and non-asphalt solutions believed to benefit asphalt binders. Various tests, including viscosity, flash point, particle charge, storage stability, compatibility, and penetration depth, were conducted to assess their effectiveness. The study recommended distinguishing between general pavement maintenance products and true rejuvenators based on their ability to penetrate and restore asphalt properties. It also proposed specifications for materials used as rejuvenators in the field.

A study by Shoenberger (2003) evaluated the field performance of proprietary petroleum-based and coal tar-based rejuvenators, as well as seal coat materials. The tested rejuvenators included AR-2000, APR-100, BCR-2000, BCR-3000, CBRT-SO, CPR, GSB-mod, Reclamite, RejuvaSeal N, RejuvaSeal 50, and RejuvaSeal 500, while the seal coats tested were CRF, LAS-320, PAS, PolyTar, and Antiskid (Promak A). The study assessed these products based on their impact on skid resistance, visual appearance, and surface texture. Results showed that rejuvenators temporarily reduced skid resistance, sometimes below acceptable levels. Additionally, some rejuvenators left residual material on the surface, affecting long-term skid resistance. However, applying sand or fine aggregate helped maintain the minimum required skid resistance. The study also emphasized the need for a standardized test method to evaluate rejuvenator effectiveness, given the wide range of proprietary products available in the market.

A study by Chiu and Lee (2006) evaluated the effectiveness of three rejuvenators; two asphalt emulsions and one asphalt cut-back on a 12-year-old severely raveled asphalt parking lot in Taiwan. The study measured skid resistance and surface texture before and 60 days after rejuvenation. Cores from both control and rejuvenated sections were analyzed to determine penetration depth by measuring viscosity changes in the extracted binder. Results showed that asphalt emulsion rejuvenators were cured within two hours, while the cut-back rejuvenator took seven hours. All rejuvenators softened the asphalt binder within the top 10 mm, with the cut-back showing the highest reduction; 90% viscosity decrease at 60°. Despite a high void content (9.7%), none of the rejuvenators penetrated beyond 20 mm. Additionally, surface friction and macro-texture depth decreased by 20% and 10%, respectively.

Medina and Clouser (2009) from the Pennsylvania Department of Transportation (PennDOT) evaluated the impact of the RePlay (soy-based) rejuvenator on asphalt pavement surfaces. The study included skid resistance tests, permeability tests, and field observations. Results showed no significant benefits from using RePlay, but pavement friction decreased, raising safety concerns. Additionally, permeability values remained unchanged one year after application.

A study by Lee et al. (2013) evaluated the performance and limitations of a maltene rejuvenator applied on US-40 in Henry County, IN. Tests conducted included surface friction, permeability, viscosity, and contact-angle measurements. Results showed that the rejuvenator penetrated up to 12.5 mm into the pavement. On the day of application, surface friction decreased significantly by 47%. However, the rejuvenation process had no notable effect on pavement permeability.

Lin et al. (2014) tested three commercially available rejuvenators to determine their effective penetration depth. Asphalt binder samples were taken from different depths of the rejuvenated pavement and analyzed using Dynamic Shear Rheometer (DSR) and Fourier-Transformed Infrared Spectroscopy (FTIR). The study found that penetration depth could not be identified by peaks in the FTIR spectrum but was instead calculated using the carbonyl area index. Results showed that the effective penetration depth of the rejuvenators ranged from 10 to 20 mm.

Kebede (2016) studied three types of rejuvenators; polymer-modified, coal tar, and soybean—applied on thirteen roads in Indiana. The study assessed their impact on pavement condition, surface friction, and the rheological and chemical properties of asphalt binders. Pavement condition was evaluated using

the PASER rating, while surface friction was measured using the friction coefficient from a dynamic friction tester. Binder properties were analyzed with Dynamic Shear Rheometer and Fourier-Transformed Infrared Spectroscopy. Results showed that the soybean rejuvenator caused the least reduction in surface friction. However, despite variations in friction, PASER ratings remained largely unchanged after one year, suggesting it may not be a reliable method for evaluating rejuvenators. Binder tests indicated that polymer-modified and soybean rejuvenators performed better in restoring asphalt binder viscosity compared to the coal tar rejuvenator.

Quintus and Raghunathan (2017), in a study funded by the Ohio Department of Transportation, evaluated the surface conditions of four seal-treated test sections before and after treatment. Three rejuvenators: Biorestor, Replay, and Reclamite were applied, and pavement performance was monitored over four years to assess the difference in service life between treated and control sections. The study found little difference in permeability between treated and control sections, with time being the primary factor affecting permeability rather than the treatment itself. After four years, it remained unclear whether the treatment was cost-effective. Additionally, while some variations were observed in reflection cracking, raveling, and transverse cracking, the differences were not significant.

Bastola et al. (2021) conducted a field implementation study in Nebraska to assess high-RAP mixtures with and without a bio-oil rejuvenator. Using Hamburg Wheel Tracking (HWT) and Semi-Circular Bending (SCB) tests, this study evaluated rutting, moisture susceptibility, and cracking resistance over two years. While the rejuvenator improved cracking resistance in the lab, field-aged samples showed diminished effectiveness over time. Notably, the surface layer exhibited more fatigue and thermal cracking when the rejuvenated mixture was used in the lower layer. These results raised concerns about long-term field benefits and suggested that rejuvenators might not consistently mitigate aging effects in high-RAP pavements.

A wide variety of rejuvenators are available in the market, each manufactured with different compositions and properties to restore aged asphalt pavement. Rejuvenators available on the market are classified into two main types based on their composition: petroleum-based and bio-based. Petroleum-based rejuvenators contain petroleum-derived components, while bio-based rejuvenators are made entirely or partially from agricultural or plant-based materials. Common petroleum-based rejuvenators include CMS-1PF, CRF® Restorative Seal, GSB-88®, PASS® QB, Ravel Check®, Reclamite®, RegenX®, and RejuvaSeal®. Examples of bio-based rejuvenators include Anova®, BioRestor®, Delta Mist™, and Replay™.

2.4 Study motivation

Spray-on rejuvenation is an established pavement preservation technique that has been in use for several decades. Past studies have evaluated different types of rejuvenators using various laboratory and field tests such as surface friction, viscosity, penetration depth, and permeability. While some studies have shown performance benefits such as reduced stiffness and improved binder characteristics, others have highlighted potential drawbacks, including reductions in surface friction or no measurable

long-term improvements. These studies have largely focused on proprietary products and specific test conditions, often providing isolated insights that are difficult to generalize.

However, there remained a lack of comprehensive research that evaluated a wide range of spray-on rejuvenators (SORs) under consistent field and laboratory conditions across different binders and pavement environments. This study was motivated by the need to fill that gap by assessing 12 commercially available SORs using a standardized experimental design. In doing so, the research aimed to evaluate their effectiveness in field applications as well as controlled lab conditions. For local roadway owners and engineers, this study offers practical insights into how SORs perform under varying pavements and environmental conditions. With products sourced voluntarily from manufacturers and applied by vendor-selected contractors, the goal was not to endorse any rejuvenator but to generate transparent, comparative data to inform product selection and maintenance planning. Results from this work are especially relevant for rural agencies looking to extend pavement life while minimizing safety risks and budget constraints.

In summary, this study builds upon existing knowledge while addressing gaps in the literature. It offers a broad comparison of SORs under uniform conditions, with recommendations for their selection and use based on performance outcomes, traffic levels, binder compatibility, and environmental exposure.

Chapter 3: Laboratory study

This laboratory study aims to evaluate the performance and key characteristics of spray-on rejuvenators (SORs). While previous studies have primarily focused on short-term effects, there is limited data on long-term results. This chapter addresses the gap by evaluating SOR effectiveness over 36 months, and the following tests were conducted:

- Creep stiffness (Bending Beam Rheometer)
- Rutting resistance (Hamburg Wheel Tracking Test)
- Abrasion and raveling resistance (Modified Hamburg Wheel Tracking Test)
- Friction (British Pendulum Test)
- Permeability (Falling Head Rising Tailwater Permeameter)

3.1 SOR-treated test sections

Three test sections were selected for the Spray-on Rejuvenator (SOR) application; two at the MnROAD research facility and one on 15th Street in St. Michael, MN. The 15th Street was paved in 2020 (1 year before application), and the two MnROAD test sections were newly resurfaced (two months before the SOR application) with asphalt mixtures having the same aggregate gradation, but two different asphalt binders. These sections, named MnROAD28 and MnROAD34, correspond to the binders PG 58S-28 and PG 58H-34, respectively. The third test section is an in-service pavement located in the city of St. Michael, MN, which is denoted as "15th Street" in this report. Each section was further divided into multiple test cells, with different SORs applied to each cell. Since pavement aging was a major consideration during the experimental setup, the manufacturers/suppliers generally recommend applying the products within 1 to 3 years after paving, preferring newer pavements over older ones. It should be noted that thermal cracking on 15th Street was minimal, with cracks more closely aligning with the slope gradients rather than the typical evenly spaced thermal cracking patterns. In the MnROAD sections, transverse thermal cracks were present; however, concluding cracking within the 50-foot sections was challenging, since these were constructed over an existing overlay with pre-existing thermal distress. Additionally, the past two winters in Minnesota have been relatively mild, and significant thermal cracking has not been observed in other test sections of similar age.

3.1.1 Overview of SORs used in this study

Table 3.1 shows the twelve different products evaluated in this study. Each test section included two control cells along with the SOR-treated test cells. For certain SORs (e.g., ARA1 Ti, CRF®, GSB-88®, Reclamite®, and Replenify™), sand or fine gravel was spread over the pavement surface after SOR application, to enhance surface friction. To compare the outcomes later, the SORs were grouped into two categories: Group A, with no gravel/fine sand applied, and Group B, where gravel/fine sand was added after the SOR application. Some SORs were derived from petroleum, while others were bio-based, as shown in the table.

Table 3.1 Summary of SORs and their manufacturers/suppliers

Group ID	SORs	Composition	Supplier/Manufacturer
Group A	BioMAG™	Bio-based	Iowa State University
	BioRestor®	Bio-based	BioBased Spray Systems, LLC
	BioRestor® Low VOC	Bio-based	BioBased Spray Systems, LLC
	Delta Mist®	Bio-based	Collaborative Aggregates, LLC
	Invigorate™	Bio-based	Iowa State University
	RePlay™	Bio-based	BioSpan Technologies
	RPE-R	Bio-based	H.G. Meigs, LLC
Group B	ARA1 Ti	Petroleum-based	D&D Emulsions, Inc.
	CRF®	Petroleum-based	Tricor Refining, LLC
	GSB-88®	Petroleum-based	Asphalt Systems, Inc.
	Reclamite®	Petroleum-based	Pavement Technology, Inc.
	Replenify™	Petroleum-based	Flint Hills Resources

Figure 3.1 shows the SOR-treated test cells approximately a month after application.

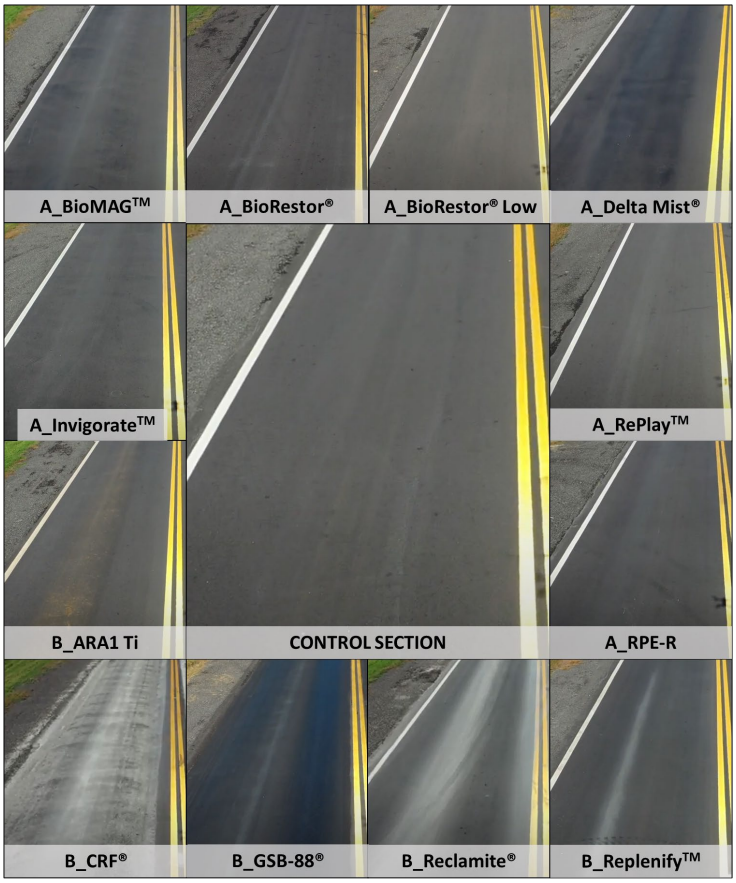

Figure 3.1 Control and SOR-treated test cells at MnROAD28 test section

All SORs were donated for the study and applied by manufacturer-selected contractors. MnDOT and the research team were not involved in the application process but monitored the procedures. Most of the products were applied within a two-week window in July 2021 under dry conditions. However, ARA1 Ti was applied separately in August 2021, and during the application of GSB-88, a sudden rain event occurred. This caused the material to break, changing color from brown to black and then back to brown. As a result, the black sand material applied with GSB-88 was visibly washed out along the section edges. Although the manufacturer offered to reapply the product, MnDOT did not pursue this, as it was not considered a safety concern, and the affected area was limited to approximately 600 feet.

3.1.2 Collection of field cores at different aging periods

Field cores were collected from all test cells at the MnROAD test sections at a one-year interval over three years. The coring process was carried out by MnROAD staff, and the cores were sent to MSU for testing. To date, field cores have been collected at four intervals:

1. 0-year field-aged (F0): Collected field cores after one month of SOR application
2. 1-year field-aged (F1): Collected field cores after 12 months of SOR application
3. 2-year field-aged (F2): Collected field cores after 24 months of SOR application
4. 3-year field-aged (F3): Collected field cores after 36 months of SOR application

Besides all the field-aged conditions, long-term aging (LA) was simulated in the lab by aging some unaged samples (0-year field-aged). Two-inch thick cylindrical slices were cut from field-extracted cores and placed in a forced draft oven at 95°C for 7 days. The cores were secured with stainless steel wire mesh and hose clamps to prevent probable deformation at high temperatures. Figure 3.2 shows snapshots of the cores during the lab aging process. After aging, the cores were left undisturbed for 48 hours to cool to room temperature before preparing the required samples.

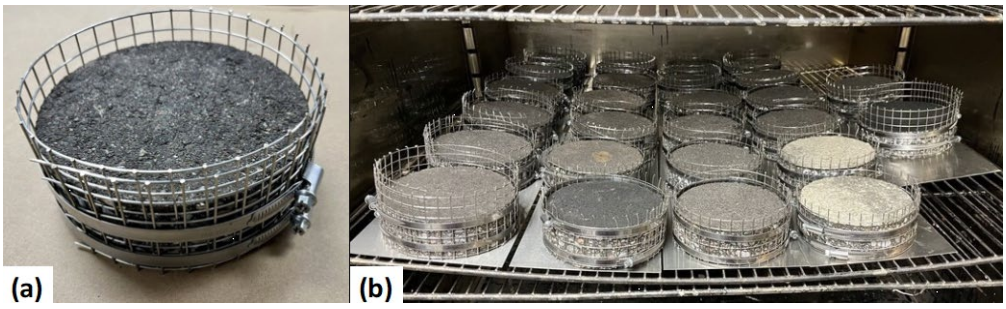

Figure 3.2 (a) Close-view of a core wrapped with steel mesh and hose clamps and (b) SOR-treated and control cores placed in an oven for lab aging

3.1.3 Visual observations

This section presents the research team's visual observations. Since this study focuses on the surface characteristics of SOR-treated asphalt pavements, examining the surface of field cores can help explain certain properties. Figure 3.3 shows the top views of the cores at 0-year field-aged (F0) condition. The Group A SOR-treated surfaces appeared similar to the control section, though there were slight color

variations. Group B SORs included sand/fine gravel which was applied on the surface to improve surface friction. However, it was observed that the sand/fine gravel applied to ARA1 Ti and Replenify did not remain on the surface and was swept away. The main intention of this section is not to highlight surface appearance but to illustrate the presence of microcracks. These observations might provide useful context for understanding pavement surface conditions.

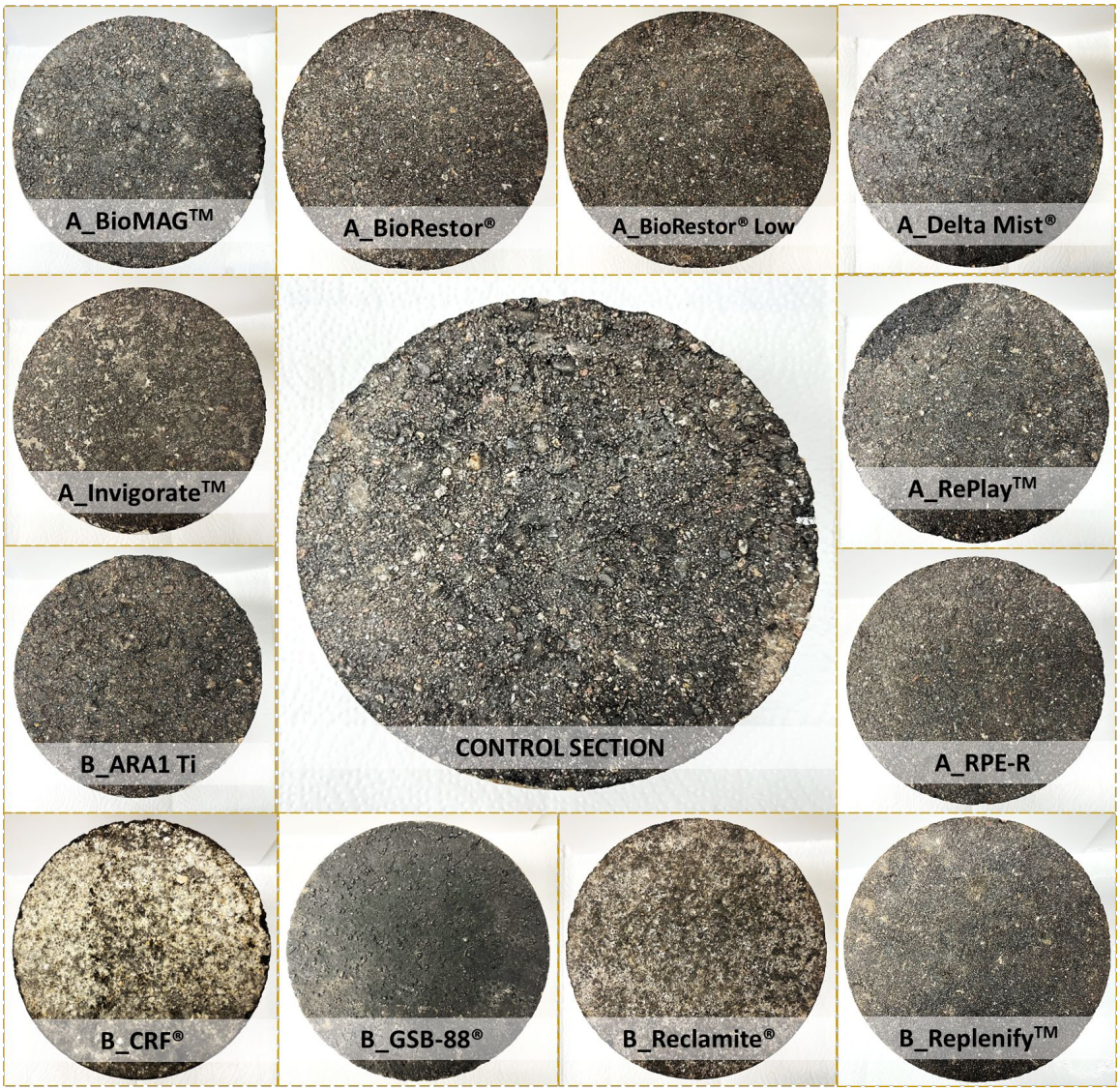

Figure 3.3 Close view of the SOR-treated surface of extracted cores (MnROAD28 test section)

Furthermore, microcracks were observed in the substrate of the MnROAD34 test section. A comparison with the MnROAD28 control section (Figure 3.4) suggests that these cracks might have resulted from compaction issues or other construction-related factors. Similar microcracks were found in other SOR test cells where little SOR residue remained, exposing the pavement surface. Figure 3.5 shows examples of SOR-treated surfaces in the MnROAD34 section. Based on these observations, it is assumed that

microcracks were already present throughout the MnROAD34 test section before the SORs were applied.

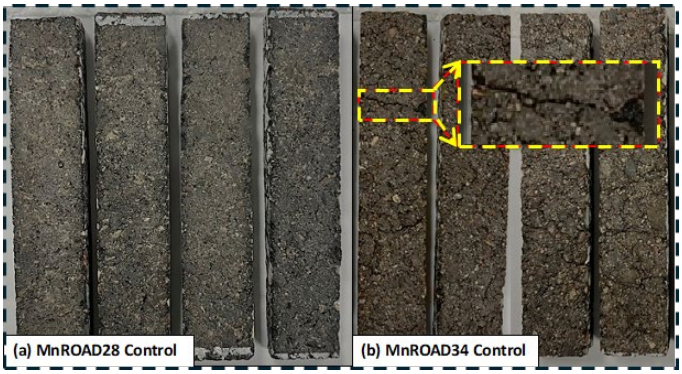

Figure 3.4 (a) Surface of the MnROAD28 samples and (b) microcracks observed in MnROAD34 samples

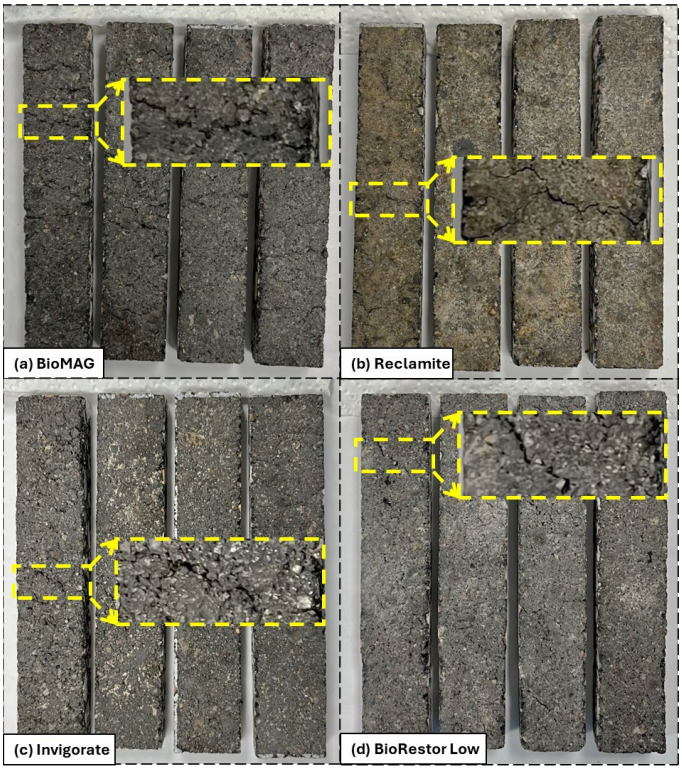

Figure 3.5 Illustration of the presence of surface microcracks in MnROAD34 sections treated with SORs

3.2 Creep stiffness of SOR-treated surfaces

The primary objective of applying SORs is to reduce the stiffness of asphalt surfaces that have stiffened over time due to aging. To evaluate the effectiveness of SORs, the stiffness of treated surfaces was measured. Thin beam asphalt specimens were prepared from the top layers of field-extracted cores and tested for creep stiffness using a Bending Beam Rheometer (BBR). The testing followed the flexural

creep stiffness measurement procedure for asphalt binders (AASHTO T313 and AASHTO TP125) (AASHTO, 2019, 2020) with a few modifications.

3.2.1 Experimental setup

3.2.1.1 Conventional test procedure

According to the conventional test procedure following AASHTO T313 and AASHTO TP125, a thin beam measuring 127 mm × 12.7 mm × 6.35 mm is prepared using an asphalt binder (AASHTO, 2019, 2020). The beams are placed on BBR supports, and a 980 mN (for binder) or 4000 mN (for mixture) load was applied at its center for 240 seconds. The deflection of the beam at the center is measured with the help of an LVDT. The stiffness of the beam is calculated using **Equation 1**. Typically, creep stiffness and the m-value at 60 sec were used for comparative analysis of binders. The BBR machine that was used to determine creep stiffness of binder or asphalt concrete is shown in Figure 3.6.

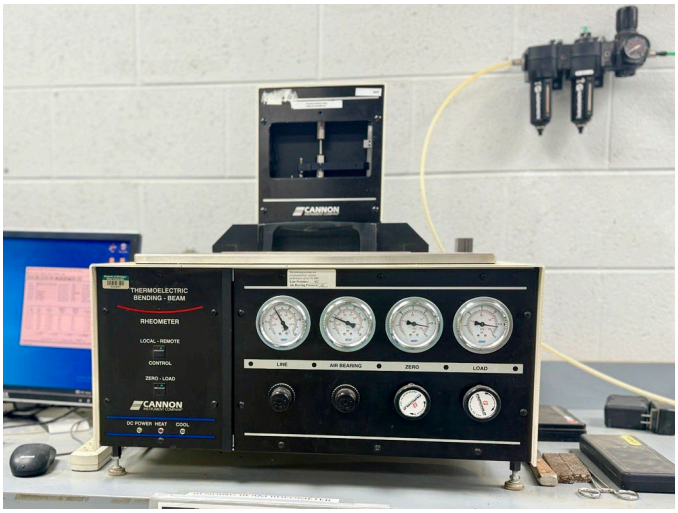

Figure 3.6 Bending Beam Rheometer (BBR) device

$$S(t) = \frac{PL^3}{4bh^3\delta(t)} \quad (1)$$

where:

S(t) = time-dependent flexural creep stiffness at time t (calculated), MPa;
P = constant load, N;
L = span length, mm;
b = width of the beam, mm; and
h = height (thickness) of the beam
δ(t) = deflection of the beam at time t, mm.

A second-order polynomial equation is fitted to the log(S(t)) versus log(t) curve and the slope of the fit at

60 sec (represented as m-value) is measured. The second-order polynomial fit and the slope equations are given in **Equations 2 & 3**.

$$\log S'(t) = \mathrm{A} + \mathrm{B}[\log(\mathrm{t})] + C[\log(t)]^2 \quad (2)$$

$$|m(t)| = \frac{d[\log S'(t)]}{d[\log(t)]} = B + 2C[\log(t)] \quad (3)$$

where:

S' (t)	=	time-dependent flexural creep stiffness (fitted) estimated using Eq. 2, MPa;
t	=	time in seconds; and
A, B, and C	=	regression coefficients.

3.2.1.2 Modified test procedure

The AASHTO T313 test procedure has been widely used in past studies to measure the flexural creep stiffness of asphalt mixtures (*20–28*). Typically, the surface of field-extracted cores or laboratory-prepared gyratory-compacted specimens was trimmed to obtain a smooth surface (*27–29*). However, this study focused on evaluating the impact of SORs on the top pavement layer. Previous research also indicates that effective SOR penetration is less than 10 mm. Additionally, the surface of compacted asphalt mixtures, whether field or gyratory compacted, has a higher void content than the inner layers (*30–32*). To accurately assess the effectiveness of SORs, the surface of the treated specimens was not trimmed before testing. The rationale for these modifications and related preliminary studies were published in the Transportation Research Record (TRR) (*33*).

PRELIMINARY STUDY 1 - FOCUSING ON THE TEST SPECIMEN SIZE

The preliminary study was conducted using cores from two test cells in the MnROAD28 section (one control and one treated with SOR). The intention was to investigate the feasibility of using the conventional BBR test methodology on the test specimens. Initially, the plan was to prepare 16 test specimens (127 mm × 12.7 mm × 6.35 mm) from each test cell's cores. However, only eight specimens could be successfully prepared, as many broke during cutting, likely due to the high void content near the surface as mentioned earlier. Additionally, excessive chipping of fine aggregate particles was observed (Figure 3.7a), creating a big void space (relative to the height of 6.35 mm) that could affect test results. Despite these challenges, thin beam specimens were prepared from the control and one SOR-treated test cell (BioMAG) for flexural creep stiffness testing. The tests were conducted at -18°C (low PG +10°C) with a 450-gram load, which is close to the maximum load that can be applied using the BBR without additional dead load. It should be noted that three of the eight specimens (BioMAG) broke during testing.

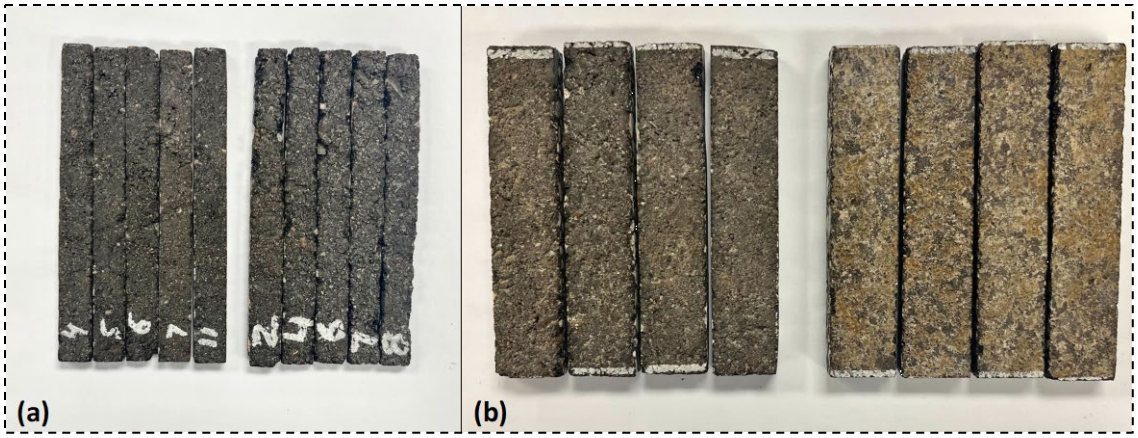

Figure 3.7 (a) Regular BBR sized thin beams (127 mm x 12.7 mm x 6.35 mm); and (b) modified beams (127 mm x 25.4 mm x 12.7 mm)

The BBR test results are presented in Figure 3.8 as a box plot. In each plot, the average value is marked with an "**x**," while the median is shown as a solid line inside the box. The lower and upper edges of the box represent the 25th and 75th percentiles, while the whiskers indicate the minimum and maximum values, excluding outliers. Any outliers, defined as data points more than 1.5 times the interquartile range from the average, are shown as small circular dots outside the plot. Figure 3.8 shows that while there is a difference in the average creep stiffness values, the variation in BioMAG results is too large to be statistically significant. Additionally, with only five test specimens, it is difficult to exclude outliers, making it challenging to draw solid conclusions from the results.

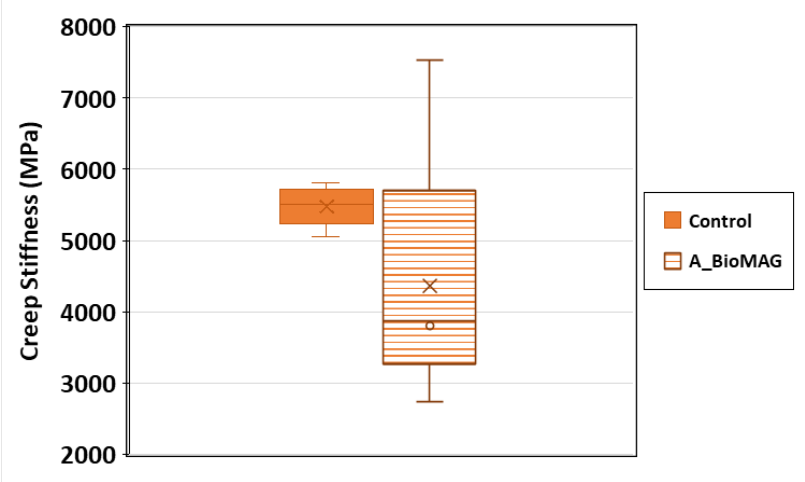

Figure 3.8 Creep stiffness results of the thin beam test specimens (127 mm x 12.7 mm x 6.35 mm)

To conclude, the preliminary tests on thin beam specimens (127 mm × 12.7 mm × 6.35 mm) showed that extracting and testing thin beams from the core surface is not practical. To prevent breakage during cutting and testing, a larger beam size is needed, which would also reduce fine aggregate chipping. However, the existing BBR cannot accommodate a longer specimen. Therefore, while keeping the length at 127 mm, the beam's width and height were increased from 12.7 mm × 6.35 mm to 25.4 mm × 12.7 mm, maintaining the original 2:1 width-to-height ratio. The new height (12.7 mm) covers the area affected by SORs, aligning with research by Lee et al. (2013), which measured an effective penetration

depth of approximately 12.5 mm (Lee et al, 2013). It is noted that the Federal Aviation Administration (FAA) specifies a minimum penetration depth of 9 mm (USDOT, 1980).

PRELIMINARY STUDY 2 - FOCUSING ON THE EFFECTIVENESS OF THE MODIFIED TEST METHODOLOGY

A second preliminary study evaluated whether the BBR test, using modified beam dimensions (127 mm × 25.4 mm × 12.7 mm), could distinguish between asphalt mixtures with significantly different dynamic modulus (|E*|) values. Two asphalt mixtures from Michigan, 4E30 and 5E10, were selected due to their distinct dynamic modulus properties. The dynamic modulus values for these mixtures at a 10Hz frequency across different temperatures are presented in Figure 3.9.

The creep stiffness calculation method was re-evaluated with the change in beam specimen dimensions. The AASHTO T313 recommends using **Equation 1** for BBR testing, which is based on Euler's beam theory for slender beams with a span-to-depth ratio greater than 10. According to this theory, mid-span deflection in the BBR beam is assumed to result only from bending, while deflection due to flexural stress is neglected. Since the standard BBR beam has a span-to-depth ratio of 16 (greater than 10), this assumption holds. However, the modified beam has a span-to-depth ratio of 8 (less than 10), meaning **Equation 1** from AASHTO T313 is not applicable to the modified beam size.

The behavior of shorter beams (span-to-depth ratio <10) can be explained using Timoshenko beam theory, which includes the effects of shear and bending stresses. In a three-point loading test, mid-span deflection is calculated using **Equation 4**, which is derived from Timoshenko's theory (Gere & Timoshenko, 1984). **Equations 5-7** describe the relationships between various elastic material properties (AASHTO, 2019a; Gere & Timoshenko, 1984; Mamlouk & Sarofim, 1988). By substituting these equations into **Equation 4**, a simplified and rearranged form, **Equation 8** is obtained.

$$\delta = \frac{PL^3}{48EI}\left(1 + \frac{12\alpha_s EI}{GAL^2}\right) \tag{4}$$

$$I = \frac{bh^3}{12} \tag{5}$$

$$\frac{E}{G} = 2(1+\nu) \tag{6}$$

$$\alpha_s = \frac{12+11\nu}{10(1+\nu)} \tag{7}$$

$$\mathrm{E} = \frac{PL^3}{4\mathrm{b}h^3\delta}\left(1 + \beta\frac{h^2}{L^2}\right) \tag{8}$$

where:

δ = mid-span deflection, mm
I = moment of inertia, mm^4
E = modulus of elasticity, MPa
G = shear modulus, MPa
A = area of cross section, mm^2
L = span length, mm
b = width of beam, mm
h = thickness of beam, mm
ν = Poisson's ratio
α_s = shear coefficient
β = $(12 + 11\nu)/5$

In **Equation 8**, Poisson's ratio is a required input for calculating the resultant modulus of an asphalt mixture. However, Poisson's ratio is not always known or measured for every mixture. To assess its impact, the sensitivity of the second term in **Equation 8**, $\beta h^2/L^2$, was calculated for typical asphalt mixture Poisson's ratio values ranging from 0.2 to 0.35. The results, shown in Table 3.2, indicate that for a modified beam size of 127 mm × 25.4 mm × 12.7 mm, the effect of shear stresses on the resultant modulus is minimal, ranging from 4.44% to 4.95%. Since this variation is small, an average Poisson's ratio of 0.25 is used in all further calculations. Additionally, the modulus E in the elastic case can be replaced with 1/D(t), which is equivalent to S(t) (AASHTO, 2019a), allowing the creep stiffness equation to be expressed accordingly as:

$$S(t) = \frac{PL^3}{4bh^3\delta(t)}\left(1 + 2.95\frac{h^2}{L^2}\right) \quad (9)$$

where:

S(t) = time-dependent flexural creep stiffness at time t, MPa;
P = constant load, N;
L = span length, mm;
b = width of the beam, mm; and
δ(t) = deflection of the beam at time t, mm.

BBR tests were conducted on the prepared specimens at a test temperature of 4°C using a 700 g (6865 mN) load. The measured creep stiffness values are presented in Figure 3.10. The ratio of |E*| at 4°C for the 4E30 and 5E10 mixtures was 1.28, which closely matched the BBR-based creep stiffness ratio of 1.3 at the same temperature. To determine if the difference in average creep stiffness values was statistically significant, a student t-test was performed. The results, with a p-value of 0.002 at a 95% confidence level, confirmed a significant difference between the two mixtures. This validates that the proposed methodology effectively differentiates the creep stiffness of asphalt mixtures.

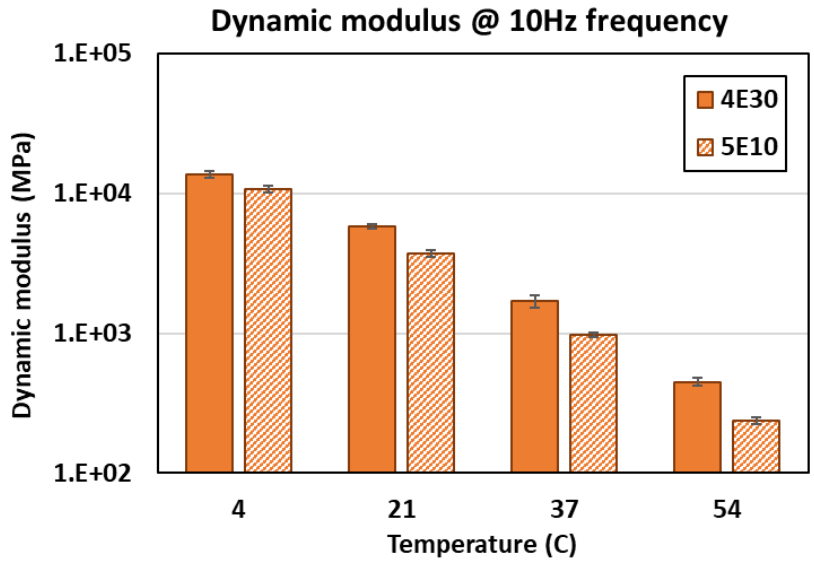

Figure 3.9 Dynamic moduli of selected mixtures

Table 3.2 Effect of Poisson ratio on the modulus measurements

Poisson ratio	Shear coefficient	E/G	$\beta h^2/L^2$
0.2	1.1833	2.4	2.84
0.25	1.1800	2.5	2.95
0.3	1.1769	2.6	3.06
0.35	1.1741	2.7	3.17

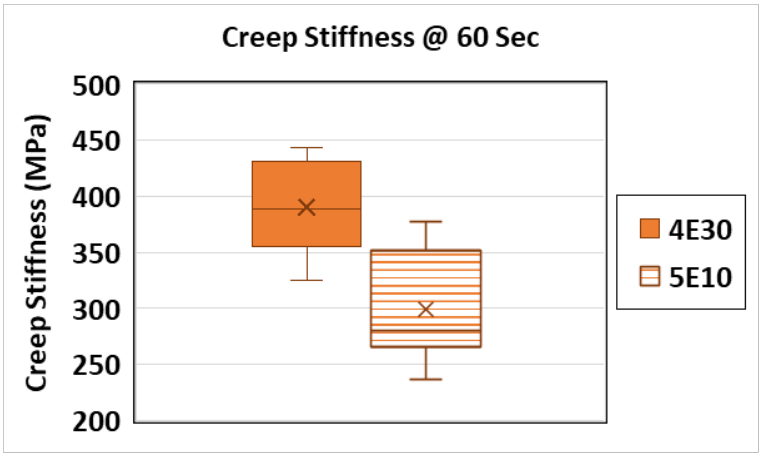

Figure 3.10 Creep stiffness of soft and stiff asphalt mixtures

PRELIMINARY STUDY 3 - FOCUS ON THE TEST TEMPERATURE AND LOAD

The preliminary studies (1 & 2) showed that creep stiffness variations in asphalt mixtures change at different test temperatures. To examine this effect in SOR-treated mixtures, it was decided to test the same specimens at multiple temperatures due to the limited number of available cores. It was important to ensure that the test specimens did not undergo permanent deformation during testing.

Since the objective of this preliminary study was to figure out BBR test loads at each temperature, trial tests were conducted using 200 g, 400 g, 500 g, and 600 g loads at -10°C, 4°C, and 21°C. After testing, the specimens were allowed to rest for 24 hours to regain their original shape. The BBR tests were then repeated on these same samples, to check whether the applied load had caused any unrecoverable damage.

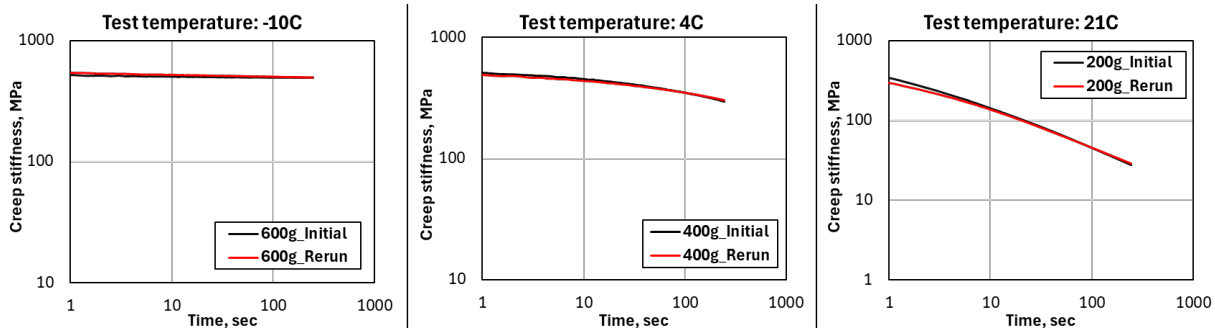

Figure 3.11 Effect of temperature and load on the creep stiffness of an asphalt mixture

The creep stiffness variation with time was measured for both initial and rerun cases, and the percentage difference between creep stiffness values at 60 sec was compared. The results (Figure 3.11) showed minimal differences: 2% at -10°C with 600 g, 1% at 4°C with 400 g, and 1% at 21°C with 200 g. Based on these findings, 600 g, 400 g, and 200 g were selected as the appropriate test loads for -10°C, 4°C, and 21°C, respectively.

FINAL TEST METHODOLOGY WITH THE PROPOSED MODIFICATIONS

From the insights from preliminary studies 1, 2, and 3 above, a final test methodology was developed for testing the cores (*33*). We prepared eight BBR beams, each measuring 127 mm × 25.4 mm × 12.7 mm from four field cores for both control and SOR-treated test cells. The cutting sequence for specimen preparation is illustrated in Figure 3.12. Due to height restrictions in the conventional BBR setup, the 12.7 mm high beams could not fit properly. To accommodate this, the standard BBR beam supports were replaced with shorter supports designed according to AASHTO T313 guidelines. A comparison of the original and modified supports is shown in Figure 3.13.

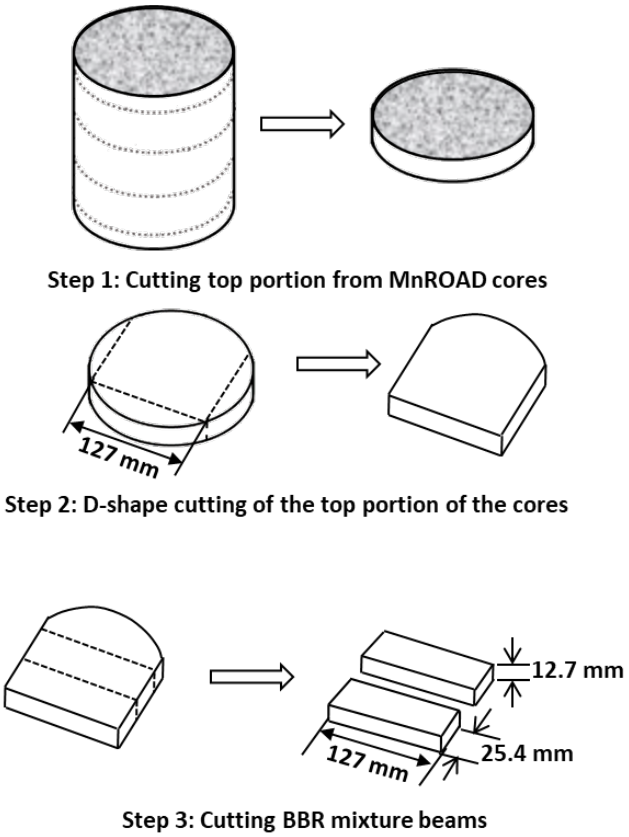

Figure 3.12 Preparation of BBR test samples from field-extracted cores

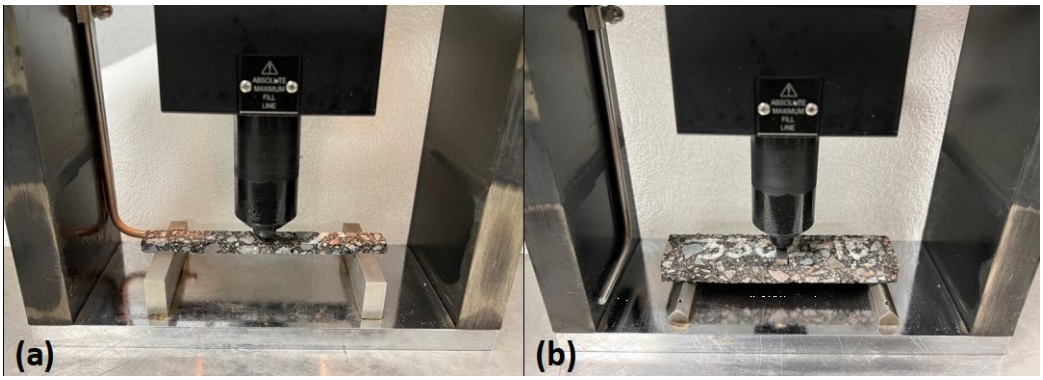

Figure 3.13 (a) The original and (b) the modified support of the BBR test setup

The BBR load cell, LVDT, and temperature sensors were calibrated following the AASHTO T313 standard procedure without any modifications. The original BBR supports were used only during calibration. The tests were conducted at three temperatures: 20°C, 4°C, and -10°C in the specified order. The BBR beams were conditioned at the target test temperature for at least one hour before testing. During the test, the beams were submerged in ethanol (ethyl alcohol), which was used as the thermal bath fluid in accordance with AASHTO T313 standards. During the test, the beams were submerged in ethanol (ethyl alcohol), which was used as the thermal bath fluid in accordance with AASHTO T313 standards. Ethanol

was selected for its ability to maintain the low temperatures required for BBR testing. The beams remained in the ethanol bath only for the duration of the test (approximately 4 to 6 minutes per sample). Given this short exposure time and the guidance provided by the standard, no interaction between ethanol and the asphalt binder or SOR-treated surfaces is expected. No softening, swelling, or other interactions were noticed that would suggest adverse effects of ethanol on the test specimens. Each test was run with a seating load of 35 ± 15 mN, followed by the specified test loads: 200 g at 20°C, 400 g at 4°C, and 600 g at -10°C, applied for 240 seconds.

For the 20°C and 4°C tests, the loads were applied using the BBR control panel. However, in the case of testing with 600 g of load at the test temperature of -10℃, the total load cannot be applied using the BBR control panel alone as the maximum load that can be applied using the control panel is 500 g. A step loading method in which partial load was applied using the BBR control panel, and the rest of the load was applied by the additional dead load, following the previous studies (Marasteanu et al., 2009; Zofka, 2007).

In this study, the entire 600 g load was applied using a dead load to avoid differential loading effects. A small metal strip (Figure 3.13b) was placed on top of the specimen to ensure the load was evenly distributed rather than concentrated. Since the beams were prepared from the top portion of the cores, one side retained the original pavement surface texture. During testing, this textured surface was placed facing downward to accurately measure the SOR's effect. The deflection measurements and creep stiffness calculations followed the AASHTO T313 standard test procedure.

3.2.2 Test results

3.2.2.1 Effect of SORs on pavement aging

This section includes the results of creep stiffness tests conducted on BBR beams prepared from field cores subjected to five aging conditions: unaged (0-year field-aged), one-year field-aged, two-year field-aged, three-year field-aged, and lab-aged.

I. MNROAD28 TEST SECTION

The creep stiffness results at different aging conditions of the MnROAD28 test section measured at the test temperature of 20°C are shown in Figure 3.14. In Figure 3.14, the colored horizontal dashed lines indicate the median values for the Control section under each aging condition. Table 3.3 to Table 3.7 shows the statistical analysis using the Fisher LSD method at a 95% confidence level. In these tables, the SORs that do not share a letter mean that they are statistically different. From the Figure 3.14 and Table 3.3 through Table 3.7, the following general conclusions can be drawn:

[1] *0-year field aged samples (F0):* From Figure 3.14 and Table 3.3, the creep stiffness values for some SORs (BioMAG, RPE-R, ARA1-Ti, CRF, Reclamite, and Replenify) were significantly lower than those of the control, indicating immediate effectiveness in softening the asphalt. This suggests these SORs successfully reduced the mixture's stiffness right after application. While the other SORs (e.g.,

BioRestor, Delta Mist, Invigorate, Replay) might have needed more time to show their impact on creep stiffness (see results on 1-year field-aged samples (F1)).

[2] *1-year field-aged samples (F1):* Using the mean creep stiffness value of the control section as a baseline for the one-year field-aged samples, it is observed that the creep stiffness for *all* SOR-treated samples is lower than that of the control. This indicates that the effectiveness of the SORs became evident after a year. Table 3.4 also shows that the creep stiffness of all SORs are significantly lower than that of the control section. Also, when comparing the increase in creep stiffness from unaged to one-year field-aged samples, there was a significant increase in the control cell's stiffness, but the increase in SOR-treated cells was minimal. This suggests that all SORs were effective in retarding aging.

[3] *2-year field-aged samples (F2):* The creep stiffness values for all samples increased compared to the unaged samples. For the two-year-aged samples, taking the mean creep stiffness of the control section as a reference, the creep stiffness of six SOR-treated samples appeared lower than the control. Specifically, from Table 3.5 it is more evident that SORs like CRF, RPE-R, ARA1Ti, BioMAG, and Reclamite continued to show effectiveness even after two years of application. This indicates that the other SORs might require reapplication after two years of SOR application.

[4] *3-year field-aged samples (F3):* Compared to all 0-year-aged samples, the creep stiffness values increased in all SORs after three years of application, as shown in Figure 3.14. The rate of increase varied among different SOR types. For example, in the case of BioRestor, BioRestor Low, Invigorate, Replay, GSB-88, and Replenify, the rate of increase of creep stiffness values was similar to the control, while other SORs showed lower rates. Among all the SORs, Reclamite exhibited the lowest rate of increase in creep stiffness.

Using the mean creep stiffness of the control section as a reference for three-year-aged samples, most SOR-treated samples showed higher creep stiffness than the control. Accordingly, Table 3.6 indicates that BioMAG, CRF, RPE-R, ARA1 Ti, and Reclamite had lower creep stiffness than the control, as they do not share the same statistical grouping. Interestingly, Reclamite showed lower creep stiffness values after 3-years of field aging than that of 2-years of field aging (F3 < F2).

[5] *Lab-aged samples (LA):* The creep stiffness results for lab-aged samples from Figure 3.14 and Table 3.7 showed that laboratory aging largely affected the stiffness values for most test cells, although the variability was quite high. Since laboratory aging was intended to simulate long-term aging, the results show that SORs such as Invigorate, RPE-R, BioMAG, Replenify, Reclamite, ARA1 Ti, and CRF were effective in retarding aging, even under extreme conditions. These SOR-treated samples had lower creep stiffness compared to the control section in the lab-aged condition. Additionally, creep stiffness generally increased for most of the cells when compared to the three-year field-aged samples.

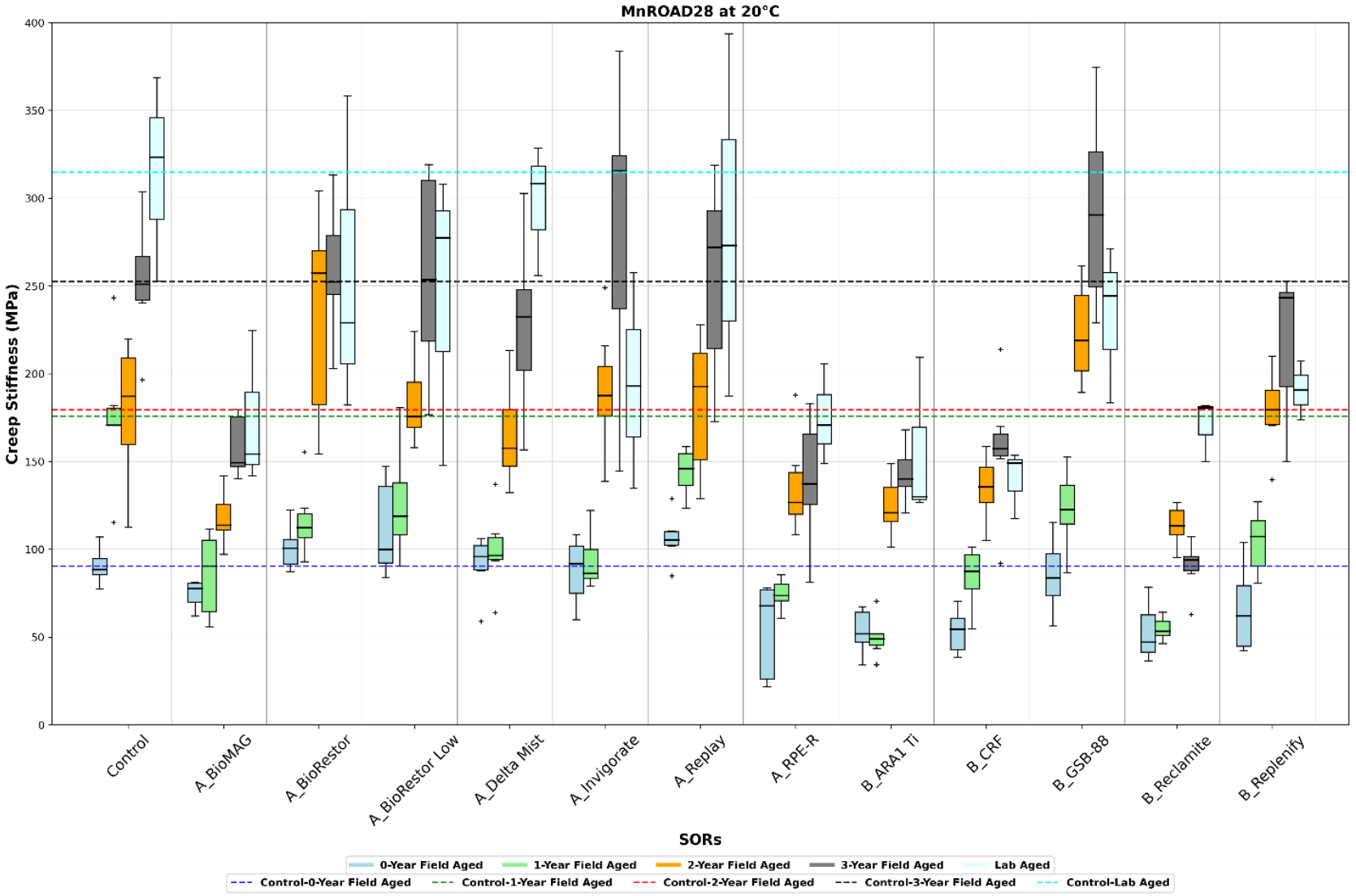

Figure 3.14 BBR test results for asphalt mixture beams for MnROAD28 test section at 20°C

Table 3.3 Fisher LSD grouping results for MnROAD28 test cells in 0-year field aged condition at 20°C

SORs	Number of Replicates	Mean Creep Stiffness (MPa)	Grouping (95% Confidence Level): At 0-year field aged condition (F0) [20°C]				
A_BioRestor Low	8	107.40	A				
A_RePlay	8	105.61	A				
A_BioRestor	8	100.43	A	B			
A_Delta Mist	8	90.88	A	B	C		
A_Invigorate	8	90.45	A	B	C		
Control	8	90.21	A	B	C		
B_GSB-88	8	85.92		B	C		
A_BioMAG	4	75.23			C	D	
B_Replenify	8	65.37				D	E
A_RPE-R	8	56.09				D	E
B_ARA1 Ti	8	51.60					E
B_CRF	8	51.45					E
B_Reclamite	8	50.17					E

Note: SORs that do not share a letter mean that they are statistically different.

Table 3.4 Fisher LSD grouping results for MnROAD28 test cells in 1-year field aged condition at 20°C

SORs	Number of Replicates	Mean Creep Stiffness (MPa)	Grouping (95% Confidence Level): At 1-year field aged condition (F1) [20°C]									
Control	8	171.0	A									
A_RePlay	8	143.8		B								
B_GSB-88	8	130.8		B	C							
A_BioRestor Low	8	126.3		B	C	D						
A_BioRestor	8	115.6			C	D	E					
B_Replenify	8	106.4				D	E	F				
A_Delta Mist	8	99.0					E	F	G			
A_Invigorate	8	94.2						F	G	H		
A_BioMAG	8	87.3						F	G	H		
B_CRF	8	81.9							G	H		
A_RPE-R	8	74.0								H	I	
B_Reclamite	8	56.2									I	J
B_ARA1 Ti	8	50.6										J

Note: SORs that do not share a letter mean that they are statistically different.

Table 3.5 Fisher LSD grouping results for MnROAD28 test cells in 2-year field aged condition at 20°C

SORs	Number of Replicates	Mean Creep Stiffness (MPa)	Grouping (95% Confidence Level): At 2-year field aged condition (F2) [20°C]		
B_GSB-88	8	232.10	A		
A_BioRestor	8	231.80	A		
A_Invigorate	8	192.40		B	
B_Replenify	8	186.50		B	
A_RePlay	8	184.60		B	
A_BioRestor Low	8	183.69		B	
Control	8	176.40		B	
A_Delta Mist	8	168.78		B	
B_CRF	8	137.35			C
A_RPE-R	8	132.84			C
B_ARA1 Ti	8	126.60			C
A_BioMAG	4	119.62			C
B_Reclamite	8	114.87			C

Note: SORs that do not share a letter mean that they are statistically different.

Table 3.6 Fisher LSD grouping results for MnROAD28 test cells in 3-year field aged condition at 20°C

SORs	Number of Replicates	Mean Creep Stiffness (MPa)	Grouping (95% Confidence Level): At 3-year field aged condition (F3) [20°C]					
B_GSB-88	8	290.3	A					
A_Invigorate	8	280.8	A	B				
A_BioRestor	8	266.6	A	B	C			
A_RePlay	8	255.6	A	B	C	D		
Control	8	250.0	A	B	C	D		
A_BioRestor Low	8	242.4		B	C	D		
A_Delta Mist	8	225.8			C	D		
B_Replenify	8	217.3				D		
A_BioMAG	8	163.5					E	
B_CRF	8	159.4					E	
A_RPE-R	8	146.6					E	
B_ARA1 Ti	8	144.9					E	
B_Reclamite	8	89.4						F

Note: SORs that do not share a letter mean that they are statistically different.

Table 3.7 Fisher LSD grouping results for MnROAD28 test cells in lab-aged condition at 20°C

SORs	Number of Replicates	Mean Creep Stiffness (MPa)	Grouping (95% Confidence Level): At lab aged condition (LA) [20°C]			
Control	4	292.80	A			
A_RePlay	4	291.80	A			
A_Delta Mist	4	274.60	A			
A_BioRestor	4	257.30	A	B		
A_BioRestor Low	4	236.90	A	B	C	
B_GSB-88	4	229.70	A	B	C	
A_Invigorate	4	199.00		B	C	D
A_RPE-R	4	186.20		B	C	D
A_BioMAG	4	183.60		B	C	D
B_Replenify	4	179.30			C	D
B_Reclamite	4	176.05			C	D
B_ARA1 Ti	4	148.20				D
B_CRF	4	146.40				D

Note: SORs that do not share a letter mean that they are statistically different.

In general, lab-aged samples were prepared to simulate long-term aging. At 20°C, most SORs followed the expected stiffness trend of F0 < F1 < F2 < F3 < LA. For most SORs, the three-year field-aged creep stiffness values were lower or comparable to those obtained from lab aging. However, for a few SORs (such as Invigorate, CRF, and GSB-88), the lab-aged creep stiffness was lower than the three-year field-aged creep stiffness. The findings suggest that RPE-R, ARA1 Ti, CRF, and Reclamite maintained the effectiveness even after three years, whereas most other SORs might require reapplication after two to three years for MnROAD28 sections.

MNROAD34 TEST SECTION

The creep stiffness results at different aging conditions of the MnROAD34 test section measured at the test temperature of 20°C are shown in Figure 3.15. In Figure 3.15, the median value for the Control section is indicated by colored horizontal dashed lines for each aging condition. Table 3.8 to Table 3.12 shows the statistical analysis by the Fisher LSD method at a 95% confidence level. Means that do not share a letter are significantly different. Based on the Figure 3.15 and Fisher LSD results shown in Table 3.8 through Table 3.12, the following general conclusions can be made:

[1] *0-year field aged samples (F0):* For unaged samples of MnROAD34 cells, a few SORs, specifically ARA1-Ti, CRF, and Reclamite, showed lower creep stiffness compared to the control, indicating their immediate effectiveness in softening the asphalt. However, most other SORs presented similar or increased stiffness levels, potentially due to the 'bridging effect' which might have contributed to a stiffness increase in some cases. The term ‘bridging effect’ herein refers to the theory that microcracks on the surface of MnROAD34 samples become filled with SORs upon application,

forming a bridge between the crack's two sides. This bridging could increase stiffness in BBR testing, particularly when the crack faces downward, as the residual material from the SOR might act similarly to filling a gap with adhesive; temporarily binding the crack surfaces and increasing resistance to deformation.

[2] *1-year field-aged samples (F1):* For the samples aged one year in the field, the majority of SORs, including BioMAG, BioRestor Low, Replay, RPE-R, ARA1Ti, CRF, Reclamite, and Replenify, showed lower creep stiffness than the control cell, highlighting their efficiency over time. Compared to the control section, the rate of increase in creep stiffness for most SOR-treated samples was observed to be less pronounced. In some cases, the creep stiffness of one-year field-aged samples was even lower than that of the unaged condition.

[3] *2-year field-aged samples (F2):* For two-year field-aged samples, the creep stiffness of most SOR-treated samples remained lower than that of the control cell, at the same time all samples exhibited an increase in creep stiffness compared to their initial states. Similar to the MnROAD28 samples, some SORs might need reapplication after 2 years of SOR application.

[4] *3-year field-aged samples (F3):* At 0-year field aging, some SOR-treated MnROAD34 samples showed higher creep stiffness than that of control, possibly due to the bridging effect of microcracks. After one year of SOR application, this bridging effect diminished, likely because the SORs penetrated the surface or due to binder wear, becoming even more prominent after three years. As shown in Figure 3.15, all SORs experienced an increase in creep stiffness after three years compared to the unaged samples, similar to the MnROAD28 samples. Here, control and Replay showed the highest rate of increment in creep stiffness values, while the other SORs had comparatively similar rates of increment. Among all of the SORs, ARA1Ti, CRF, and Reclamite had the lowest rates of increase.

Referring to the three-year-aged MnROAD34 samples, while compared to the mean control creep stiffness, most SOR-treated samples had lower creep stiffness, except for Replay and GSB88. This trend is also evident from the data in Table 3.11.

[5] *Lab-aged samples (LA):* In the lab-aged samples, only the creep stiffness for CRF-treated cells was observed to be lower than that of the control, indicating that the softening effect of this SOR was effective even under extreme conditions and in the presence of surface microcracks. Similarly, throughout all samples, there was an observed increase in creep stiffness compared to their initial measurements.

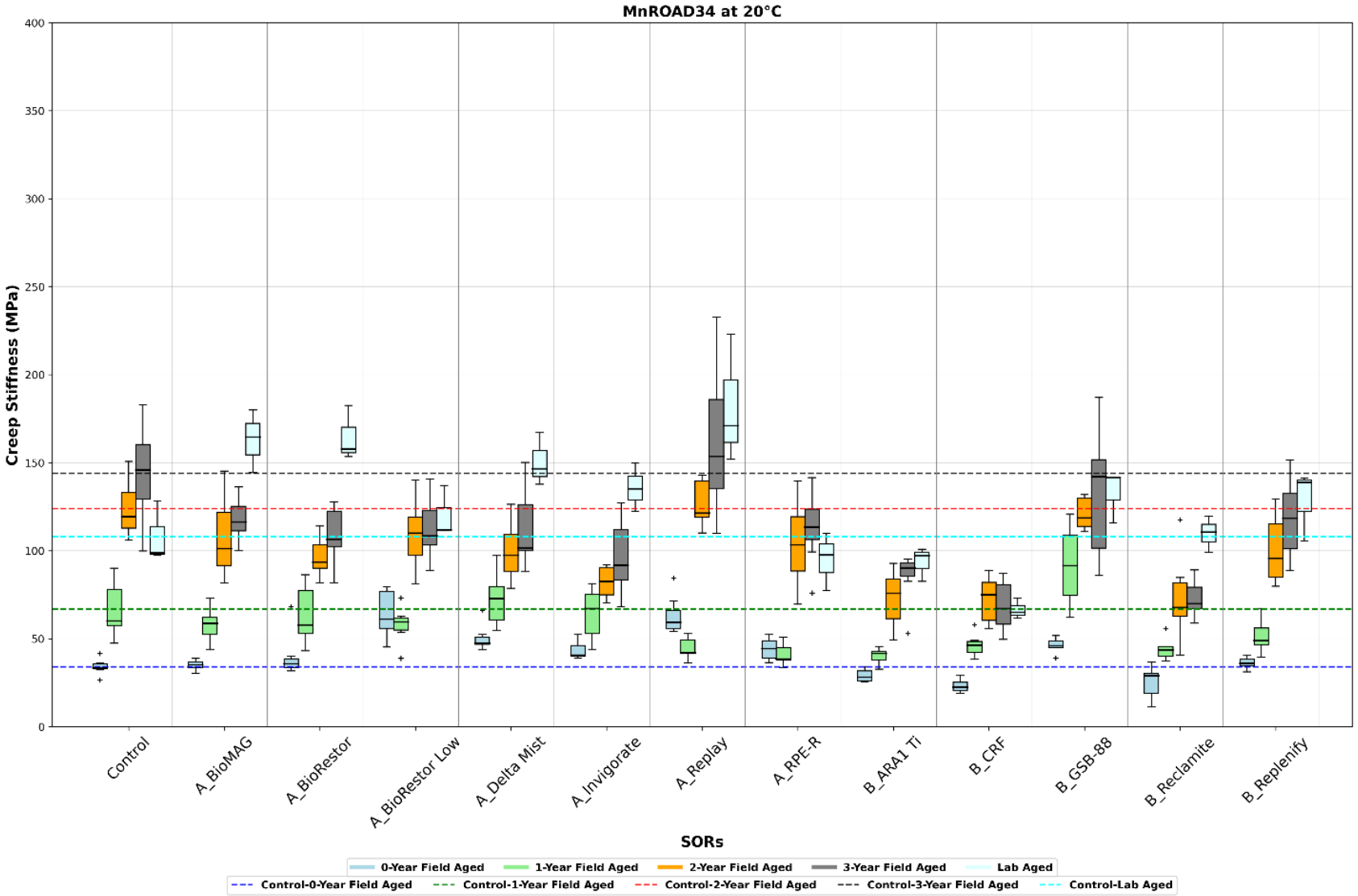

Figure 3.15 BBR test results for asphalt mixture beams for MnROAD34 test section at 20°C

Table 3.8 Fisher LSD grouping results for MnROAD34 test cells in 0-year field aged condition at 20°C

SORs	Number of Replicates	Mean Creep Stiffness (MPa)	Grouping (95% Confidence Level): At 0-year field aged condition (F0) [20°C]						
A_BioRestor Low	8	65.7	A						
A_RePlay	8	63.1	A						
A_Delta Mist	8	49.6		B					
B_GSB-88	8	45.6		B					
A_Invigorate	8	43.6		B	C				
A_RPE-R	8	43.4		B	C				
A_BioRestor	8	42.6		B	C	D			
B_Replenify	8	36.2			C	D	E		
Control	8	35.1				D	E	F	
A_BioMAG	8	35.0					E	F	
B_ARA1 Ti	8	28.6						F	G
B_Reclamite	8	26.0							G
B_CRF	8	22.5							G

Note: SORs that do not share a letter mean that they are statistically different.

Table 3.9 Fisher LSD grouping results for MnROAD34 test cells in 1-year field aged condition at 20°C

SORs	Number of Replicates	Mean Creep Stiffness (MPa)	Grouping (95% Confidence Level): At 1-year field aged condition (F1) [20°C]						
B_GSB-88	8	88.8	A						
A_Delta Mist	8	70.7		B					
Control	8	66.8		B	C				
A_Invigorate	8	62.1		B	C	D			
A_BioRestor	8	61.8		B	C	D			
A_BioMAG	8	56.7			C	D	E		
A_BioRestor Low	8	54.9			C	D	E	F	
B_Replenify	8	50.4				D	E	F	G
B_CRF	8	46.9					E	F	G
A_RePlay	8	46.8					E	F	G
B_Reclamite	8	43.7						F	G
B_ARA1 Ti	8	41.0							G
A_RPE-R	8	40.1							G

Note: SORs that do not share a letter mean that they are statistically different.

Table 3.10 Fisher LSD grouping results for MnROAD34 test cells in 2-year field aged condition at 20°C

SORs	Number of Replicates	Mean Creep Stiffness (MPa)	Grouping (95% Confidence Level): At 2-year field aged condition (F2) [20°C]			
A_RePlay	8	132.18	A			
B_GSB-88	8	125.78	A	B		
Control	8	124.91	A	B		
A_BioRestor Low	8	113.80	A	B	C	
A_BioMAG	8	109.51		B	C	
A_RPE-R	8	108.47		B	C	
A_Delta Mist	8	103.59			C	
A_BioRestor	8	102.64			C	
B_Replenify	8	102.61			C	
A_Invigorate	8	83.61				D
B_CRF	8	74.42				D
B_Reclamite	8	73.46				D
B_ARA1 Ti	8	71.65				D

Note: SORs that do not share a letter mean that they are statistically different.

Table 3.11 Fisher LSD grouping results for MnROAD34 test cells in 3-year field aged condition at 20°C

SORs	Number of Replicates	Mean Creep Stiffness (MPa)	Grouping (95% Confidence Level): At 3-year field aged condition (F3) [20°C]					
A_RePlay	8	166.4	A					
Control	8	144.2	A	B				
B_GSB-88	8	139.5		B	C			
B_Replenify	8	117.9			C	D		
A_BioMAG	8	115.1			C	D	E	
A_Delta Mist	8	114.8			C	D	E	
A_BioRestor Low	8	109.7				D	E	
A_RPE-R	8	109.7				D	E	
A_Invigorate	8	104.9				D	E	
A_BioRestor	8	104.8				D	E	
B_ARA1 Ti	8	92.1					E	F
B_Reclamite	8	76.4						F
B_CRF	8	73.4						F

Note: SORs that do not share a letter mean that they are statistically different.

Table 3.12 Fisher LSD grouping results for MnROAD34 test cells in lab- aged condition at 20°C

SORs	Number of Replicates	Mean Creep Stiffness (MPa)	Grouping (95% Confidence Level): At lab-aged condition (LA) [20°C]					
A_RePlay	4	170.90	A					
A_BioRestor	4	161.64	A	B				
A_BioMAG	4	148.20	A	B				
A_Invigorate	4	141.58	A	B				
A_Delta Mist	4	139.80	A	B	C			
B_GSB-88	4	138.10		B	C			
B_Replenify	4	133.98		B	C	D		
A_BioRestor Low	4	132.00		B	C	D		
A_RPE-R	4	108.50			C	D	E	
Control	4	105.07				D	E	
B_Reclamite	4	102.98				D	E	
B_ARA1 Ti	4	99.17					E	
B_CRF	4	64.29						F

Note: SORs that do not share a letter mean that they are statistically different.

At 20°C, most SORs followed the expected stiffness incremental trend similar to the MnROAD28 section. Only in the case of Control and RPE-R, lab-aged samples exhibited lower creep stiffness than the 3-year field-aged samples. The overall discussion indicates that RPE-R, ARA1 Ti, CRF, and Reclamite showed sustained effectiveness even after three years in MnROAD34, consistent with their performance in MnROAD28.

3.2.2.2 Effect of Test Temperature on Creep Stiffness

The differences in creep stiffness between the control and SOR-treated test cells were most pronounced at the test temperature of 20°C. At lower temperatures (-10°C and 4°C), the variations in creep stiffness were less significant, as the binder became stiffer, reducing the differences. This phenomenon, referred to as low-temperature stiffening (*37*), was consistently observed across different aging conditions in a specific test section.

A consistent trend in low-temperature behavior was observed across different aging conditions in a specific test section. Since traditional fatigue cracking in the field occurs at intermediate temperatures, creep stiffness values measured at 20°C were used to assess the effectiveness of the SORs. The impact of low temperatures on asphalt mixture creep stiffness is further discussed in **Appendix A**. Past research studies have shown that as temperature decreases, asphalt binders experience increased viscosity and molecular structuring, limiting their flexibility and reducing the rate of change in creep stiffness. The reviewed literature also indicates that aged asphalt binders exhibit greater stiffness at low temperatures, and the differences between aged and unaged materials become less distinguishable. This is attributed to the viscoelastic nature of asphalt binders, which diminishes at lower temperatures, making the overall behavior of the asphalt mixture more elastic due to the dominant influence of the aggregates.

Additionally, previous studies have demonstrated that oxidation, physical hardening, and molecular aggregation at low temperatures further contribute to reduced variability in stiffness measurements.

Creep stiffness results for the MnROAD test section cells at -10°C and 4°C, provided in **Appendix B**, indicate that stiffness values increased as the temperature decreased for both MnROAD sections. At low temperatures, most SOR-treated lab-aged samples exhibited lower stiffness compared to the 3-year field-aged samples. In the MnROAD28 section, SORs such as ARA1Ti, CRF, and Reclamite exhibited lower creep stiffness compared to the control at 4°C after 3 years of SOR application. Similarly, in the MnROAD34 section, BioRestor Low, CRF, GSB88, and Reclamite exhibited lower stiffness than the control at 4°C, even 3 years after SOR application. After 3 years of SOR application, most SORs showed minimal differences in creep stiffness compared to the control in the MnROAD28 section at -10°C, except for RPE-R. In the case of the 3-year field-aged MnROAD34 section, CRF also exhibited a noticeable difference at -10°C. These findings suggest that certain SORs may remain effective at lower temperatures, even after 3 years, despite the low-temperature stiffening phenomenon.

3.2.2.3 Effect of Binder Types: MnROAD28 versus MnROAD34

As previously mentioned, the MnROAD34 test section exhibited microcracks, which were partially or completely filled by SOR residue, a phenomenon referred to as the “bridging effect” in this report. Due to the combined effects of “softening” and “bridging,” MnROAD34 test sections showed lower creep stiffness compared to MnROAD28 at 20°C. Performance differences between the two sections were also affected by SOR compatibility with binders. During 0-year field aging, most SORs exhibited similar or increased stiffness levels compared to the control, likely due to the "bridging effect," which might have contributed to higher stiffness in some cases, as previously discussed. However, after one year of field aging (F1), most SORs performed better in the MnROAD34 section. This suggests that the bridging effect might have diminished over time and indicates improved binder-SOR interactions in MnROAD34 (as shown in Figure 3.14). In addition to the microcracks, the observed trends might also be influenced by chemical interactions between certain SORs and the SBS-modified PG 58H-34 binder. Notably, the PG 58H-34 binder used in MnROAD34 was derived from a different base binder (PG 49-34) and subsequently modified on the high end, which might have affected the compatibility and performance of some SORs. This possibility highlights the need for further investigation into binder-SOR chemistry, especially for modified binders.

3.3 Rutting resistance

3.3.1 Experimental setup

Spray-on rejuvenators are believed to soften the asphalt binder in the surface layer, which helps improve cracking resistance, such as top-down or block cracking. However, excessive softening could lead to plastic deformation near the surface. To evaluate this risk, rutting resistance was tested using the Hamburg Wheel Tracking (HWT) device on both control and SOR-treated test sections. The test followed the AASHTO T324 standard (2019).

The HWT device consists of steel wheels with a diameter of 203.8 mm and a width of 47 mm, applying a force of 705 N on the test specimen. These wheels roll on the top of the specimen at a speed of 52 ± 2 passes per minute, while the device tracks the rutting profile throughout the test. In this study, cylindrical field cores (150 ± 3 mm in diameter) were cut into the HWT mold shape before testing, following the standard. The tests were conducted at 45°C with 10,000 cycles (20,000 passes). The HWT equipment used is shown in Figure 3.16.

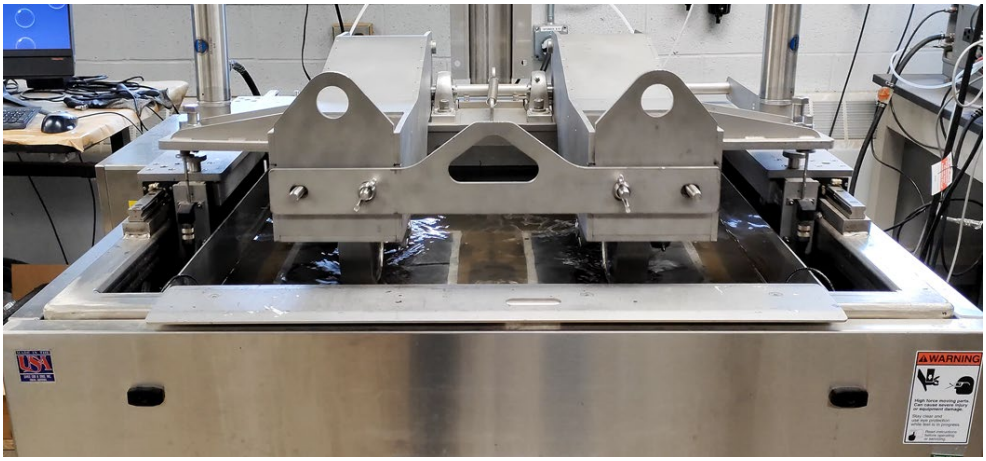

Figure 3.16 Hamburg Wheel Tracker (HWT) device used in this study

The failure threshold for the HWT test on asphalt surface sections varies based on specific requirements. Generally, a rut depth of 10 mm or more is considered a failure. However, some specifications might allow deeper rutting depending on the pavement's intended use and expected traffic load. A pavement section is considered to have failed when it exceeds the rut depth limit within a set number of wheel passes, typically between 20,000 and 50,000. Conventionally, the rutting resistance is assessed by measuring the rut depth at a fixed number of cycles, such as 10,000 cycles (20,000 passes). In this study, the research team introduced a new image-analysis-based method to calculate heave height in HWT-tested specimens, which was published in Journal of Transportation Engineering (Vaddy et al., 2024). The primary analysis in the Hamburg Wheel Tracking Device (HWTD) test focused on conventional rut depth measurements. However, this new approach aims to additionally incorporate the heave height as a complementary long-term performance parameter for asphalt mixtures, offering a more comprehensive evaluation of surface deformation behavior over time.

3.3.2 Test results

The HWT test results of both MnROAD test sections are presented in Figure 3.17. The solid line in the figures represents the control rut depth; values above the line indicate higher rut depth than the control, while values below the line indicate lower rut depth. The results are also analyzed statistically and grouped using the Fisher LSD method (see Table 3.13 and Table 3.14). The results indicated that there is no consistent statistically significant difference between the control and respective SOR-treated test cells. Though the results of the MnROAD34 test section seem to differ between the control and SOR-treated test cells, the difference was statistically insignificant, due to the high variability in the

results within a test cell. It is a good sign that none of the tested SORs had any serious rutting-related concerns compared to their respective control test cell.

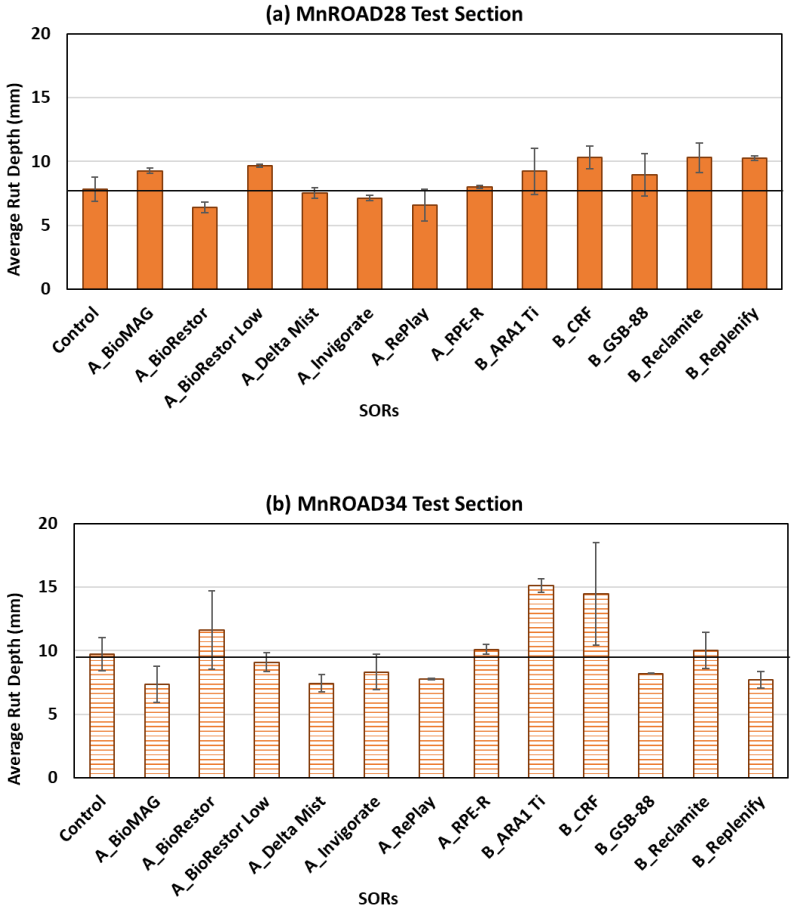

Figure 3.17 Hamburg Wheel Tracker (HWT) test results at 45°C with 20,000 passes

Table 3.13 Grouping HWT results of MnROAD28 test section using Fisher LSD method

SORs	Number of replicates	Mean rut depth (mm)	Confidence interval				
			95%				
B_CRF	2	10.31	A				
B_Reclamite	2	10.28	A				
B_Replenify	2	10.25	A				
A_BioRestor Low	2	9.66	A	B			
A_BioMAG	2	9.26	A	B	C		
B_ARA1 Ti	2	9.22	A	B	C		
B_GSB-88	2	8.95	A	B	C	D	
A_RPE-R	2	7.98		B	C	D	E
Control	2	7.81		B	C	D	E
A_Delta Mist	2	7.51			C	D	E

SORs	Number of replicates	Mean rut depth (mm)	Confidence interval 95%				
A_Invigorate	2	7.12				D	E
A_RePlay	2	6.56					E
A_BioRestor	2	6.38					E

Note: SORs that do not share a letter mean that they are statistically different.

Table 3.14 Grouping HWT results of MnROAD34 test section using Fisher LSD method

SORs	Number of replicates	Mean rut depth (mm)	Confidence interval 95%		
B_ARA1 Ti	2	15.13	A		
B_CRF	2	14.46	A		
A_BioRestor	2	11.62	A	B	
A_RPE-R	2	10.09		B	C
B_Reclamite	2	10.02		B	C
Control	2	9.71		B	C
A_Invigorate	2	8.32		B	C
B_GSB-88	2	8.19		B	C
A_RePlay	2	7.77			C
A_BioRestor Low	2	7.77			C
B_Replenify	2	7.69			C
A_Delta Mist	2	7.41			C
A_BioMAG	2	7.35			C

Note: SORs that do not share a letter mean that they are statistically different.

In addition to the measurement of conventional rut depths of HWT-tested specimens, the research team developed a new image-based test methodology to measure the heave height at the end of the HWT test (Vaddy et al., 2024). The team is working on measuring the heave height using the developed method. Once the heave height results are available, the team will compare the heave height in HWT-tested specimens of both control and SOR-treated sections.

3.4 Permeability

3.4.1 Experimental setup

Permeability tests were conducted on cores taken from both control and SOR-treated test cells. The tests followed ASTM D5084 (Method C - falling head and rising tail) using a flexible wall permeameter (ASTM, 2016). A schematic and actual test setup are shown in Figure 3.18. The setup included a permeameter (or pressure cell) and a hydraulic system to apply head differences (flex panel). According to the standard procedure, the test specimen was placed in a "sandwich" structure with porous stones between the top and bottom plates of the permeameter (Figure 3.18a). A flexible membrane was used to cover the sides to prevent leakage. The cell was pressurized, so that the membrane adhered tightly to

the sample. Additionally, high-pressure vacuum gel was applied, and O-rings were inserted between the plates and membrane to ensure no water leaks from the setup.

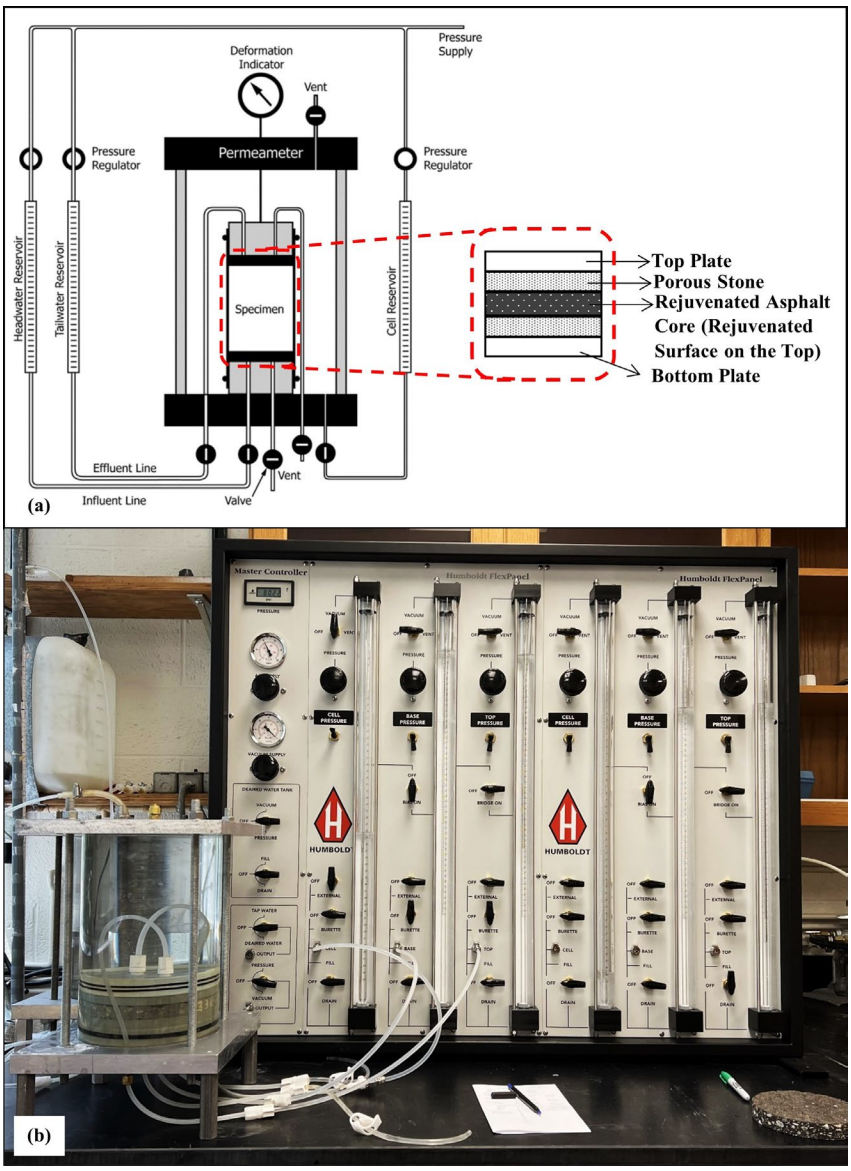

Figure 3.18 Permeability test setup: (a) schematic diagram of the test setup (ASTM, 2016) and (b) laboratory test setup

Since this research focused on the surface properties of the SOR-treated asphalt pavements, to evaluate permeability, we cut a 20 mm thick, 150 mm diameter cylindrical slice from the top of field-extracted cores. According to standard procedures, test specimens must be fully saturated and free of air bubbles. To achieve this, the specimens were submerged in water for 24 hours and subjected to a vacuum to remove trapped air. The permeability tests were conducted at atmospheric pressure to maintain water heads, with an applied cell pressure of 80 psi. A constant head difference of 20 mm was maintained for all samples to ensure consistency and avoid variations due to variable head levels.

3.4.2 Test results

Proper saturation (or removal of air) of test specimens is crucial in permeability testing, as it affects the accuracy of the results. In this study, specimens were submerged in water for 24 hours and vacuum was applied before testing to ensure full saturation. If a specimen is properly saturated, its permeability should remain constant over time. To verify the effectiveness of the saturation process, one specimen from each control test cell at the MnROAD sections was tested for permeability at different time intervals. The first test (t = 0 min) followed the standard procedure. Without dismantling the setup, the same specimens were retested every 60 minutes. As shown in Figure 3.19, the permeability remained consistent over time, confirming that the saturation method used was effective and the test procedure was correctly followed.

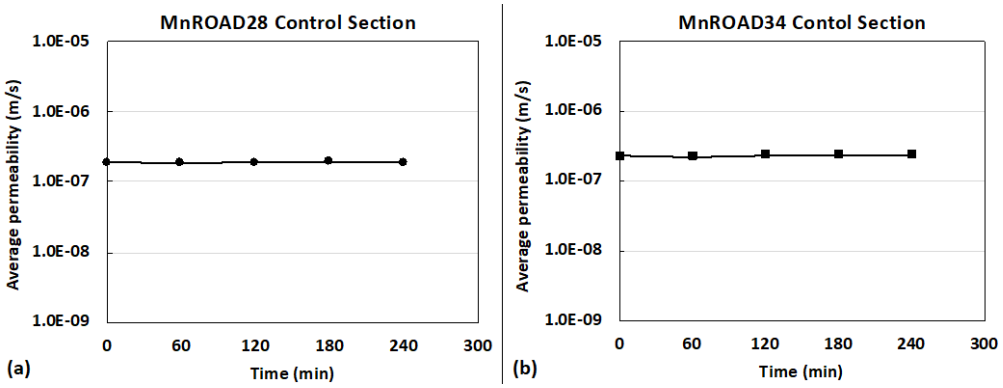

Figure 3.19 Effectiveness of the saturation process by the maintenance of constant permeability with time

The permeability test results for cores from the control and SOR-treated test sections are shown in Figure 3.20. The solid and dashed lines in the figures represent the permeability values of the control section for MnROAD28 and MnROAD34 section respectively; values above the line indicate higher permeability than the control, while values below the line indicate lower permeability.

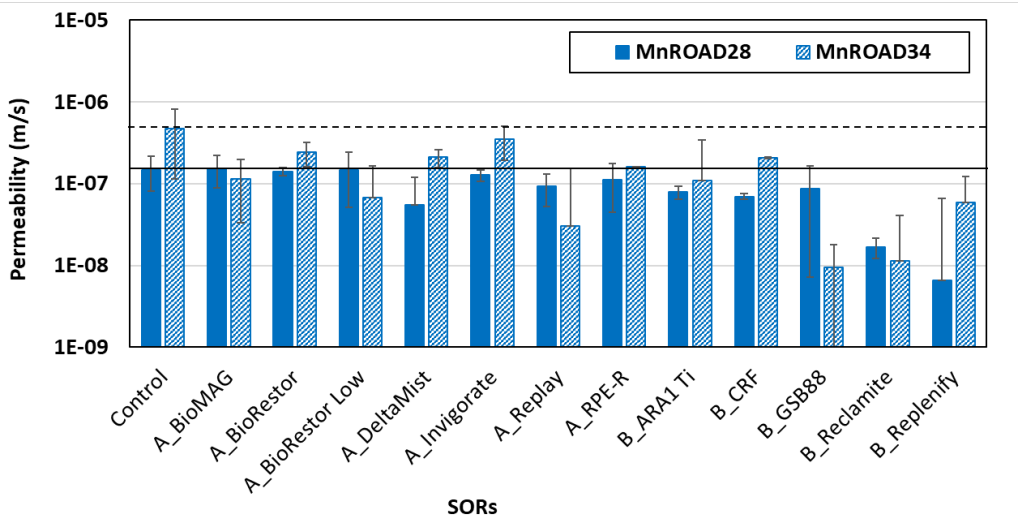

Figure 3.20 Permeability results of MnROAD28 and MnROAD34 sections

It was observed that the permeability of the control cell in the MnROAD34 section is higher than in the MnROAD28 section. This aligns with hypothesis for the presence of microcracks on the MnROAD34 surface, which likely contributed to the increased permeability. The results were statistically analyzed and grouped using the Fisher LSD method (Table 3.15 and Table 3.16). Overall, there was no significant difference in permeability between the control and SOR-treated test cells in most cases. However, in both MnROAD sections, Reclamite and Replenify consistently showed a reduction in permeability compared to the control sections. This decrease may be due to the filling of surface voids in the pavement surface.

Table 3.15 Grouping permeability results of MnROAD28 test section using Fisher LSD method

SORs	Number of replicates	Log (average *k*) (m/s)	Confidence interval 95%			
A_BioMAG	4	-6.81	A			
A_BioRestor Low	4	-6.88	A			
Control	4	-6.88	A			
A_Invigorate	4	-6.90	A			
A_BioRestor	4	-6.98	A	B		
A_RPE-R	4	-7.01	A	B		
A_RePlay	4	-7.13	A	B		
B_CRF	4	-7.18	A	B		
B_ARA1 Ti	4	-7.24	A	B		
B_GSB-88	4	-7.26	A	B		
A_Delta Mist	4	-7.37		B	C	
B_Reclamite	4	-7.79			C	
B_Replenify	4	-8.28				D

Note: SORs that do not share a letter mean that they are statistically different.

Table 3.16 Grouping permeability results of MnROAD34 test section using Fisher LSD method

SORs	Number of replicates	Log (avg *k*) (m/s)	Confidence interval 95%						
Control	4	-6.45	A						
A_Invigorate	4	-6.57	A						
A_BioRestor	4	-6.65	A	B					
A_Delta Mist	4	-6.72	A	B	C				
A_RPE-R	4	-6.82	A	B	C				
B_CRF	4	-6.84	A	B	C	D			
A_BioMAG	4	-7.02		B	C	D	E		
B_ARA1 Ti	4	-7.08			C	D	E		
A_BioRestor Low	4	-7.25				D	E	F	
B_Replenify	4	-7.27					E	F	
A_RePlay	4	-7.53						F	

SORs	Number of replicates	Log (avg *k*) (m/s)	Confidence interval 95%						
B_Reclamite	4	-7.95							G
B_GSB-88	4	-8.03							G

Note: SORs that do not share a letter mean that they are statistically different.

The permeability of dense-graded Hot Mix Asphalt (HMA) typically ranges from 10^{-3} to 10^{-6} cm/s, as reported in various studies(Chen et al., 2019; Cooley et al., 2001; Gogula et al, 2004; Guada et al., 2018; Ryan et al., 2007). Dense-graded HMA is designed to have low permeability to prevent water infiltration and improve resistance to moisture damage. This is achieved by using a well-graded aggregate mix, which creates a tightly interlocked structure with minimal air voids. Additionally, adjusting the asphalt binder content helps ensure proper coating and adhesion of aggregate particles, further reducing permeability. However, it is important to note that HMA permeability can vary depending on the testing method used.

3.5 Abrasion and friction resistance

3.5.1 Experimental setup

To analyze the effects of SORs on the abrasion resistance of pavement surfaces, a modified Hamburg Wheel Tracking (HWT) system was used (Boz et al., 2019). This device (shown in Figure 3.21) simulated the braking/acceleration effect and allowed for the evaluation of skid resistance and abrasion after SOR application. This adaptation involved replacing the Hamburg Wheel Tracking device's steel wheel with a rubber wheel and reducing the load to 125 lb (same load level used for assessing bleeding of micro-surfacing mixtures, as described in ASTM D 6372 (ASTM, 2015). In addition, the rubber wheel was locked in place to enable sliding rather than rolling, simulating the effect of a rubber wheel sliding across the pavement surface.

The cylindrical cores from the field test sections were cut into the shape of the HWT mold specified by the AASHTO T324 (2019) standard before the testing. As a part of sample preparation, a very-thin layer (2-3 mm) of quick-setting concrete was applied at the bottom to maintain consistent surface levels between adjacent samples. This avoided any elevation change during the tests, as shown in Figure 3.22.

The skid resistance of the samples was evaluated by quantifying friction loss using British Pendulum Tester (BPT) before and after the HWT-abrasion action. This evaluation aimed to determine if there was any reduction in skid resistance due to the application of SORs. The BPT device (Figure 3.23a) operates on the principle of a dynamic pendulum impact, where a rubber slider is propelled across the surface of the specimen. For this test, a smaller slider of 1.25 inches in width (Figure 3.23b) was used instead of the 3-inch width slider recommended by ASTM E303 (ASTM, 2022). The adjustment was made to measure skid resistance changes specifically within the abrasion testing wheel path after 0-, 50-, and 100-wheel passes (Figure 3.23c). To ensure accuracy, comparative tests with the standard-sized slider at 0-wheel passes (before abrasion testing) were also conducted. These tests revealed similar trends in the results, as shown in **Appendix C** (Figure C. 1 and Figure C. 2).

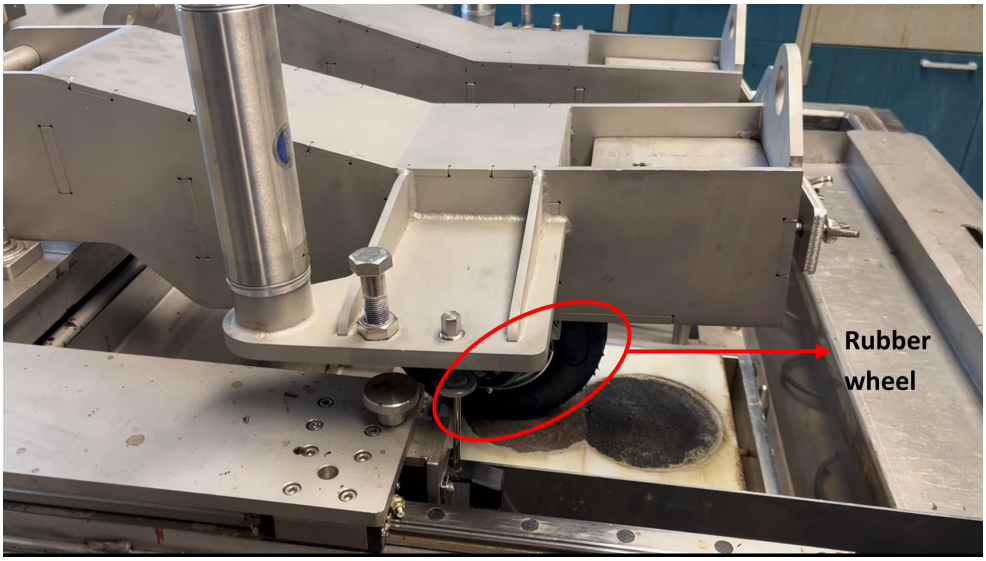

Figure 3.21 Modified Hamburg wheel tracking device used in this study

Figure 3.22 Sample preparation before abrasion testing

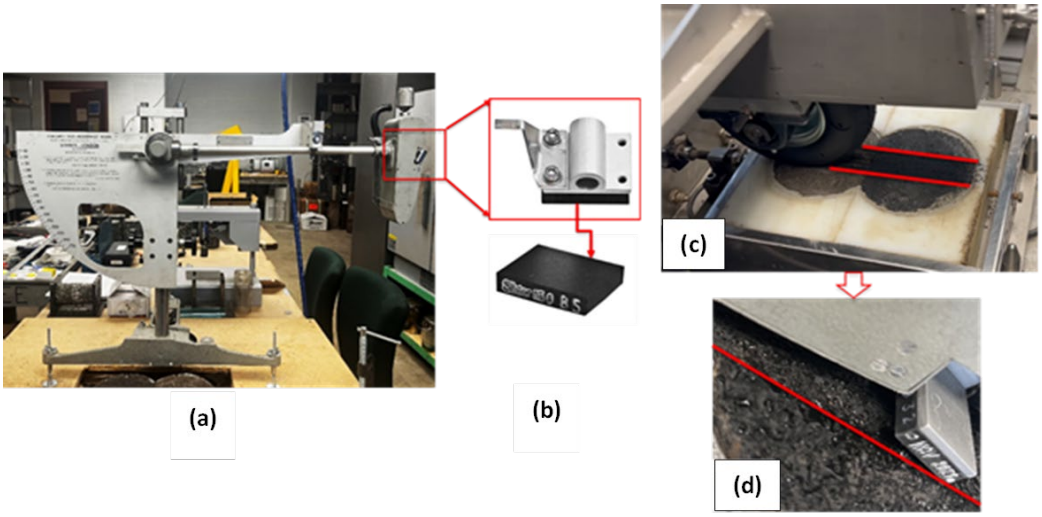

Figure 3.23 Abrasion and Friction Testing (BPT): (a) BPT device, (b) slider used in this study, (c) rubber wheel passing over the specimen surface, and (d) BPT testing along with the wheel path

3.5.2 Test results

The skid resistance values obtained from British pendulum testing (BPT), both before and after HWT-wheel passes, are outlined below. It should be noted that the wear from rubber tires might affect the skid resistance results measured by the British Pendulum testing.

3.5.2.1 MnROAD28 test section

Figure 3.24 shows how different SORs affect the skid resistance of asphalt over time with increasing wheel/tire passes in the MnROAD28 section.

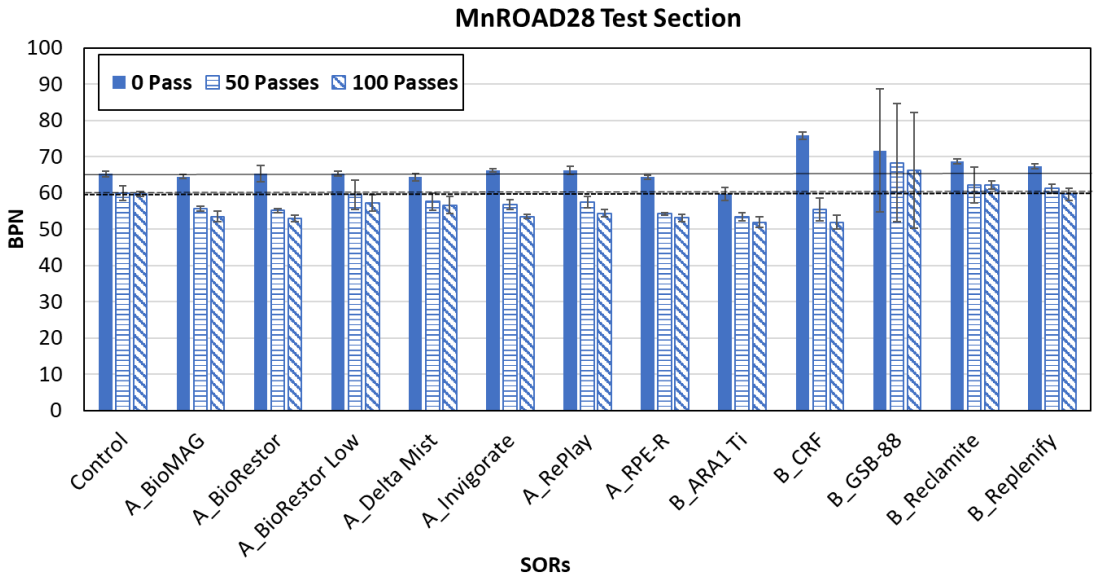

Figure 3.24 Skid resistance of MnROAD28 section

Both the control section and the SOR-treated sections experienced a slight decrease in BPN after wheel passes, indicating a gradual decrease in skid resistance. Some SORs, like BioRestor and CRF, had a more noticeable decrease in BPN after 50 and 100 passes, implying they might not be as effective in maintaining skid resistance over time.

On the other hand, some SORs (e.g., BioRestor Low, ARA1 Ti, Reclamite) showed less reduction in BPN after 50 and 100 passes, indicating they might better preserve skid resistance under traffic conditions. Initially, only CRF and GSB-88 had considerably higher skid resistance than the control. After 50 and 100 passes, GSB-88 continued to maintain higher skid resistance compared to the control, however, the skid resistance of CRF became lower than that of control.

3.5.2.2 MnROAD34 test section

Figure 3.25 illustrates how different SORs impact skid resistance in the MnROAD34 section as wheel/tire passes increase over time. Like in the MnROAD28 section, both the control and SOR-treated areas experienced a decrease in BPN, showing a decline in skid resistance after the increase of wheel passes.

Some SORs, such as Reclamite and CRF, showed a noticeable decrease in BPN after 50 and 100 passes. Similar to MnROAD28, CRF initially had a higher BPN than the control, but it decreased after 50 and 100 passes. In contrast, GSB-88 started with a lower BPN than the control, but the skid resistance slightly increased after 50 and 100 passes, which is a different trend compared to the other sections. This could suggest that GSB-88 maintained better skid resistance after the passes, possibly due to the presence of fine sand/gravel.

Figure 3.25 Skid resistance of MnROAD34 section

The Group A SORs showed consistent results with no significant decrease in skid resistance over wheel passes. In contrast, the variations in Group B SORs might be due to the uneven distribution of sand or fine gravel. It is also possible that some materials were displaced during transportation, leading to these differences. While certain SORs initially showed greater skid resistance compared to the control, the repeated wheel passes might have exposed the underlying pavement surface, leading to a gradual decline in skid resistance that eventually reached levels similar to the control. Establishing a benchmark for minimum skid resistance on the pavement would be beneficial to ensure safety.

3.6 Ranking of the SORs

To assess the extent of the effects of the SORs, a ranking score was established based on the laboratory studies. This ranking is determined by calculating the percentage difference between the control cells and the different SOR-treated cells. Compared to the control cells, the SORs with lower values for creep stiffness, permeability, and rut depth and higher values for skid resistance (friction) were ranked in order. For BBR, rut depth, and permeability, a lower value compared to the control is desirable. However, for skid resistance (friction), a higher value compared to the control is preferred. Considering

all of these conditions, a formulation to calculate the SOR scores was developed and shown in **Equation 10**:

$$\textbf{Ranking Score} = \left[\sum(\mathrm{F0_x} + \mathrm{F1_x} + \mathrm{F2_x} + \mathrm{F3_x} + \mathrm{LA_x}) + \mathrm{k} + \mathrm{RD}\right] - \sum BPN_y \quad (10)$$

where:

$F0_x$ = Creep stiffness of 0-year-field-aged-samples (unaged) samples @ x°C [x = 20°C, 4°C, -10°C]
$F1_x$ = Creep stiffness of 1-year-field-aged-samples @ x°C
$F2_x$ = Creep stiffness of 2-year-field-aged-samples @ x°C
$F3_x$ = Creep stiffness of 3-year-field-aged-samples @ x°C
LA_x = Creep stiffness of lab-aged-samples @ x°C
k = Lab permeability test values on field-extracted cores
RD = Rut depth of field extracted samples by HWT test
BPN_y = Skid resistance at y-wheel passes [y = 0, 50, 100-wheel passes]

The ranking scores are shown in Table 3.17. The ranking indicates that the SORs within the groups of "Best", "Better" and "Good" were consistent across both MnROAD28 and MnROAD34 test sections. Although some SORs generally performed better than others, all treatments demonstrated lower creep stiffness, permeability, and rut depth, while maintaining higher skid resistance, making them strong candidates for field implementation.

Table 3.17 Ranking of SORs based on lab studies

Rank	Order	MnROAD28	Composition	MnROAD34	Composition
Best	1	B_Reclamite	Petroleum-based	B_CRF	Petroleum-based
	2	B_ARA1 Ti	Petroleum-based	B_Reclamite	Petroleum-based
	3	B_CRF	Petroleum-based	A_RPE-R	Petroleum-based
	4	A_RPE-R	Petroleum-based	B_ARA1 Ti	Petroleum-based
Better	5	A_BioMAG	Bio-based	A_BioMAG	Bio-based
	6	B_Replenify	Petroleum-based	A_Invigorate	Bio-based
	7	B_GSB-88	Petroleum-based	B_GSB-88	Petroleum-based
	8	A_Invigorate	Bio-based	B_Replenify	Petroleum-based
Good	9	A_Delta Mist	Bio-based	A_BioRestor Low	Bio-based
	10	A_BioRestor	Bio-based	A_Delta Mist	Bio-based
	11	A_RePlay	Bio-based	A_RePlay	Bio-based
	12	A_BioRestor Low	Bio-based	A_BioRestor	Bio-based
Control	13	No Treatment			

It is important to note that the performance ranking presented in this study is based solely on the laboratory experiments. Within these defined parameters, no SOR was identified as a poor performer.

However, factors such as cost, aesthetics, and environmental product declarations (EPDs), which might significantly influence roadway owners' product selection, were beyond this study's scope and were not evaluated.

Chapter 4: Field study

Field test sections were monitored at different intervals before SOR application and at 1 month, 12 months, 24 months, and 36 months after application. All the data provided in this report was collected by MnROAD personnel. The following key properties were assessed:

- Rejuvenation Application Rate (RAR)
- Reflectivity
- Albedo
- Mean texture depth
- Dynamic friction coefficient (Surface friction)
- Permeability

4.1 Rejuvenation application rate (RAR)

In this study, the recommended application rate for each product was determined by the manufacturers of each product and measured by the research team. The rejuvenator application rate (RAR) was assessed using 1 ft × 1 ft square measuring pads. Three pads were placed on the pavement test cell before application, and rejuvenators were sprayed while the pads remained in place (Figure 4.1). The RAR was then calculated as the ratio of the weight increase of the pad to its cross-sectional area.

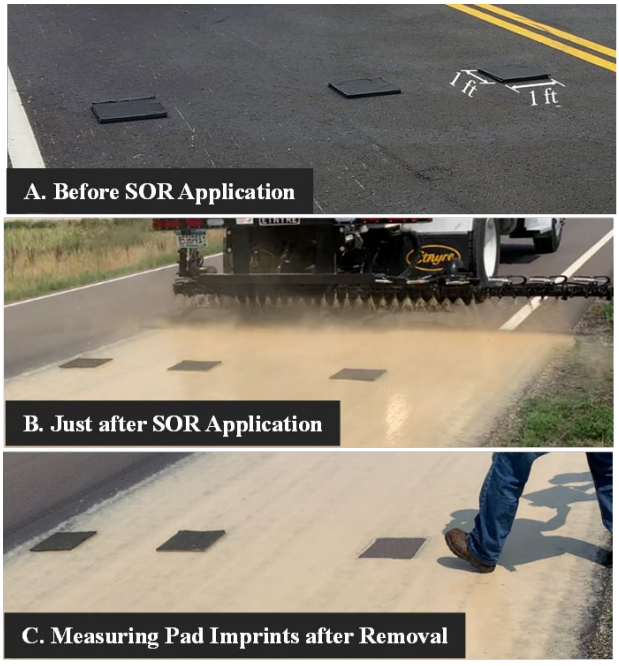

Figure 4.1 Sequence of activities in measuring the application rate of rejuvenator

The rejuvenator application rates (RARs) for different products are shown in Figure 4.2. Most SORs were applied at a consistent rate across the three test sections, but significant variations were observed

between different products. BioMAG®, BioRestor®, BioRestor® Low, Invigorate™, and RePlay™ had RARs below 0.2 lb/yd^2, while Delta Mist®, ARA1 Ti, CRF®, Reclamite®, and Replenify™ had RARs between 0.5 and 0.7 lb/yd^2 on average. GSB-88® had the highest application rate, and RPE-R showed variation across the test sections. For GSB-88®, granular material was applied simultaneously with the SOR using the same truck, which contributed to its high RAR measurement.

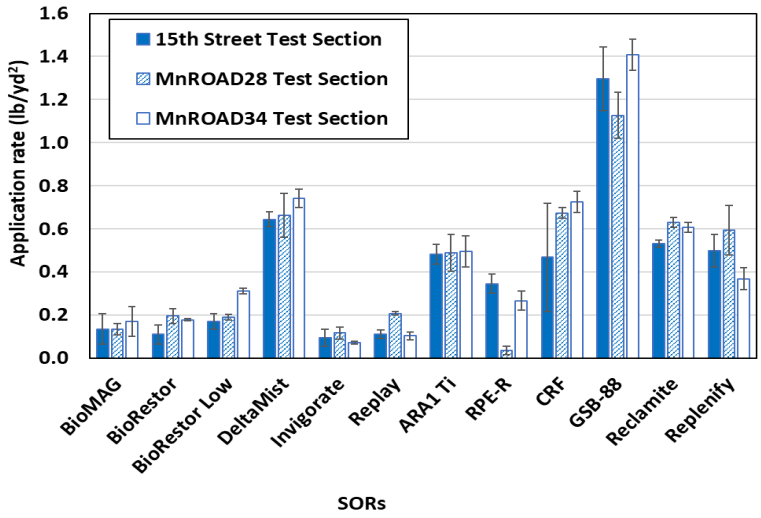

Figure 4.2 Application rates of the SORs

4.2 Reflectivity

4.2.1 Test method

In this study, the reflectivity of pavement markings was measured before and after SOR application across all test cells. Reflectivity was quantified using the coefficient of retroreflected luminance (CRL, cd/m^2/lux), which represents the ratio of reflected light to incident light. Measurements were taken for both control and SOR-treated sections using a Delta LTL-X portable retro reflectometer (shown in Figure 4.3), following ASTM E1710 standards (ASTM, 2018).

4.2.2 Observations

The reflectivity data was collected from all test cells before and approximately two months after application. The results, shown in Figure 4.4, indicate that all SORs reduced pavement marking reflectivity to some extent. At MnROAD28 and MnROAD34 sections, GSB88 and CRF were applied over existing stripes due to field constraints, and the resulting reflectivity data might not reflect typical field application practices. For this reason, based on feedback and manufacturer application guidance, these SORs have been excluded from the reflectivity data reporting (by 'x' mark), as these products are not intended to be applied directly over pavement markings without appropriate restriping considerations. Several other SORs also caused a more than 30% reduction in reflectivity. Post-SOR application measurements showed that not all test cells had statistically similar reflectivity values across the three

test sections. However, most SORs, except CRF and GSB-88, allowed pavement markings to remain visible after application.

Figure 4.3 Photograph of Delta LTL-X portable retro reflectometer

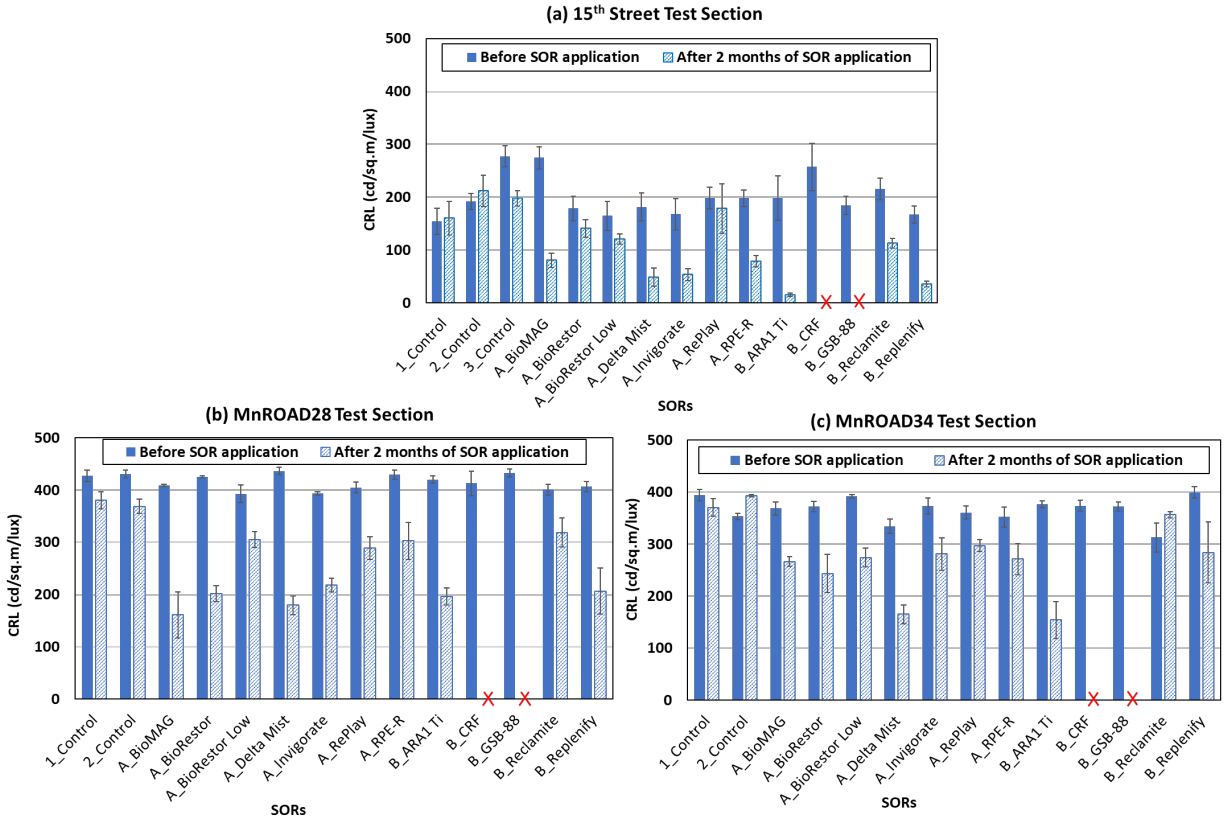

Figure 4.4 Results of reflectivity analysis of control and SOR-treated test cells: (a) and (b) 15th street test section, (c) and (d) MnROAD28 test section, and (d) and (e) MnROAD34 test section

Note: 1. CRL means Coefficient of Retroreflective Luminance, and 2. "X" in graphs denotes the unavailability/exclusion of data at a specific location. Products B1 and B2 were not applied on pavement marks at 15th street due to their high reduction in reflectivity, and 15th street is an in-service road.

A change in reflectivity was also observed in the control test cells over two months. The change was more significant with the 15th Street control test cells compared to those at MnROAD. This difference may be due to 15th Street being an active roadway, while the MnROAD test cells were dedicated research sections with minimal traffic. Additionally, the pavement markings at MnROAD were freshly applied within two months of testing. In contrast, the 15th Street markings had been in place for about a year, which might have contributed to the lower absolute reflectivity values observed on 15th Street.

4.3 Albedo

4.3.1 Test method

Albedo is an important part of the mechanistic-empirical pavement design, as it greatly influences the pavement's temperature profile. A higher albedo means the surface reflects more sunlight and stays cooler, while a lower albedo absorbs more heat, potentially accelerating aging. Some SORs can change the pavement's surface color, affecting its albedo. To evaluate this, albedo was measured before and after applying SORs on all the SOR-applied test cells. Field measurements were taken using a portable dual pyranometer (Type 8104) Model 240-8104 Albedometer, following the ASTM E1918 standard (ASTM, 2021). The test setup in the field is shown in Figure 4.5. The goal was to determine whether SORs increased or decreased surface reflectivity, which might have implications for pavement performance.

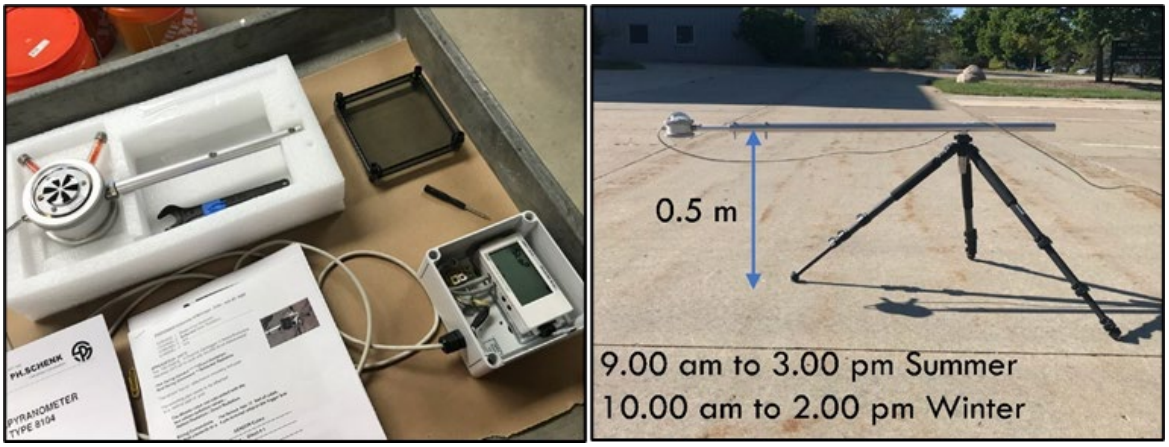

Figure 4.5 Albedo testing setup using a dual pyranometer

4.3.2 Observations

The albedo of both control and SOR-treated sections in the MnROAD28 and MnROAD34 test sections was measured at three intervals: 2 months, 24 months, and 36 months after the application of SORs, as presented in Figure 4.6. Additionally, albedo data for the 15th Street test section was collected, but only at 2 months following the SOR application, and is also showed in Figure 4.6. Missing data are indicated by 'x' symbol.

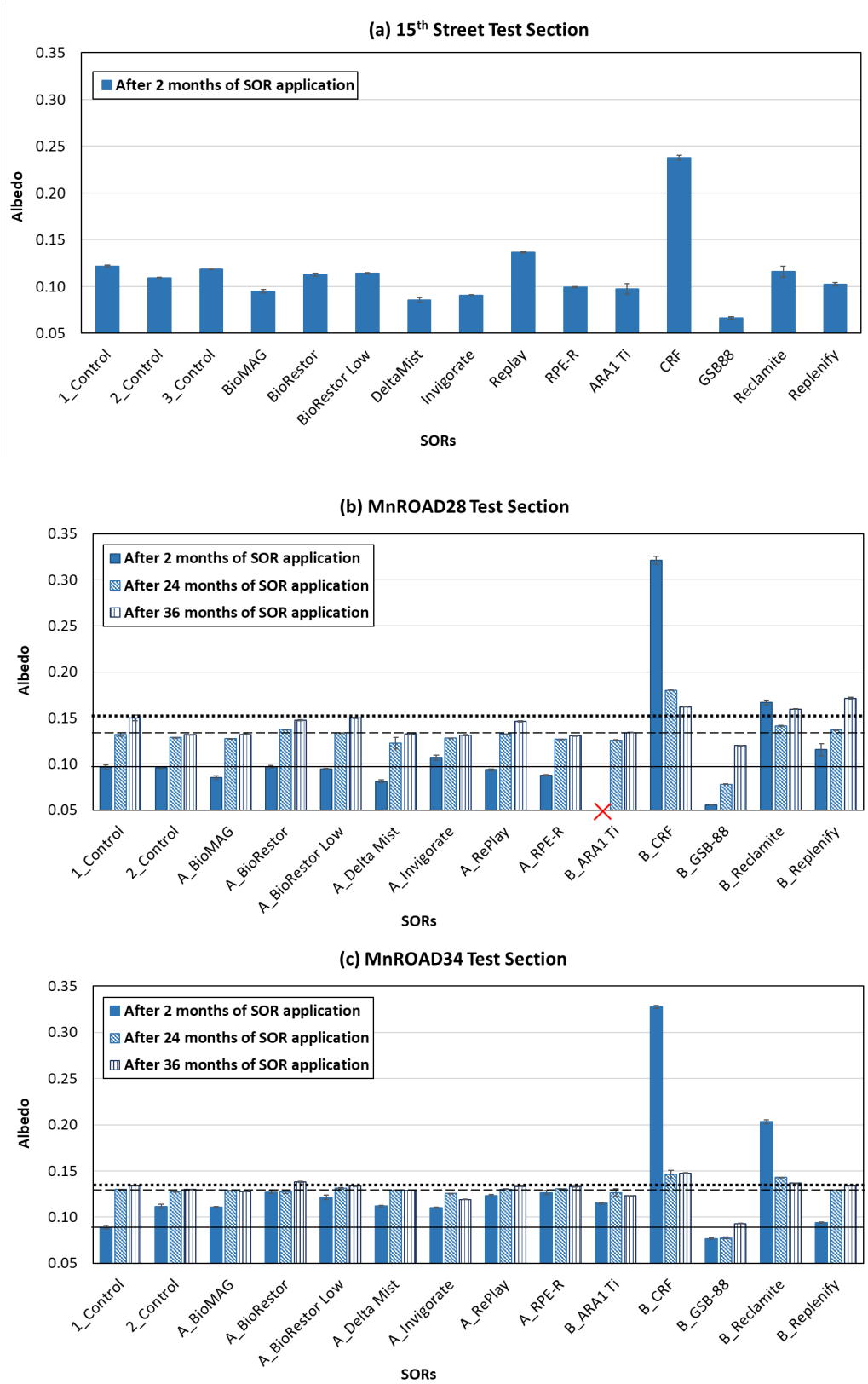

Figure 4.6 Albedo results of (a) 15th Street, (b) MnROAD28 test section, and (c) MnROAD34 test section

The solid, dashed, and dotted lines in the figures represent the control albedo after 2 months, after 24 months, and after 36 months respectively; values above the line indicate higher albedo than the control, while values below the line indicate lower albedo. All albedo testing was conducted under direct sunlight (no shade condition).

For 15th Street, MnROAD28 and MnROAD34 test cells, all Group A SORs exhibited minimal to no change in comparison to the control sections. In contrast, the albedo values of a few Group B SORs were higher than those of the control sections, due to the presence of bright fine sand/gravel. These test sections with fine sand/gravel had a higher effective albedo compared to the control sections, as they reflected a greater amount of light than the black asphalt surface. However, after 2 months of SOR application, CRF exhibited the highest albedo in all of the test sections. This can be attributed to its relatively light color and the heavy application of light-colored sand, which was designed to be worked into the pavement surface through traffic. Despite the anticipation that Group B products, with applied fine sands/gravel, would yield higher albedo values, GSB88 had the lowest albedo among all the SORs, due to the inherently dark appearance of GSB-88, which provided a deep black surface finish, contributing to its aesthetic appeal. Additionally, this might be possible as during the application of this SOR, coal slag (Gilsonite sand) was applied in parallel. But in the case of CRF, a heavy sand layer was applied, which was intended to be worked into the pavement surface by traffic. The sand was light in color.

4.4 Macrotexture

4.4.1 Test method

The macrotexture of the control and SOR-treated test sections were measured using the sand patch tests. The sand patch test was conducted following the ASTM E965 (ASTM, 2019a), in which a known volume of fine sand or glass beads was spread on a pavement surface in a circular shape (shown in Figure 4.7). Then, the average diameter of the circular spread was measured to calculate the mean texture depth (MTD) using **Equation 11**:

$$MTD = \frac{4\,V}{\pi D^2} \tag{11}$$

where:
MTD = mean texture depth, mm;
V = volume of the sand spread, mm^3;
D = average diameter of the area covered by the sand, mm^2.

The sand patch tests were performed on four locations (two on the wheel path of the inner lane and the other two in the middle of the outer lane) in each test cell to evaluate the effect of SOR application on the macrotexture of the pavement surface. It is noted that the inner lanes of the MnROAD28 and MnROAD34 test sections were subjected to MnROAD truck traffic.

Figure 4.7 Photograph of sand patch testing in the field

4.4.2 Test results

4.4.2.1 15th Street test section

The MTD results for the 15th Street test section are shown in Figure 4.8, with measurements taken before and one month after the application of SORs at both the wheel path and mid-lane locations. Since all cells were untreated before the application, their MTD values were expected to be similar. However, as shown in Figure 4.8a and Figure 4.8b, the values varied between 0.3 and 0.5 mm, reflecting testing or spatial variability. After the SOR application, even the control sections showed a reduction in MTD, as highlighted by the red circle. Taking all these variations into account, the overall patterns between the wheel path and mid-lane sections can be considered consistent. Most SOR-treated cells showed no significant change in MTD after one month, remaining within the observed variability range. Notable exceptions were the CRF and GSB-88 treated cells, which showed a significant increase in MTD, likely due to the application of fine sand/gravel during SOR treatment. This indicates that such materials might temporarily increase the pavement surface texture.

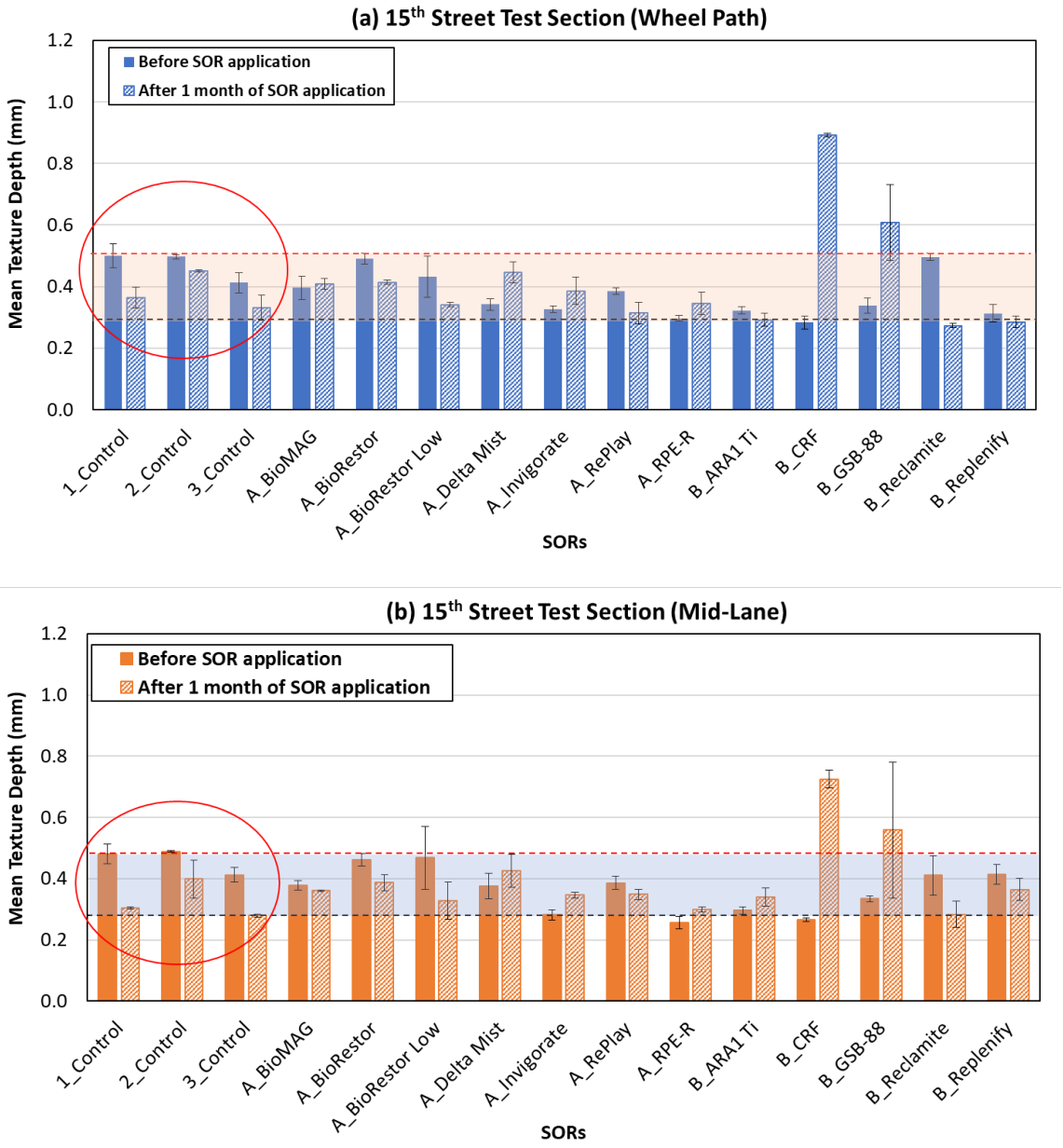

Figure 4.8 Sand patch test result comparison before, after 1 month of SOR application for 15th Street test section: (a) in the Wheel path and (b) in the Mid-lane

4.4.2.2 MnROAD28 test section

Figure 4.9 shows the MTD results for the MnROAD28 section before, after 1 month, 12 months, and 24 months of SOR application. Before applying SORs, all cells act as control sections, indicating that the MTD values across these sections should be relatively consistent. However, Figure 4.9a and Figure 4.9b reveal a variation in MTD values, which range between approximately 0.3 and 0.5 mm (shown by the shaded area between the dashed lines), illustrating the spatial variability of the MTD from one location to another. Therefore, the MTDs within the 0.3 to 0.5 mm range could be considered within testing or spatial variability. There was no big difference between the values measured in the wheel path and

those in the middle of the lane, although the variability was less pronounced in the mid-lane compared to the wheel path.

Figure 4.9 also shows that in most cells treated with SORs, the MTD values did not significantly change at 1 month or 12 months after the SOR application considering the overall variability. The notable exceptions were the cells treated with CRF and GSB-88, where a significant increase in MTD was observed. This increase might be attributed to the fine sand or gravel spread over the surface in those specific cells. After 24 months of SOR application, the MTD values were consistent with those observed at 12 months, accounting for all variability.

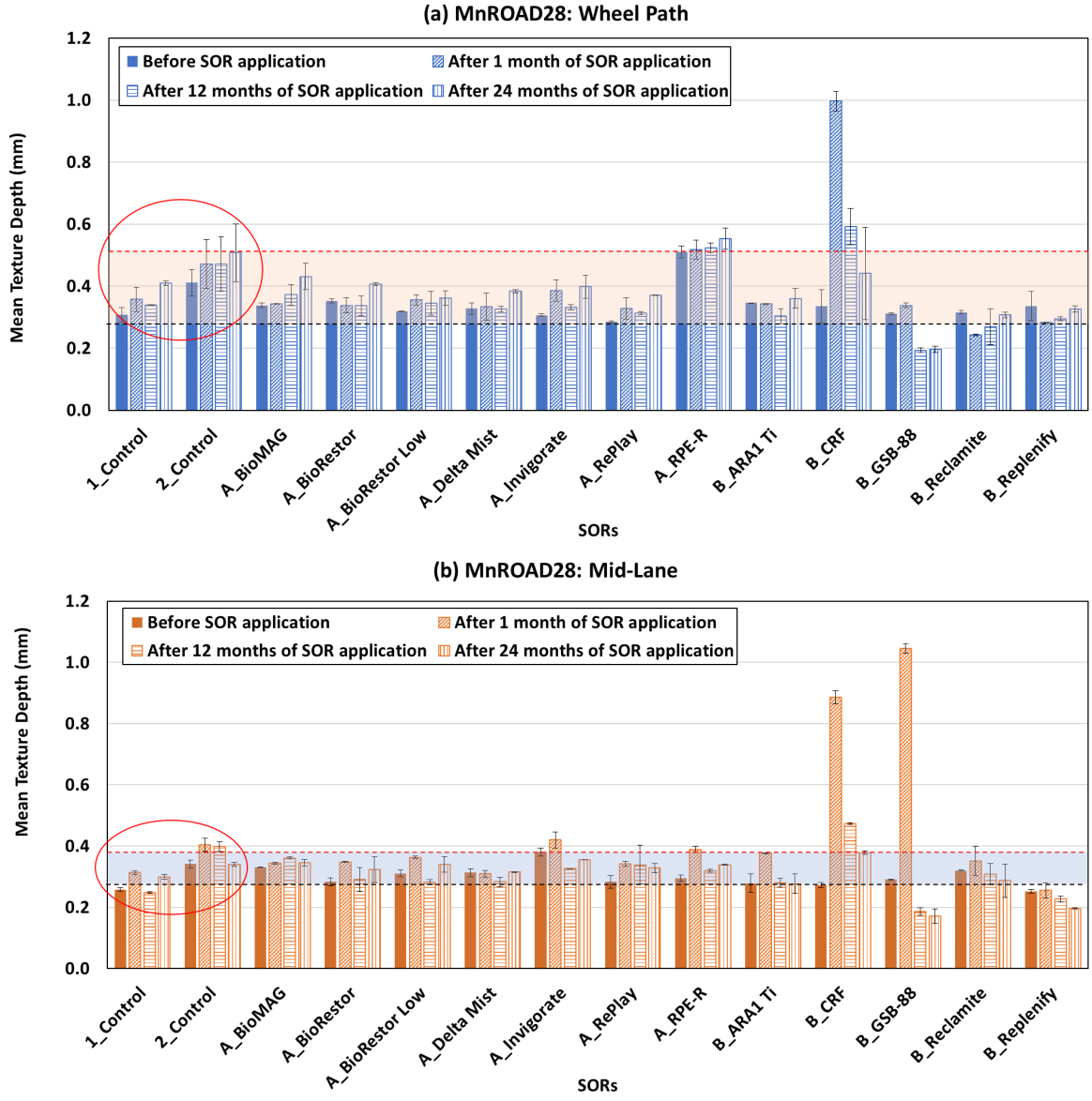

Figure 4.9 Sand patch test result comparison before, after 1 month, after 12 months, and after 24 months of SOR application for MnROAD28 test section: (a) in the Wheel path and (b) in the Mid-lane

4.4.2.3 MnROAD34 test section

Figure 4.10 shows the MTD results for the MnROAD34 section before, after 1 month, 12 months, and 24 months of SOR application. The spatial variability ranged from 0.3 to 0.4 mm for this section (shown by the shaded area between the dashed lines). Therefore, compared to the MnROAD28 section, the MnROAD34 section showed slightly less variation in MTD values. Figure 4.10 illustrates that one month after applying the SORs, considering the spatial variability, the MTD values in the SOR-treated cells were consistent with those of the untreated control section.

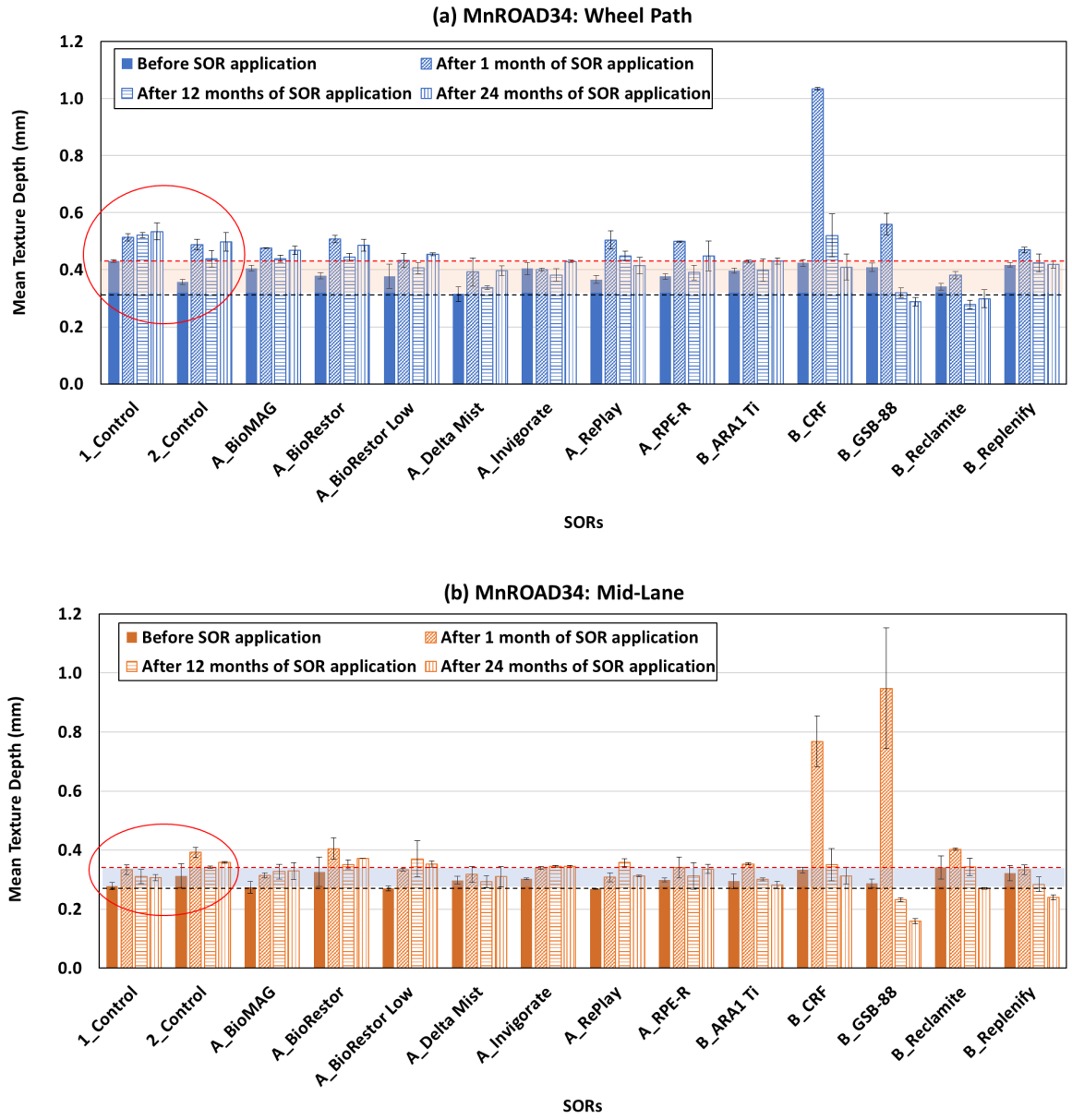

Figure 4.10 Sand patch test result comparison before, after 1 month, after 12 months, and after 24 months of SOR application for MnROAD34 test section: (a) in the Wheel path and (b) in the Mid-lane

However, in the case of CRF and GSB-88 (again), a significant rise in MTD values because of the addition of sand or fine gravel was observed, similar to the MnROAD28 cells. Afterward, the MTD decreased after 12 months and remained consistent 24 months after the SOR application (similar to the behavior observed in the MnROAD28 section). Considering all the variability, the Group A SORs had a minimal impact on the surface texture. However, the hypothesis behind the conditions observed in Figure 4.9 and Figure 4.10 can be illustrated by Figure 4.11 for Group B SORs, particularly with CRF and GSB88.

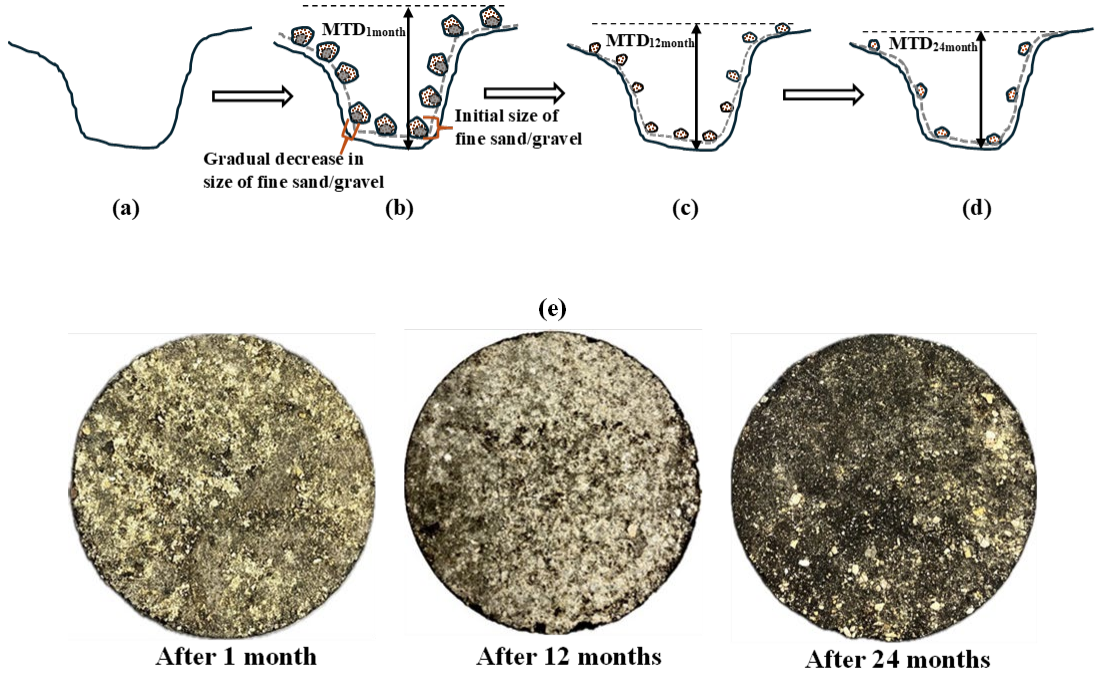

Figure 4.11 Micro-level hypothesis on surface texture change for Group B SORs: (a) before SOR application, (b) after 1 month of SOR application, (c) after 12 months of SOR application, (d) after 24 months of SOR application, (e) Surface profile of field cores treated with CRF

In the case of Group B SORs, fine sand/gravel was applied along with a higher SOR application rate (Figure 4.11b) compared to the other SORs. After 12 months (Figure 4.11c), the SORs might have filled out the voids and the fine sand/gravel swept off by the MnROAD trucks and/or snowplows, resulting in a noticeable reduction in MTD values. This trend continued over the next 24 months, with MTD either decreasing further or remaining relatively stable as a lot of fine sand/gravel was worn away (Figure 4.11d). The changes in the surface profile over time for Group B SORs can be observed in Figure 4.11e, using images captured from field-extracted cores with CRF. The images demonstrate a gradual reduction in the fine sand/gravel particles on the surface, as well as changes in the overall layout of the SOR over time. This might explain why MTD values were highest after 1 month, while they gradually decreased after 12 months and further after 24 months. However, based on the discussion from the sand patch tests, most of the SORs did not affect the MTD adversely.

4.5 Surface friction

4.5.1 Test method

We measured the pavement surface friction values using a Dynamic Friction Tester (DFT), which consists of three rubber sliders that rotate at a set speed with the help of a motor (shown in Figure 4.12). The tests were carried out following the standard ASTM E1911 procedure (ASTM, 2019b). The friction coefficient of the pavement surface was measured at three different speeds: 20, 40, and 60 kph (12, 25, and 37 mph) at each of the three test sections before and one month after the SOR application, to investigate potential decrease in surface friction due to the SOR application. The friction coefficient was also measured after 12 months and 24 months to evaluate the extent to which they may restore the friction of the pavement to its original state before the application of the SOR. The measured DFT results of the three test sections at a test speed of 40 kph (25 mph) are shown in Figure 4.13 to Figure 4.15. The DFT measurements in other test speeds are shown in **Appendix D**. Friction tests were conducted at four specific locations: two on the wheel path of the inner lane and two in the middle of the outer lane. It is noted that the inner lanes of the MnROAD28 and MnROAD34 test sections were subjected to MnROAD truck traffic.

Figure 4.12 Dynamic Friction Testing (DFT) Machine used in the field measure

In the testing, the skid trailer was operated in the traffic direction, with the steepest downhill slope observed in the control cells and the Reclamite section positioned at the hill's crest. The SOR ARA1 Ti section had a moderate downward slope, though less pronounced than the control cells, whereas the SOR BioRestor section contained the greatest uphill slope. Other sections, including Delta Mist and BioRestor low, were relatively flat. Despite these variations, the Dynamic Friction Tester (DFT) measured friction within a localized circular path and applied force perpendicular to the pavement surface, making it unaffected by orientation or vehicle travel direction.

4.5.2 Test results

4.5.2.1 15th Street test section

As shown in Figure 4.13, prior to the application of SORs, the 15th Street cells exhibited some spatial variability in friction coefficient measurements. It is noted that all cells at that stage functioned as

control sections. Also, variability within the control cells (1, 2, and 3) was observed before, 1 month after, and 12 months after the SOR application, even though no SOR was applied to these cells, and some of this variability exceeded the previously mentioned variability (shown by the shaded area between the dashed lines). After 1 month of SOR application shown in Figure 4.13, a decrease in friction values was observed through all cells at varying levels.

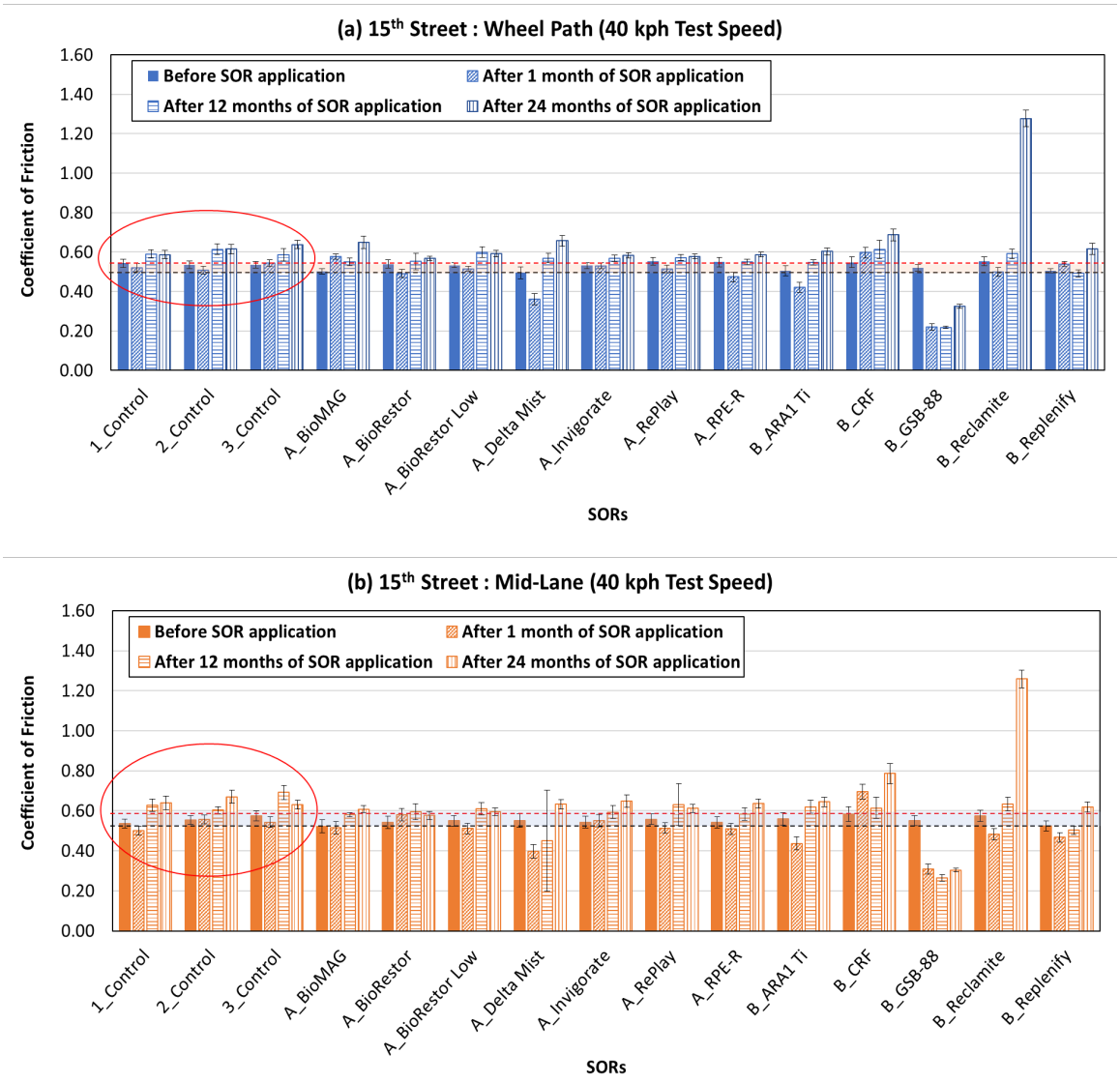

Figure 4.13 DFT result comparison before, after 1 month, after 12 months, and after 24 months of SOR application of the 15th Street test section at a test speed of 40 kph: (a) at the Wheel path and (b) at the Mid-lane

However, 12 months after the SOR application, the friction values for SOR-treated cells were restored to their original levels before the application, except for GSB-88. Here, even with the variability, the friction coefficient in GSB-88 cells remained lower, indicating a sustained reduction in friction due to the loss of fine sand/gravel. After 24 months of SOR application, friction values either increased or remained similar in most cells. GSB-88, which was impacted by an unexpected rain event during application also showed a

gradual increase, indicating a slow restoration of friction. However, Reclamite exhibited a significant increase in both the wheel path and mid-lane.

4.5.2.2 MnROAD28 test section

In MnROAD28 cells, a similar pattern of spatial variability (shown by the shaded area between the dashed lines) before the application of SORs was observed along with the comparable variability within control cells after SOR application. Similar to the 15th test cells, the friction coefficient in most of the MnROAD28 cells decreased 1 month after the SOR application (Figure 4.14).

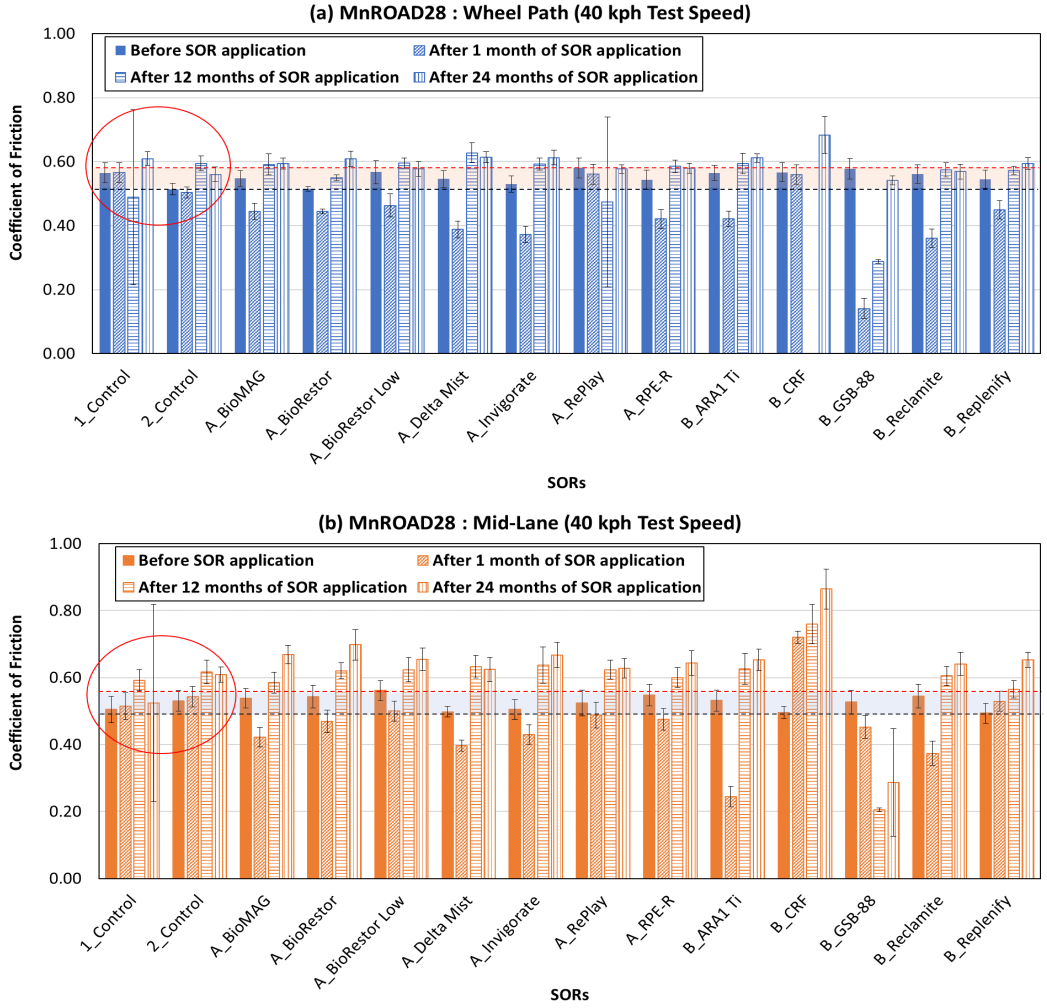

Figure 4.14 DFT result comparison before, after 1 month, after 12 months, and after 24 months of SOR application of MnROAD28 test section at a test speed of 40 kph: (a) in the Wheel path and (b) in the Mid-lane

After twelve months of application, the friction values returned to the same levels as before the SOR application, similar to the results seen in the 15th test cells. The exception was once again GSB-88, where the friction values remained lower than the pre-SOR application scenario. Similar to the 15th test cells, friction values either increased or remained consistent after 24 months of SOR application. This includes GSB-88 also, indicating a gradual restoration of friction values for this SOR.

4.5.2.3 MnROAD34 test section

For the MnROAD34 section (Figure 4.15), a consistent trend of variability (shown by the shaded area between the dashed lines) before SOR application within cells, and spatial variability within control cells after SOR application was observed.

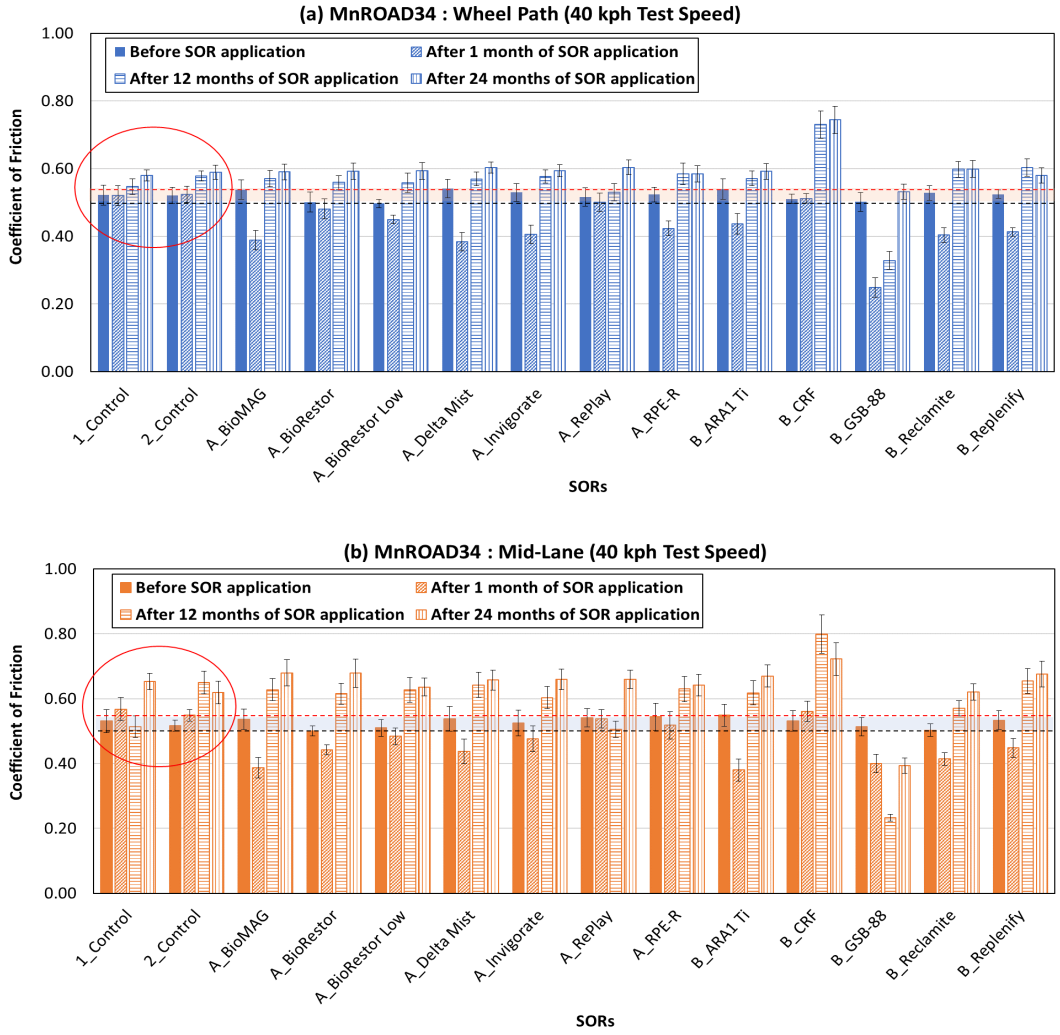

Figure 4.15 DFT result comparison before, after 1 month, after 12 months, and after 24 months of SOR application of MnROAD34 test section at a test speed of 40 kph: (a) in the Wheel path and (b) in the Mid-lane

Following the trend observed in the 15th Street and MnROAD28 sections, the friction coefficient in MnROAD34 decreased 1 month after the SOR application. After 12 months, it increased to levels similar to those before the SOR application, except GSB-88. However, the friction values of GSB-88 also increased after 24 months, along with the other SORs. The DFT measurements were also taken at test speeds of 20 kph (12.5 mph) and 60 kph (37 mph), as shown in **Appendix D**. These results were also consistent with the observations from 40 kph. Considering all variabilities, only minor variations in the DFT results among most Group A SORs were observed.

It was expected that Group B SORs would provide higher friction coefficients because of the application of additional granular material. However, if the applied granular particles were to be displaced due to the abrasion action of MnROAD trucks and/or snowplows, a reduction in friction is possible. It can be concluded that the application of sand or fine gravel was not always effective in keeping the friction high in all Group B SORs. Although Group B SORs were categorized as a general classification, the specific characteristics of each product, such as the nature and rate of the aggregate application, might have influenced the friction outcomes. For example, CRF and GSB-88 were applied with a higher amount of fine sand and had higher residue compared to others.

The potential reasons for reduced surface friction like inconsistent distribution of fine sand or gravel and their possible displacement during friction testing are illustrated in Figure 4.16. This figure presents a micro-level hypothesis showing how surface texture and friction might have changed over time following the application of SORs. Figure 4.16a shows the pavement surface before treatment, representing its original condition. Figure 4.16b shows the pavement surface shortly after the application of the SOR, when a decrease in surface friction might have occurred by the SORs. In the cases of Group B SORs, additional factors that might have influenced the results include the uneven application of sand or gravel and the possible displacement of these materials during the Dynamic Friction Test (DFT). Due to traffic and environmental exposure, the fine sand or gravel applied with the SORs might have either become embedded into the pavement surface or gradually worn off. The presence of residual SOR material on the surface could also have contributed to temporary reductions in friction. Specifically, GSB-88 was applied with blackjack coal slag, which might have contributed to the lowest friction observed one month after the SOR application compared to the other SORs.

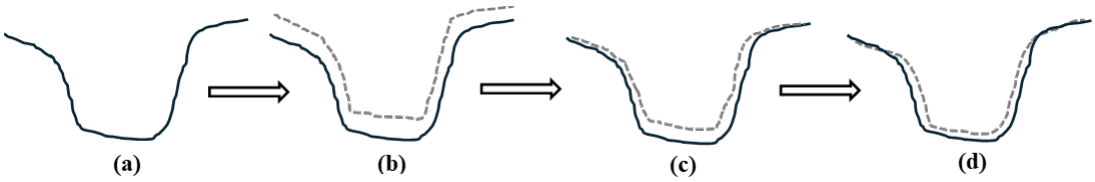

Figure 4.16 Micro-level hypothesis for surface friction: (a) before SOR application, (b) after 1 month of SOR application, (c) after 12 months of SOR application, (d) after 24 months of SOR application

Finally, Figure 4.16c and Figure 4.16d show the surface condition after 12 and 24 months, respectively, suggesting that the surface might have gradually returned to a state similar to its original condition over time. After 24 months the smoother surface texture, likely caused by the coal slag, diminished possibly by the SORs penetrating the voids, or surface abrasion taking place, resulting in a slight increase in friction. As previously illustrated in Figure 4.11, a gradual reduction in fine gravels over 24 months was visually observed. Also, results from the DFT tests indicate that, in the case of some SORs, friction values decreased after one month of application but gradually recovered over the 24 months. The rate of recovery varied depending on the type of SOR applied. It should be noted that, MnDOT engineers confirmed that the road surface always remained safe, and there were no safety concerns.

4.6 Permeability

4.6.1 Test setup

The application of SORs might improve pavement durability by reducing surface permeability and water percolation capacity. Field permeability values were determined using a National Center for Asphalt Technology (NCAT) permeameter (Mallick et al, 2003) by the falling head permeability method. The permeability of the pavement surface was measured to investigate the possible reduction in permeability on the surface layer due to SOR application. Tests were carried out before, as well as one month, 12 months, 24 months and 36 months after the application of the SORs.

4.6.2 Test results

4.6.2.1 MnROAD28 test section

Figure 4.17 shows the permeability test results for the MnROAD28 test sections. Although uniform permeability values are expected before SOR application as the conditions were theoretically the same, a significant variability is observed. This variability extends to a 50% difference between the highest and lowest permeability values when measured on a logarithmic scale (shown by the shaded area between the dashed lines).

Permeability in two control cells of MnROAD28 sections decreased from 1.7×10^{-4} cm/sec to 4×10^{-5} cm/sec and 7×10^{-5} cm/sec (% decrease of 10% and 17%) after one month of SOR application, as shown in Figure 4.17 (encircled). Figure 4.17 also shows that after 12 months of SOR application, the permeability values in the two control cells dropped from 1.7×10^{-4} cm/sec to 2×10^{-5} cm/sec and 3×10^{-6} cm/sec, respectively, representing a 25% and 46% decrease. Ideally, the control cells' permeability is expected to be the same over time as there was minimal traffic action. This decrement in permeability values of control cells might be attributed to either dust settling over time or testing variation within the test cell. However, after 24 months and 36 months, the permeability of most cells including the control cells increased. In comparison to pre-SOR application, permeability in the two control cells increased to 5.3×10^{-4} and 1.5×10^{-3} cm/sec (increases of 13% and 26%). This rise, compared to 12 months post-SOR can be attributed to environmental factors, such as rain washing away the surface dust, leading to greater water percolation. Additionally, potential variability in field testing conditions or equipment sensitivity over time might have contributed to the observed changes.

Considering all variability, the permeability values in the MnROAD28 cells remained unaffected after one month and 12 months of the SOR application (with the exceptions of Biorestor Low, GSB-88, and Reclamite). Given the variability observed, the reduction in permeability for these exceptions can be considered significant. Also, for CRF and GSB-88, there was variability related to the location of the testing stations before and after the 12-month period, which might have influenced the results. However, after 24 months, permeability increased in all SOR-applied cells, including Biorestor Low, GSB-88, and Reclamite. The permeability values were higher than those measured before the SOR application, but considering all variabilities, the increment is not significant. It is also possible that the

SORs, which were somewhat effective initially, no longer helped reduce permeability after 12 months. After 36 months of SOR application, most test cells had permeability values similar to those recorded after 24 months. The permeability values in GSB-88 and Reclamite, which initially showed significant reductions, increased further. Additionally, in some test cells, permeability values exceeded the pre-application values after 36 months of application, supporting the possibility that SORs provided only temporary permeability reduction. It is also possible that variability in field testing conditions or limitations in the testing methodology contributed to these results.

4.6.2.2 MnROAD34 test section

Figure 4.18 shows that the permeability values in the two control cells of MnROAD34 sections remained relatively consistent before and after the SOR application. In the case of the MnROAD34 section, significant testing variability (43%) in the permeability results was observed also within all the test cells (shown in the shaded area between the dashed lines). After one month of the SOR application in the MnROAD34 section, the difference in permeability between the two control sections was less than MnROAD28 (0.8 and 1.2%), showing no significant additional variability compared to the MnROAD28 section (encircled in Figure 4.18).

A reduction in permeability was observed in the case of CRF, although this observation was based on a single data point, which might affect the reliability of this specific finding. After 12 months of the SOR application, the control cells in the MnROAD34 section experienced a slight increase in testing variability compared to one month after the SOR application (2.4 and 20.4%). A significant reduction in permeability was observed for SORs such as BioMAG, BioRestor, CRF, and GSB-88. However, the findings for BioMAG and BioRestor were based on just a single data point, which might limit the conclusiveness of these results. Also, similar to what was observed in the MnROAD28 section, there was variability in the testing station locations for CRF and GSB-88. Despite these factors, the available data suggests a decrease in permeability for these specific SORs.

After 24 months, permeability increased in both the control and SOR-applied cells in the case of MnROAD34, similar to the MnROAD28 section. Considering all variability, these values are close to the permeabilities observed before the SOR application, except Replay, ARA1 Ti, GSB-88, and Replenify. These SORs showed lower permeability than before the SOR application, although these values are still higher than permeabilities after 12 months. This suggests that most SORs might have lost effectiveness after 12 months, except for these SORs, which are also gradually becoming less effective in terms of reduction in permeability.

After 36 months of SOR application, the permeability values in most test cells of the MnROAD34 section decreased, likely due to debris accumulation. Although some SORs, such as BioRestor Low, Replay, ARA1 Ti, GSB-88, and Replenify, showed lower permeability than before application, the variability in results and reliance on a single data point make it difficult to draw definitive conclusions.

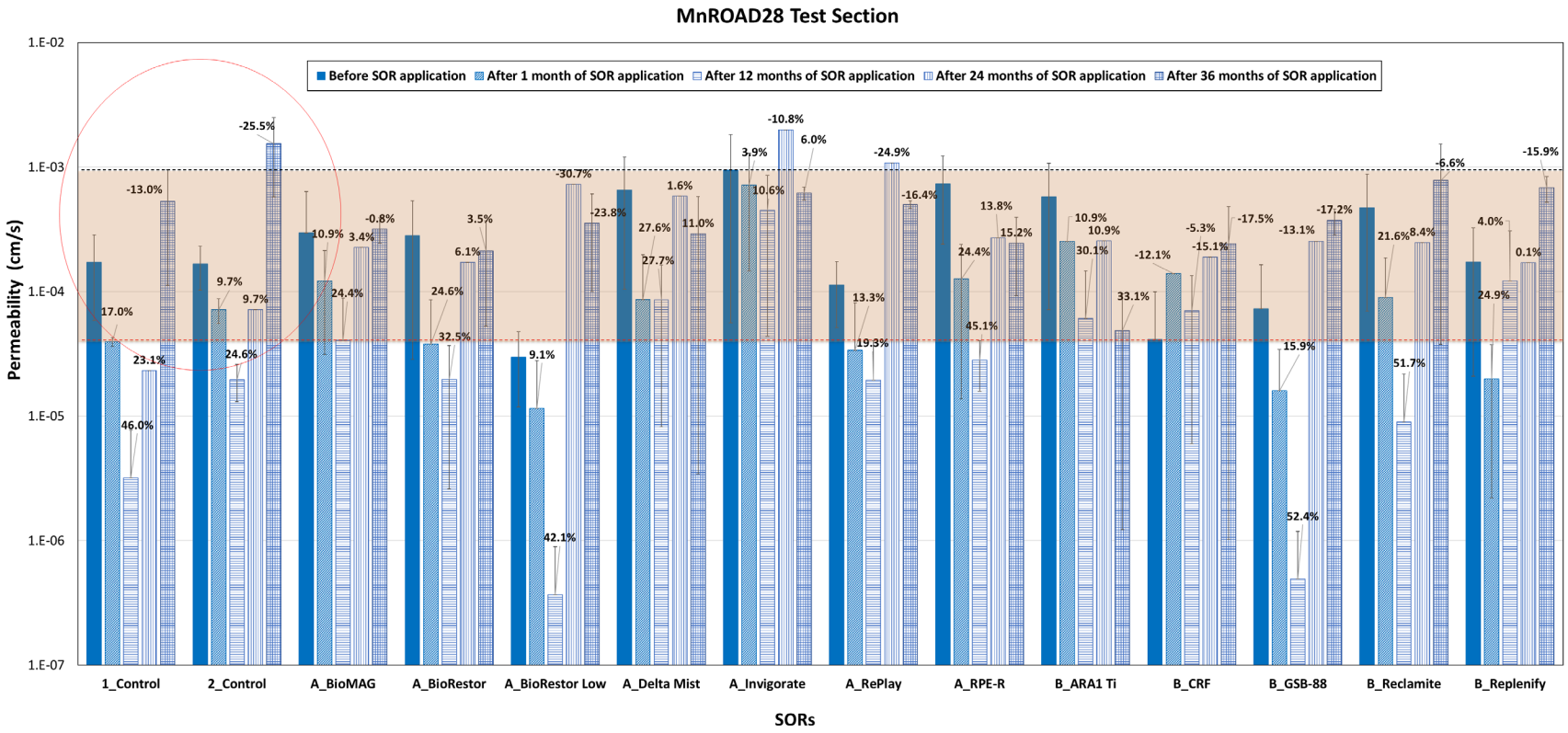

Figure 4.17 Permeability results of control and SOR applied sections for MnROAD28 test cells

Note: % decrease in permeability values is shown compared to the permeability values before SOR application

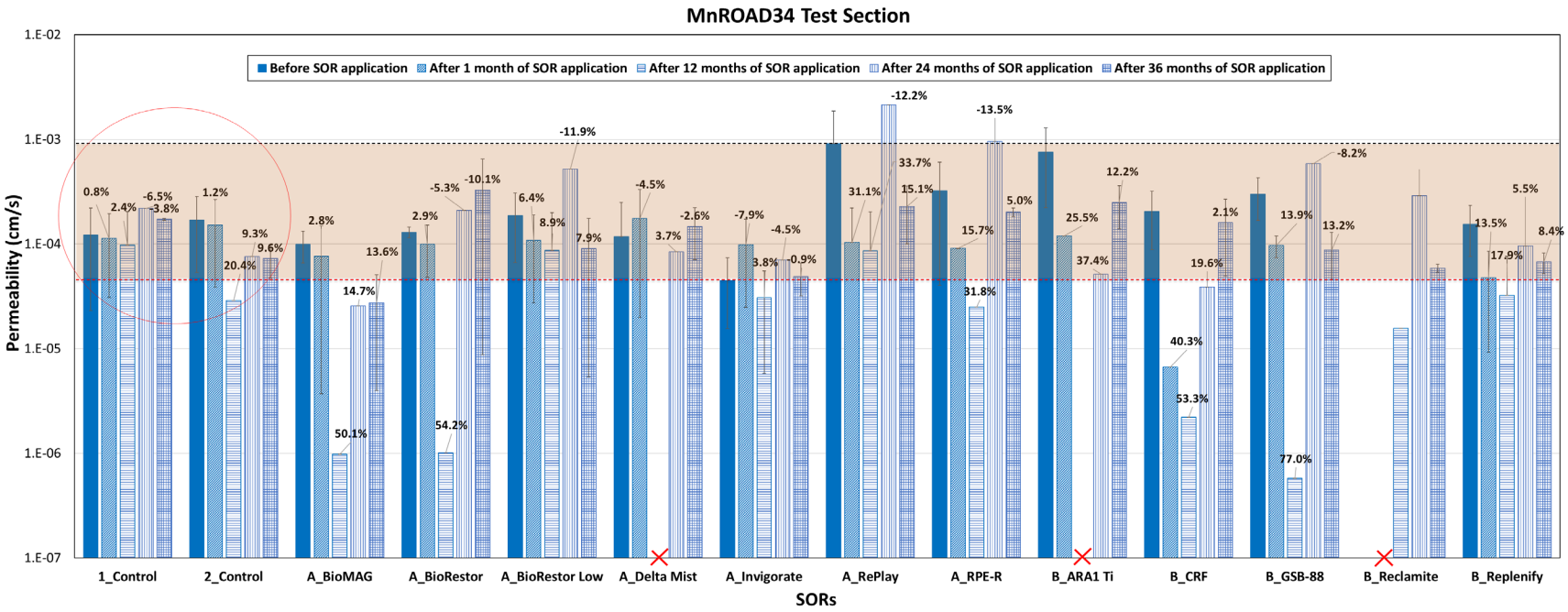

Figure 4.18 Permeability results of control and SOR applied sections for MnROAD34 test cells

Note: % decrease in permeability values is shown compared to the before rejuvenation permeability values

Chapter 5: Conclusions

This research provided a comprehensive evaluation of the short-term and long-term performances of Spray-on Rejuvenators (SORs) through both laboratory and field investigations; two at MnROAD and one in St. Michael, MN. A total of 12 different SORs were successfully applied, and no safety concerns were observed for the traveling public during or after the product applications. The findings offer insights into the effects of SORs on asphalt pavement aging, structural properties, and surface characteristics, helping to assess their effectiveness in extending pavement life. From the overall study, the following conclusions can be drawn:

- Laboratory study portion of this work revealed the following conclusions and observations:
    - A modified BBR testing methodology was developed to measure the creep stiffness of small beams cut from the surface of field cores extracted from test cells at the MnROAD facility. Testing was conducted at three temperatures (20°C, 4°C, and -10°C) across different aging conditions, including 0-year, 1-year, 2-year, 3-year, and laboratory-aged specimens. The results showed that the most significant effects of SORs were observed at higher temperatures (20°C), where SORs effectively softened the asphalt binder. In contrast, at lower temperatures (-10°C and 4°C), the differences between control and treated sections were less pronounced due to the stiffening of the binder.
        - In the MnROAD28 section, about half of the SORs did not show an immediate reduction in creep stiffness after application, suggesting they might require time to penetrate the asphalt binder to exert their softening effect. However, all SORs showed significantly lower creep stiffness compared to the control cells after one year, with some continuing to show effectiveness even after two years. However, by the third year, only a few products, such as Reclamite, ARA1 Ti, CRF, and RPE-R, maintained their effectiveness. This indicates that reapplication is necessary at different times depending on the product.
        - The visual observations revealed the presence of microcracks in some of the MnROAD34 test cells, likely due to construction-related issues. These microcracks on the pavement surface might have influenced SOR performance. Initially, some SORs filled the cracks, creating a ‘bridging effect’ and leading to increased creep stiffness compared to the respective control section, but over time, the softening effect of the SORs became more dominant. After one year of field aging, most SOR-treated cells showed lower creep stiffness compared to the control, indicating improved binder-SOR interactions. By the third year, SORs such as ARA1Ti, CRF, and Reclamite showed effectiveness, while others exhibited reduced performance. The creep stiffness in MnROAD34 test cells is thus influenced by both the softening and bridging effects, with the latter diminishing over time.

- It is necessary to ensure the SORs are not excessively softening the binder to cause plastic deformations near the surface. To evaluate the potential for plastic deformation, Hamburg Wheel Tracking (HWT) tests were conducted at 45°C with 20,000 passes. The results showed that the application of SORs did not significantly affect the rutting resistance of the asphalt mixture, ensuring that they do not lead to excessive softening.

- The top 20 mm of field cores were tested for permeability using a flexible wall permeameter. The results showed that most SORs had little impact on permeability. Only Reclamite and Replenify led to a consistent reduction in permeability across both test sections. In general, it is not easy to reproduce field conditions in a controlled environment, hence it is probable that laboratory results might not be similar to the field scenario.

- Skid resistance measurements indicated no significant reductions for most SORs, particularly Group A products. The addition of sand or fine gravel improved friction in some cases, but inconsistent application led to variability in results. While the application of all SORs was carried out consistently by manufacturer-selected contractors under the observation of the research team, it is noted that the surface condition of the extracted cores, particularly from the non-trafficked outer lane might have influenced certain test results. For example, products like CRF, which include sand applications, might require traffic to embed the material effectively, which did not occur in the outer lane sections used for core sampling.

- A ranking of SORs was proposed based on their overall performance in laboratory tests compared to untreated control sections. Reclamite, RPE-R, CRF, and ARA1Ti consistently performed well in both MnROAD28 and MnROAD34, demonstrating compatibility with different binder types across different temperature conditions.

o Field portion of the study revealed that:

- SOR applications reduced pavement marking reflectivity, with some products causing a decline of more than 30%. Therefore, post-application reflectivity should be checked against local agency requirements.

- Albedo measurements indicated that Group A SORs showed minimal change in albedo compared to the control sections. Some Group B SORs displayed higher albedo values, possibly due to the presence of bright fine sand or gravel except GSB-88 due to its dark color. Over time, albedo increased in most of the test sections, possibly due to the aging of the asphalt surface. This suggests that as observed in some SORs, the higher albedo might help reduce UV damage to the pavement surface by reflecting more sunlight.

- The mean texture depth (MTD) of the control sections showed variation, possibly due to the testing or spatial variability. Most of the SOR-treated cells exhibited no significant changes in their MTD values either after one month, 12 months, or 24 months of SOR application. In contrast, CRF and GSB-88 treated cells showed a significant increase in the MTD after one month of SOR application because of the presence of fine sand/gravel applied over the

surface. However, the MTD in those SORs (CRF and GSB-88) decreased significantly after 12 months and 24 months, indicating that the SORs might have filled the voids, or the fine sand/gravel have been swept off. Therefore, it is imperative to implement measures that ensure the preservation of fine grains to maintain the integrity of the application of fine sand/gravel.

- The Dynamic Friction Test (DFT) results were mostly consistent in most of the Group A SORs. Friction measurements indicated minor reductions in Group B SOR-treated sections immediately after application, but most products regained or exceeded their initial friction values after one year, indicating recovery or improvement of friction properties over time. However, after 24 months the friction values were likely to be restored. This implies that the use of sand or fine gravel in Group B SORs might not have been fully effective in maintaining high friction values. This variation could be possible due to uneven application of sand or gravel, or potential displacement of these materials during the friction test itself.

- Permeability test results showed that there were slight changes in most SOR-treated cells both one month and twelve months after treatment. These minor variations could be attributed to dust settling or the inherent spatial variability of the test sites. A decrease in permeability was observed in some SORs over both time intervals, suggesting that certain SOR applications can reduce the pavement's ability to allow water to pass through. However, after 24 months of SOR application, permeability increased in most cases, indicating a decline in the effectiveness of SORs in reducing permeability. After 36 months, most test cells showed similar permeability to 24 months, with some SORs, like GSB-88 and Reclamite, increasing further. In some cases, permeability values exceeded the pre-application levels, supporting the possibility that SORs only temporarily reduced permeability. Environmental factors, such as rain removing surface dust or debris accumulation, might have contributed to the loss of SOR effectiveness over time, causing permeability to return to or exceed pre-application levels. Additionally, the characteristics of the dense-graded HMA used in this study, along with the sensitivity of the testing apparatus and methodology, might also have influenced the permeability measurements.

Overall, the findings suggest that SORs effectively slow the aging of asphalt pavements, although their effectiveness varies by product and diminishes over time. While SORs provide benefits in softening aged binder and improving pavement durability, reapplication might be necessary after two to three years to maintain their effectiveness. The results indicate that SORs can be a valuable pavement preservation tool, but factors such as permeability, friction, and marking reflectivity should be carefully monitored to ensure long-term performance and roadway safety. Considering the slight reductions in surface friction and reflectivity observed in some cases, it is important to carefully assess the condition of the pavement before SOR application. SORs should be avoided on surfaces that already exhibit low or marginal friction and texture, as further reductions could potentially lead to safety concerns.

5.1 Future research

This study focused on relatively new pavement surfaces, and the effects of Spray-on Rejuvenators (SORs) might vary depending on the aging level of the pavement. Therefore, we recommend conducting similar studies on pavements at different stages of aging. Further research should aim to enhance the understanding of the chemical and physical interactions between SORs and asphalt binders to improve their long-term compatibility and durability.

Future research should also examine the impact of multiple reapplications and their cumulative effects on pavement longevity. Additional studies should analyze how varying traffic loads and extreme environmental conditions influence the effectiveness of SORs over time. A comprehensive cost-benefit analysis might help to determine the most cost-effective SOR application strategies for different pavement conditions.

References

AASHTO T324. Standard Method of Test for Hamburg Wheel Track Testing of Compacted Hot Mix Asphalt. American Association of State Highway Transportation Officials, Washington, D.C., 2019.

AASHTO T324. Standard Method of Test for Hamburg Wheel Track Testing of Compacted Hot Mix Asphalt. American Association of State Highway Transportation Officials, Washington, D.C., 2019b.

AASHTO. AASHTO T313, Standard Method of Test for Determining the Flexural Creep Stiffness of Asphalt Binder Using the Bending Beam Rheometer (BBR). Washington, D.C., 2019a.

AASHTO. AASHTO TP 125-16, Determining the Flexural Creep Stiffness of Asphalt Mixtures Using the Bending Beam Rheometer (BBR). Washington, D.C., 2020.

ASTM International. ASTM D6372-15, Standard Practice for Design, Testing, and Construction of Microsurfacing. West Conshohocken, PA, 2015.

ASTM International. ASTM E303-22, Standard Test Method for Measuring Surface Frictional Properties Using the British Pendulum Tester. 2022.

ASTM International. D08 Committee. Test Method for Measuring Solar Reflectance of Horizontal and Low-Sloped Surfaces in the Field. West Conshohocken, PA, 2021.

ASTM International. D18 Committee, Test Methods for Measurement of Hydraulic Conductivity of Saturated Porous Materials Using a Flexible Wall Permeameter. Publication ASTM D5084, West Conshohocken, PA, 2016.

ASTM International. E12 Committee, Test Method for Measurement of Retroreflective Pavement Marking Materials with CEN-Prescribed Geometry Using a Portable Retroreflectometer. Publication ASTM E1710, West Conshohocken, PA, 2018.

ASTM International. E17 Committee, Publication ASTM E1911. Test Method for Measuring Surface Frictional Properties Using the Dynamic Friction Tester. West Conshohocken, PA, 2019b.

ASTM International. E17 Committee, Publication ASTM E965. Test Method for Measuring Pavement Macrotexture Depth Using a Volumetric Technique. West Conshohocken, PA, 2019a.

Bahia, H. U. Low Temperature Isothermal Physical Hardening of Asphalt Cement. The Pennsylvania State University, USA, 1991.

Bastola, A., A. K. Swamy, and M. I. Khan. Research on High RAP Mixtures with Rejuvenator: Field Implementation. Nebraska Department of Transportation.

Blanchette, A., S. T. Lee, and T. Wood. Spray on Rejuvenators Synthesis. National Road Research Alliance, Minnesota Department of Transportation, St. Paul, MN, 2020.

Boyer, R. E. Asphalt Rejuvenators "Fact, or Fable." Transportation Systems 2000 (TS2K) Workshop, 2000.

Boz, I., Y. S. Kumbargeri, and M. E. Kutay. Performance-Based Percent Embedment Limits for Chip Seals. Transportation Research Record: Journal of the Transportation Research Board, Vol. 2673, No. 1, 2019, pp. 182–192. https://doi.org/10.1177/0361198118821370.

Caro, S., A. Diaz, D. Rojas, and H. Nuñez. A Micromechanical Model to Evaluate the Impact of Air Void Content and Connectivity in the Oxidation of Asphalt Mixtures. Construction and Building Materials, Vol. 61, 2014, pp. 181–190. https://doi.org/10.1016/j.conbuildmat.2014.03.013.

Chen, S., S. Adhikari, and Z. You. Relationship of Coefficient of Permeability, Porosity, and Air Voids in Fine-Graded HMA. *Journal of Materials in Civil Engineering*, Vol. 31, No. 1, 2019, p. 04018359. https://doi.org/10.1061/(ASCE)MT.1943-5533.0002573.

Chiu, C. T., and M. G. Lee. Effectiveness of Seal Rejuvenators for Bituminous Pavement Surfaces. Journal of Testing and Evaluation, Vol. 34, No. 5, 2006, pp. 390–394. https://doi.org/10.1520/JTE100056.

Chiu, C.-T., and M.-G. Lee. Effectiveness of Seal Rejuvenators for Bituminous Pavement Surfaces. Journal of Testing and Evaluation, Vol. 34, No. 5, 2006, pp. 390–394. https://doi.org/10.1520/JTE100056.

Cooley, L., E. R. Brown, and S. Maghsoodloo. Developing Critical Field Permeability and Pavement Density Values for Coarse-Graded Superpave Pavements. Transportation Research Record: *Journal of the Transportation Research Board*, Vol. 1761, No. 1, 2001, pp. 41–49. https://doi.org/10.3141/1761-06.

Falchetto, A. C., M. O. Marasteanu, S. Balmurugan, and I. I. Negulescu. Investigation of Asphalt Mixture Strength at Low Temperatures with the Bending Beam Rheometer. Road Materials and Pavement Design, Vol. 15, No. sup1, 2014, pp. 28–44. https://doi.org/10.1080/14680629.2014.926618.

Gayle, and H. King. Spray Applied Polymer Surface Seals. 2008.

Gere, J. M., and S. P. Timoshenko. Mechanics of Materials. PWS Engineering, Boston, Massachusets, 1984.

Gogula, A. K., M. Hossain, and S. A. Romanoschi. A Study of Factors Affecting The Permeability of Superpave Mixes In Kansas. Publication Final Report (Report No. K-TRAN: KSU-00-2). The University of Kansas, 2004.

Guada, I., and J. T. Harvey. Permeability Testing on Dense-Graded Hot Mix Ashphalt (HMA) and Gap-Graded Rubberized Hot Mix Asphalt (RHMA-G) Surfaces. UCPRC, University of California Pavement Research Center (UCPRC), 2018.

Kebede, A. A. Asphalt Pavement Preservation Using Rejuvenating Fog Seals. Purdue University, 2016.

Lee, J., S. Li, Y. Kim, and J. Lee. Effectiveness of Asphalt Rejuvenator. Journal of Testing and Evaluation, Vol. 41, No. 3, 2013, pp. 433–440. https://doi.org/10.1520/JTE20120024.

Lin, J., J. Hong, C. Huang, J. Liu, and S. Wu. Effectiveness of Rejuvenator Seal Materials on Performance of Asphalt Pavement. Construction and Building Materials, Vol. 55, 2014, pp. 63–68. https://doi.org/10.1016/j.conbuildmat.2014.01.018.

Mallick, R. B., L. A. Cooley, M. R. Teto, R. L. Bradbury, and D. Peabody. An Evaluation of Factors Affecting Permeability of Superpave Designed Pavements. National Center for Asphalt Technology, Auburn University, Auburn, AL, 2003, p. 33.

Mamlouk, M., and R.T. Sarofim. "Modulus of asphalt mixtures-an unresolved dilemma." *Transportation Research Record* 1171 (1988): 193-198..

Marasteanu, M. O., R. Velasquez, A. C. Falchetto, and A. Zofka. Development of a Simple Test to Determine the Low Temperature Creep Compliance of Asphalt Mixtures. Transportation Research Board of the National Academics, Washington, D.C., 2009.

Marasteanu, M., A. Cannone Falchetto, R. Velasquez, and J.-L. Le. On the Representative Volume Element of Asphalt Concrete at Low Temperature. Mechanics of Time-Dependent Materials, Vol. 20, No. 3, 2016, pp. 343–366. https://doi.org/10.1007/s11043-016-9302-3.

Medina, J. A., and T. R. Clouser. Evaluation of RePlay Soy-Based Sealer for Asphalt Pavement. Pennsylvania Department of Transportation, 2009.

Mokhtari, A., H. David Lee, R. C. Williams, C. A. Guymon, J. P. Scholte, and S. Schram. A Novel Approach to Evaluate Fracture Surfaces of Aged and Rejuvenator-Restored Asphalt Using Cryo-SEM and Image Analysis Techniques. Construction and Building Materials, Vol. 133, 2017, pp. 301–313. https://doi.org/10.1016/j.conbuildmat.2016.12.075.

Moon, K. H., A. Cannone Falchetto, and J. W. Hu. Investigation of Asphalt Binder and Asphalt Mixture Low Temperature Creep Properties Using Semi Mechanical and Analogical Models. Construction and Building Materials, Vol. 53, 2014, pp. 568–583. https://doi.org/10.1016/j.conbuildmat.2013.12.022.

Pan, P., Y. Kuang, X. Hu, and X. Zhang. A Comprehensive Evaluation of Rejuvenator on Mechanical Properties, Durability, and Dynamic Characteristics of Artificially Aged Asphalt Mixture. Materials, Vol. 11, No. 9, 2018, p. 1554. https://doi.org/10.3390/ma11091554.

Quintus, H. L. V., and D. Raghunathan. Effectiveness of Asphalt Penetrating Sealers in Extending New Asphalt Pavement. Publication FHWA/OH-2017/3. Ohio Department of Transportation, 2017.

Romero, P. Using the Bending Beam Rheometer for Low Temperature Testing of Asphalt Mixtures. Utah Department of Transportation, Salt Lake City, Utah, 2016.

Rostler, F. S., and R. M. White. Rejuvenation of Asphalt Pavements. Publication AFWL-TR-70-83. Air Force Weapons Laboratory, 1970.

Ryan, J., S. Owusu-Ababio, J. Crovetti, and A. Cooley. Relating Permeability and Performance for HMA Pavements. *Wisconsin Highway Research*, 2007.

Shoenberger, J. E. Rejuvenators, Rejuvenator-Sealers, and Seal Coats for Airfield Pavements. Publication ERDC/GSL TR-03-1. US Army Corps of Engineers, 2003.

Sirin, O., D. K. Paul, and E. Kassem. State of the Art Study on Aging of Asphalt Mixtures and Use of Antioxidant Additives. Advances in Civil Engineering, Vol. 2018, 2018, pp. 1–18. https://doi.org/10.1155/2018/3428961.

Sirin, O., D. K. Paul, M. S. Khan, E. Kassem, and M. K. Darabi. Effect of Aging on Viscoelastic Properties of Asphalt Mixtures. Journal of Transportation Engineering, Part B: Pavements, Vol. 145, No. 4, 2019, p. 04019034. https://doi.org/10.1061/JPEODX.0000137.

Song, S., M. Liang, F. Hou, H. Gao, Y. Bi, H. Zhang, and M. Guo. Analysis of Natural Aging Behavior of Asphalt Binder in Cold and Arid Region. Advances in Materials Science and Engineering, Vol. 2022, 2022, pp. 1–9. https://doi.org/10.1155/2022/2425976.

Tashman, L. E., E. Masad, B. Peterson, and H. Saleh. Internal Structure Analysis of Asphalt Mixes to Improve the Simulation of Superpave Gyratory Compaction to Field Conditions. Vol. 70, 2001.

United States Department of Transportation. Federal Aviation Administration. "AC 150/5370-10 CHANGE 6: Standards for Specifying Construction of Airports" (1980), https://doi.org/10.21949/1513998.

Vaddy, P., T. Islam, M. E. Kutay, M. Vrtis, S. W. Haider, and B. Cetin. Evaluating the Short-Term Performance of Spray-on Rejuvenators Using a Modified Bending Beam Rheometer Test Methodology. Transportation Research Record: Journal of the Transportation Research Board, 2023, p. 03611981231209038. https://doi.org/10.1177/03611981231209038.

Vaddy, P., Z. Ahmed, and M. E. Kutay. Development of an Image-Based Methodology to Measure Heave Height in Hamburg Wheel Tracker–Tested Asphalt Specimens. Journal of Transportation Engineering, Part B: Pavements, Vol. 150, No. 2, 2024, p. 04024008. https://doi.org/10.1061/JPEODX.PVENG-1420.

Vallegra, B. A. Pavement Deficiencies Related to Asphalt Durability. No. No. 50, 1981.

Velasquez, R., A. Zofka, M. Turos, and M. O. Marasteanu. Bending Beam Rheometer Testing of Asphalt Mixtures. International Journal of Pavement Engineering, Vol. 12, No. 5, 2011, pp. 461–474. https://doi.org/10.1080/10298430903289956.

Xu, J., Z. Fan, J. Lin, P. Liu, D. Wang, and M. Oeser. Study on the Effects of Reversible Aging on the Low Temperature Performance of Asphalt Binders. Construction and Building Materials, Vol. 295, 2021, p. 123604. https://doi.org/10.1016/j.conbuildmat.2021.123604.

You, Z., S. Adhikari, and M. Emin Kutay. Dynamic Modulus Simulation of the Asphalt Concrete Using the X-Ray Computed Tomography Images. Materials and Structures, Vol. 42, No. 5, 2009, pp. 617–630. https://doi.org/10.1617/s11527-008-9408-4.

Zofka, A. M. Investigation of Asphalt Concrete Creep Behavior Using 3-Point Bending Test. The University of Minnesota, Minneapolis, MN, 2007.

Zofka, A., M. Marasteanu, and M. Turos. Investigation of Asphalt Mixture Creep Compliance at Low Temperatures. Road Materials and Pavement Design, Vol. 9, No. sup1, 2008, pp. 269–285. https://doi.org/10.1080/14680629.2008.9690169.

Zofka, A., M. Marasteanu, M. Turos, G. H. Paulino, M. J. Pindera, R. H. Dodds, F. A. Rochinha, E. Dave, and L. Chen. Investigation of Asphalt Mixture Creep Behavior Using Thin Beam Specimens. In Multiscale and Functionally Graded Materials 2006, No. 973, 2008, pp. 718–723.

Zofka, A., M. O. Marasteanu, and M. Turos. Determination of Asphalt Mixture Creep Compliance at Low Temperatures by Using Thin Beam Specimens. Transportation Research Record: Journal of the Transportation Research Board, Vol. 2057, No. 1, 2008, pp. 134–139. https://doi.org/10.3141/2057-16.

Appendix A
Literature review on low-temperature testing of asphalt binders and mixtures

This section aims to present the past literature on asphalt binders and mixtures testing at low temperatures. If one recalls, the difference in creep stiffness between control and rejuvenated test cells at 4°C and -10°C was not obvious compared to the creep stiffness results at 20°C. Therefore, it was important to review the literature to check whether the creep stiffness trends observed in the current research project follow or negate the past observations. Also, it provided the theoretical background behind the trend observed in the current study.

- In a study by Xu et al. (2021), the low-temperature performance of four types of aged asphalt binders was investigated, including two unmodified and two modified with SBR and SBS Xu et al., 2021). As temperature decreased, the asphalt binders stiffened due to a phenomenon known as "low-temperature stiffening." This was due to the increased viscosity of the binder at lower temperatures, which reduced its flexibility.

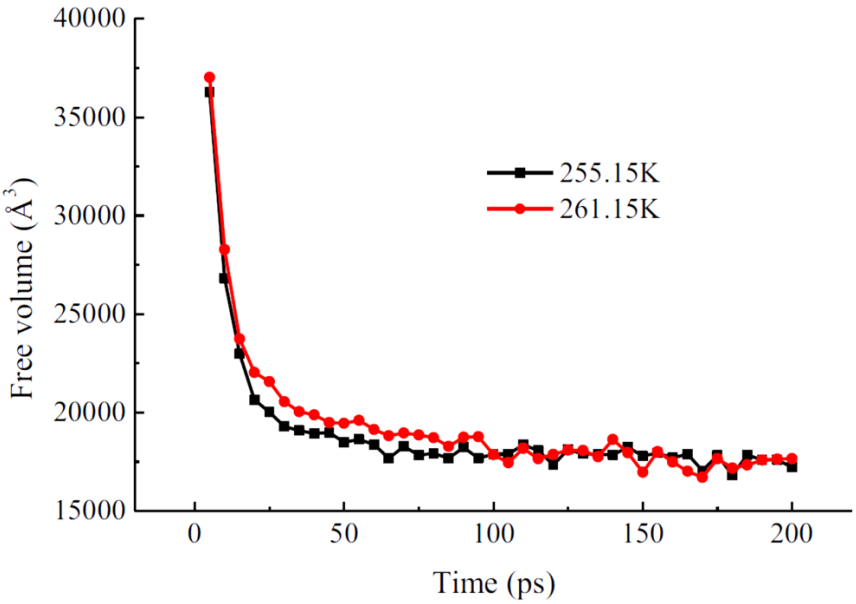

Figure A-1. Free volume of asphalt molecular model at different temperatures (Xu et al., 2021)

At lower temperatures, the asphalt binder's microstructure became more rigid and ordered, further contributing to the reduced rate of change in creep stiffness. This phenomenon was explained by measuring the free volume over time. As shown in Figure A. 1, the molecular model of asphalt experienced a substantial reduction in its free volume, which eventually reached a state of stabilization as the simulation time escalated. This resulted in the aggregation of asphaltene molecules and an increase in density, which reduced the binder's flexibility and durability, and increased brittleness. Following a prolonged duration, the free volume eventually fluctuated around the same minimum value, with the chain segment of the asphalt molecule becoming frozen when the free volume reached its minimum value. Another crucial observation made by the authors was the acceleration of the rate of stabilization at lower temperatures, which can be observed in Figure A. 1.

- Song et al. (2022) conducted a study on the natural aging of asphalt binder, using FTIR (Fourier Transform Infrared Spectroscopy) analysis, which yielded similar findings (Song et al., 2022). In this study, laboratory-aged binders were prepared by the rolling thin film oven (RTFOT), and pressure aging vessel (PAV) methods. Natural aging tests on the asphalt binders were conducted by all-weather (All) aging, thermal oxygen (TO) aging, thermal oxygen, and ultraviolet (TO + UV) aging.

  The outcomes of the research indicated that the asphalt binder's molecular weight increased due to natural aging at lower temperatures, complicating the internal ring structure of the binder. As a result, the movement of internal molecules was impeded by substantial frictional resistance. The aging process exhibited a positive correlation with the degree of aging factors. Conversely, lower temperatures were found to have a mitigating effect on the aging process of the binder, also due to the presence of wind, dust, and rain by reducing the contact area between the asphalt binder and the external environment. Figure A. 2 illustrates that as temperature decreases, the creep stiffness increases, and the rate of change of stiffness modulus and creep rate reduces.

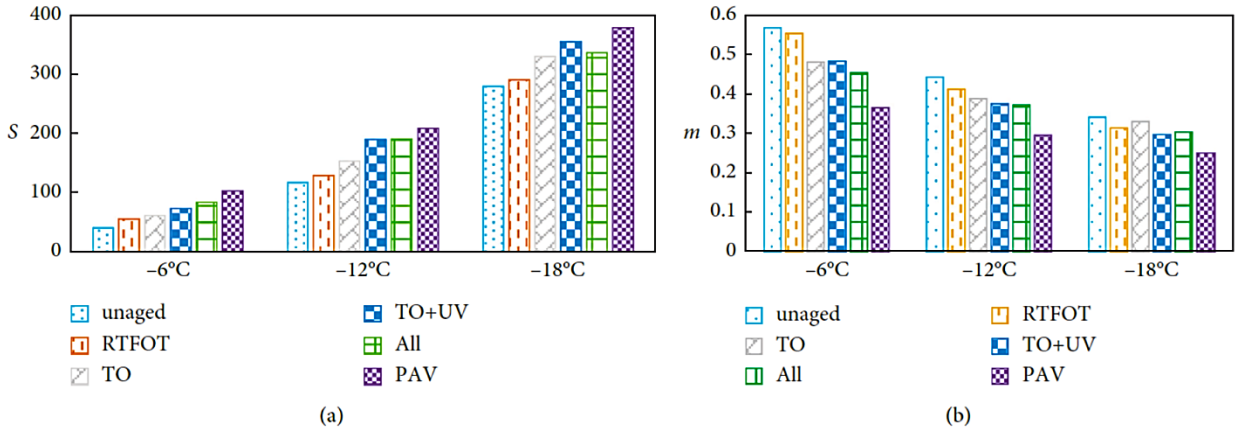

Figure A-2. (a) Creep stiffness and (b) m-values of aged and unaged binders at different temperatures (Song et al., 2022)

- In another study by Sirin et al. (2019), the authors investigated the effect of aging on asphalt mixtures (Sirin et al., 2019). This study assessed the impact of different short-term aging temperatures (125°C, 135°C, and 145°C) through four varying durations (2, 4, 6, and 8 hours). Following a brief period of aging, the mixture was compacted at 135°C by a gyratory compactor. The specimens went through long-term aging at different temperatures (75°C, 85°C, and 95°C) and durations (0, 2, 4, 6, 8, and 10 days) to replicate the field aging. Based on the results, the increase in both short-term and long-term aging conditioning temperature results in an upward shifting of the master curve, increasing the dynamic modulus. Furthermore, with an increase in the duration of aging, there was a proportional rise in the dynamic modulus, which indicates the stiffening of the binders. Figure A. 3 shows that the rate of change of dynamic modulus increases as the temperature increases.

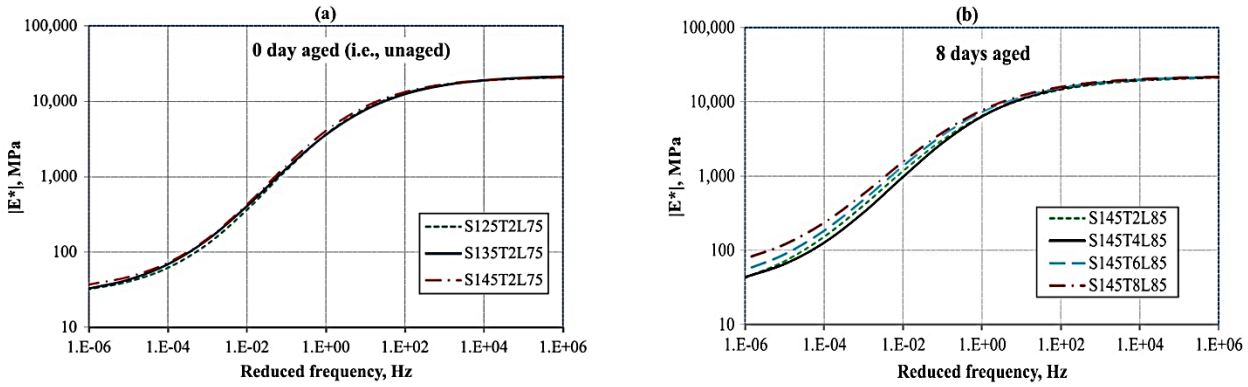

Figure A-3. Effect of short-term aging temperature on |E*| for (a) unaged sample; (b) 8 days aged sample (Sirin et al., 2019)

- Bahia (1991) conducted laboratory aging on binders for evaluating the creep behavior in the low-temperature region by TFOT and TFOT+ PAV procedures (Bahia, 1991). The influence of physical hardening on the response of oxidatively aged asphalt was measured in the identical way as for the unaged asphalt. The tests were done at temperatures of -25°C, -15°C, and -5°C. Figure A. 4 demonstrates the difference between the oxidative aging at -5°C and -25°C in terms of the creep reaction at an isothermal age of 2 hours. The creep stiffness values at -25°C are higher than those of -5°C. Also, the creep stiffness increment rate at -5°C in aged conditions is significantly larger than that of -25°.

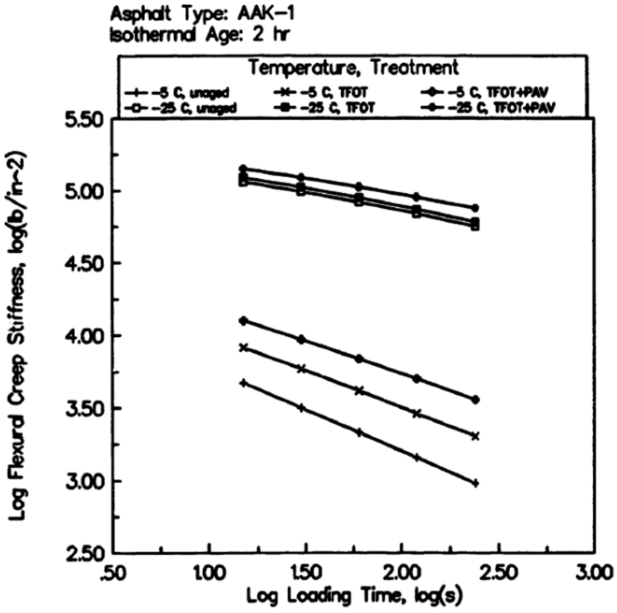

Figure A-4. Effect of oxidative aging on creep stiffness at different temperatures (Bahia, 1991)

The aged asphalt was observed to be stiffer than unaged asphalt, resulting in the creep deflection being negligible and the response was essentially elastic at -35°C. For this reason, in this study, it was suggested that, at -5°C all asphalt could be tested, therefore the temperature of -10°C or lower

temperature was no longer needed. To illustrate the extent to which the rheological or chemical properties of asphalt binder have changed with aging, the aging index of asphalt was measured in this research which is shown in Figure A. 5. It showed that the changing degree of aging was greater at -5°C compared to -15°C and -25°C. The slope of the aging index curves was almost horizontal maintaining a constant value over time at lower temperatures.

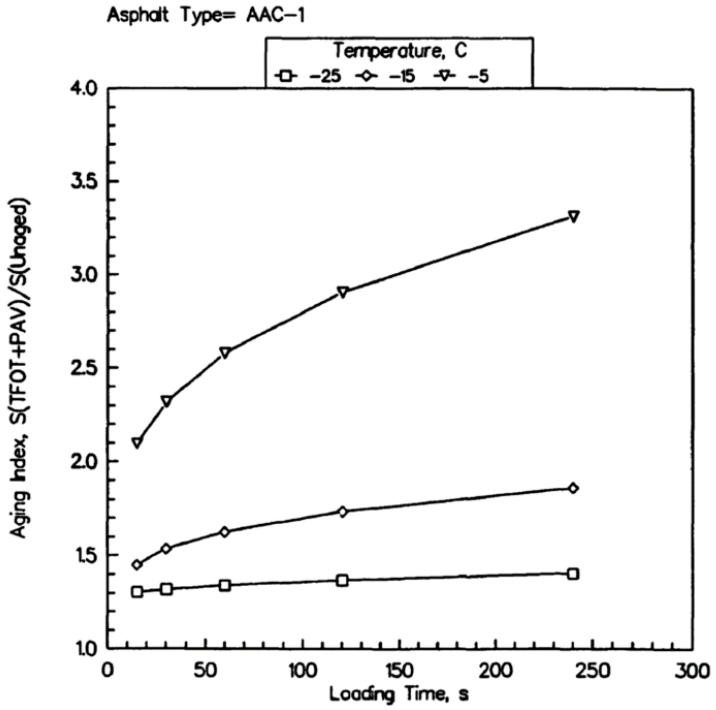

Figure A-5. Variation of aging index with temperature and loading time (Bahia, 1991)

In conclusion, after reviewing the key literature, it was understood that the change in creep stiffness at low temperatures could be very minimum, that differentiating aged and unaged binders could be challenging by testing them at low temperatures. Recall that the behavior of an asphalt mixture is governed by the combined effect of asphalt binder and aggregates, in which aggregates are mostly elastic. Because of the minimal effect of the viscoelastic nature of asphalt binder, it can be inferred that evaluation of the aged and unaged asphalt mixtures could prove more challenging at low temperatures.

Appendix B

Creep stiffness results at low temperature

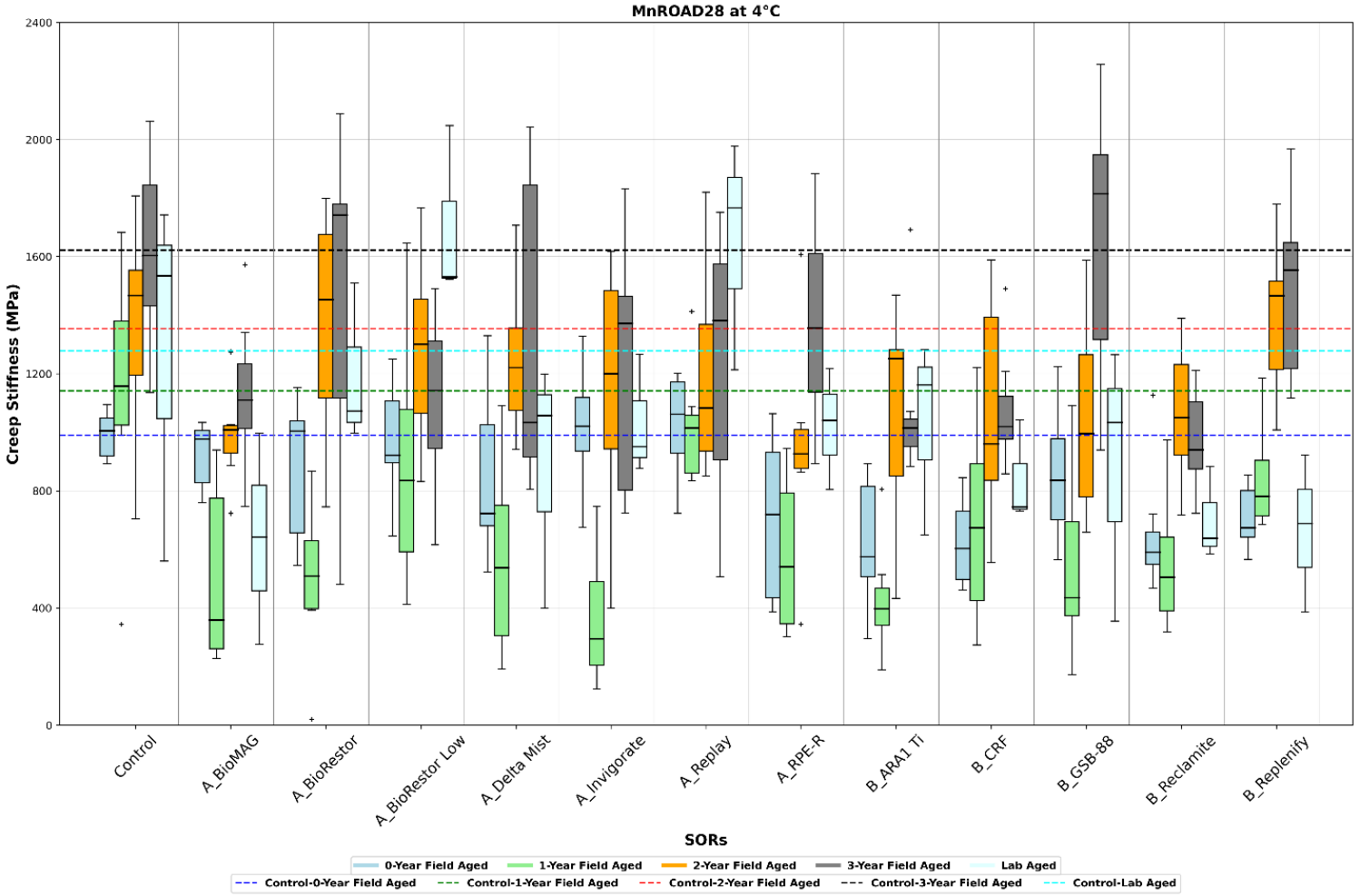

Figure B-1. BBR test results for asphalt mixture beams for MnROAD28 test section at 4°C

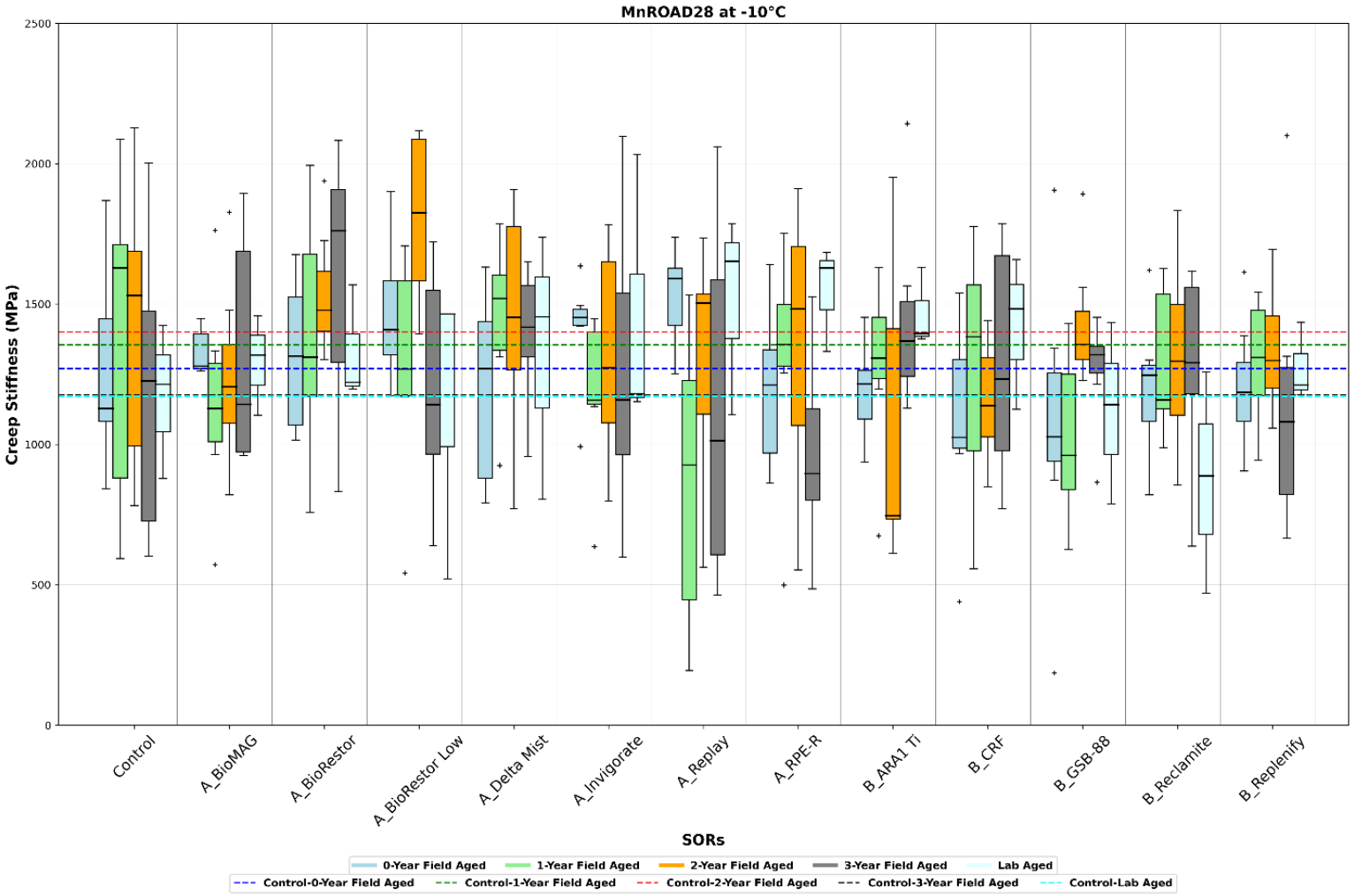

Figure B-2. BBR test results for asphalt mixture beams for MnROAD28 test section at -10°C

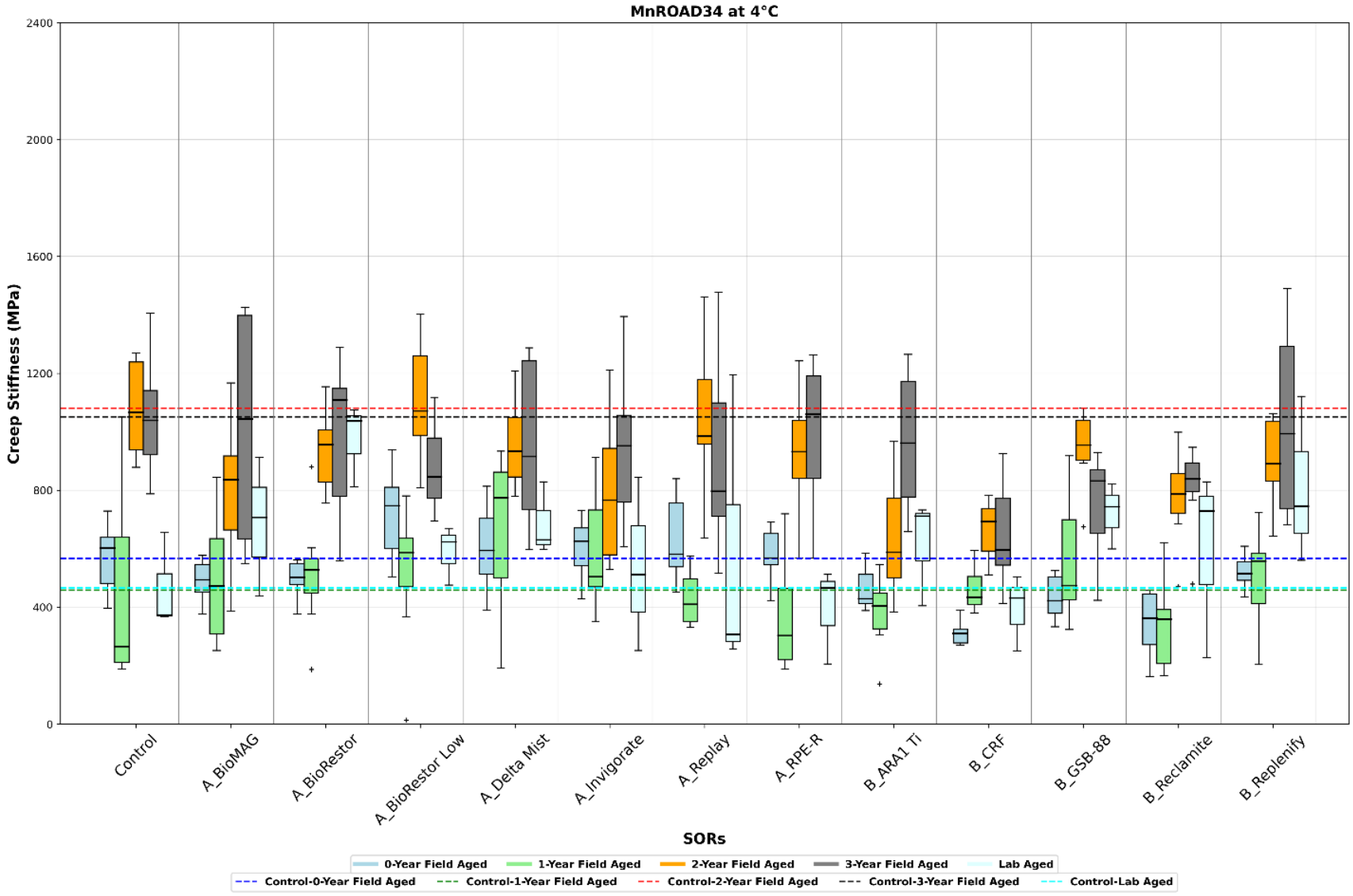

Figure B-3. BBR test results for asphalt mixture beams for MnROAD34 test section at 4°C

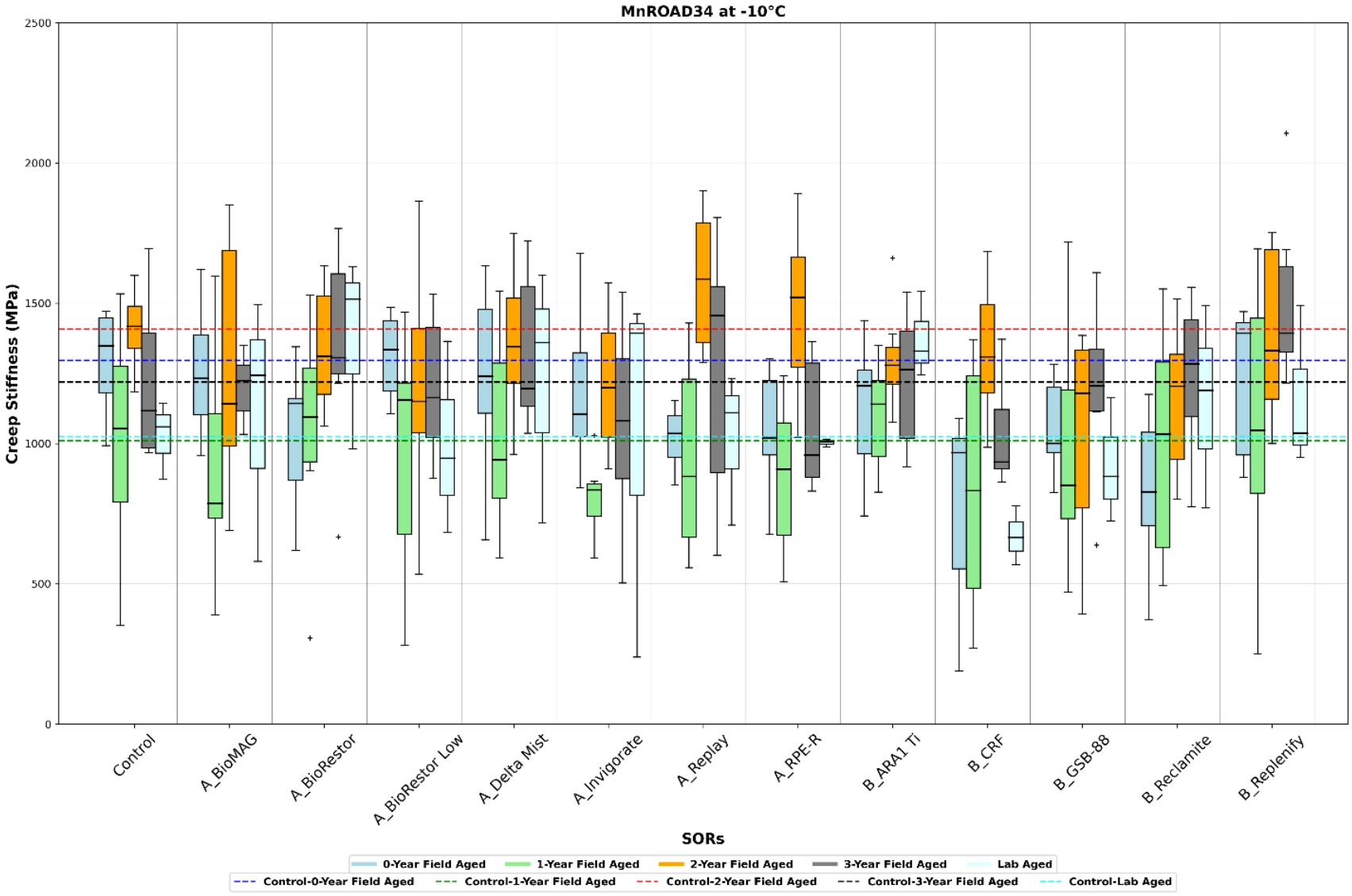

Figure B-4. BBR test results for asphalt mixture beams for MnROAD34 test section at -10°C

Appendix C
Skid resistance results

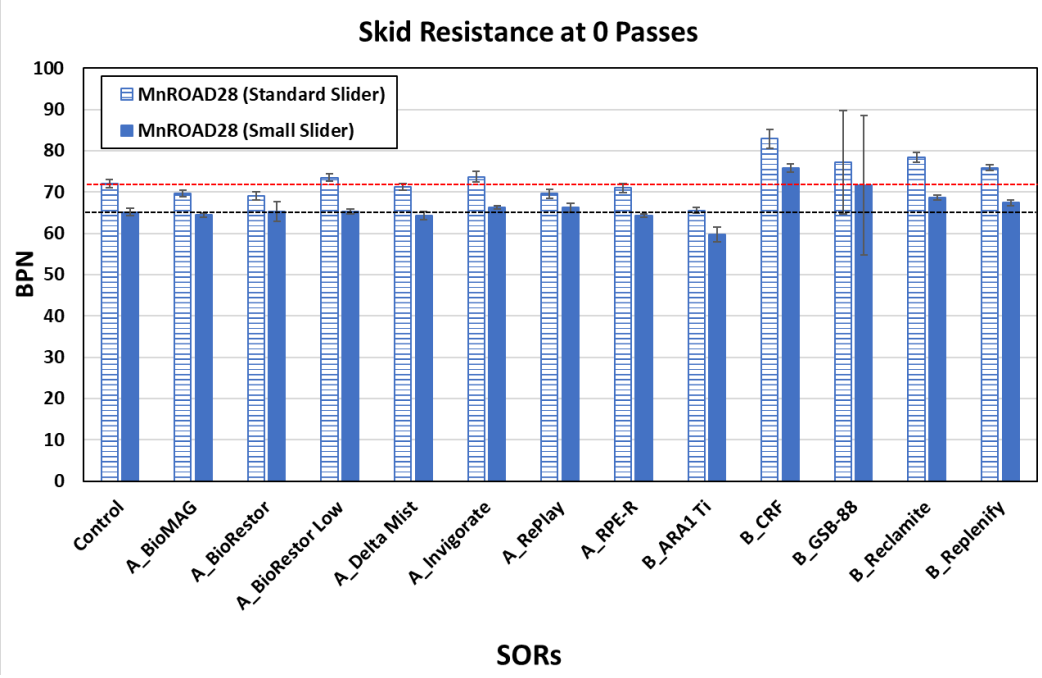

Figure C-1. Comparison of BPT test results using standard slider and modified slider before wheel passes

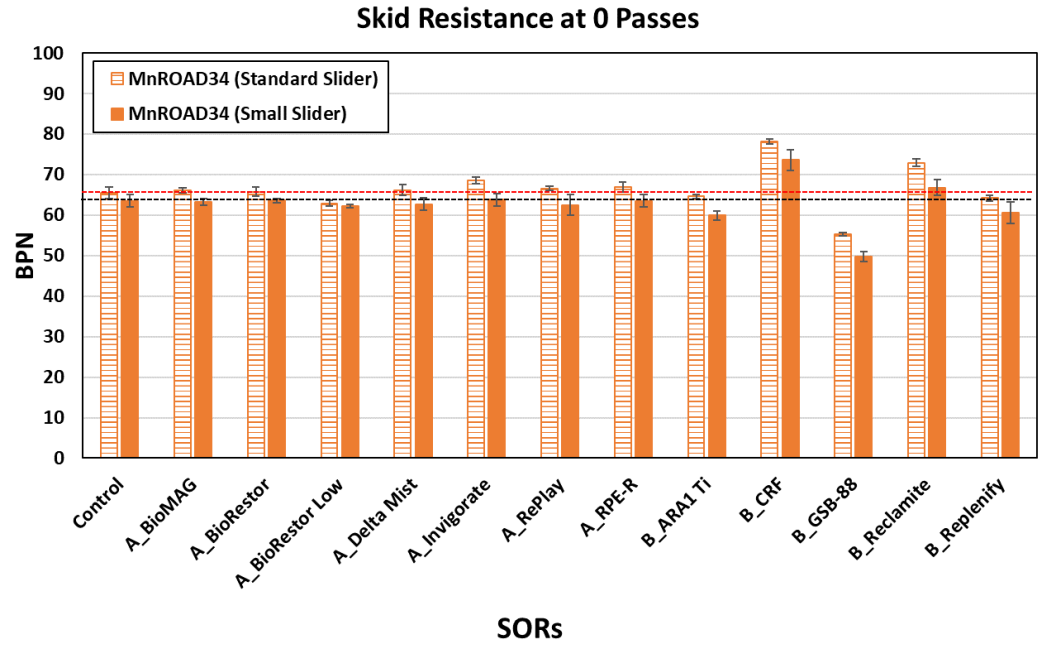

Figure C-2. Comparison of BPT test results using standard slider and modified slider before wheel passes

Appendix D
Dynamic friction test results of rejuvenated test sections at test speeds of 20 and 60 kph

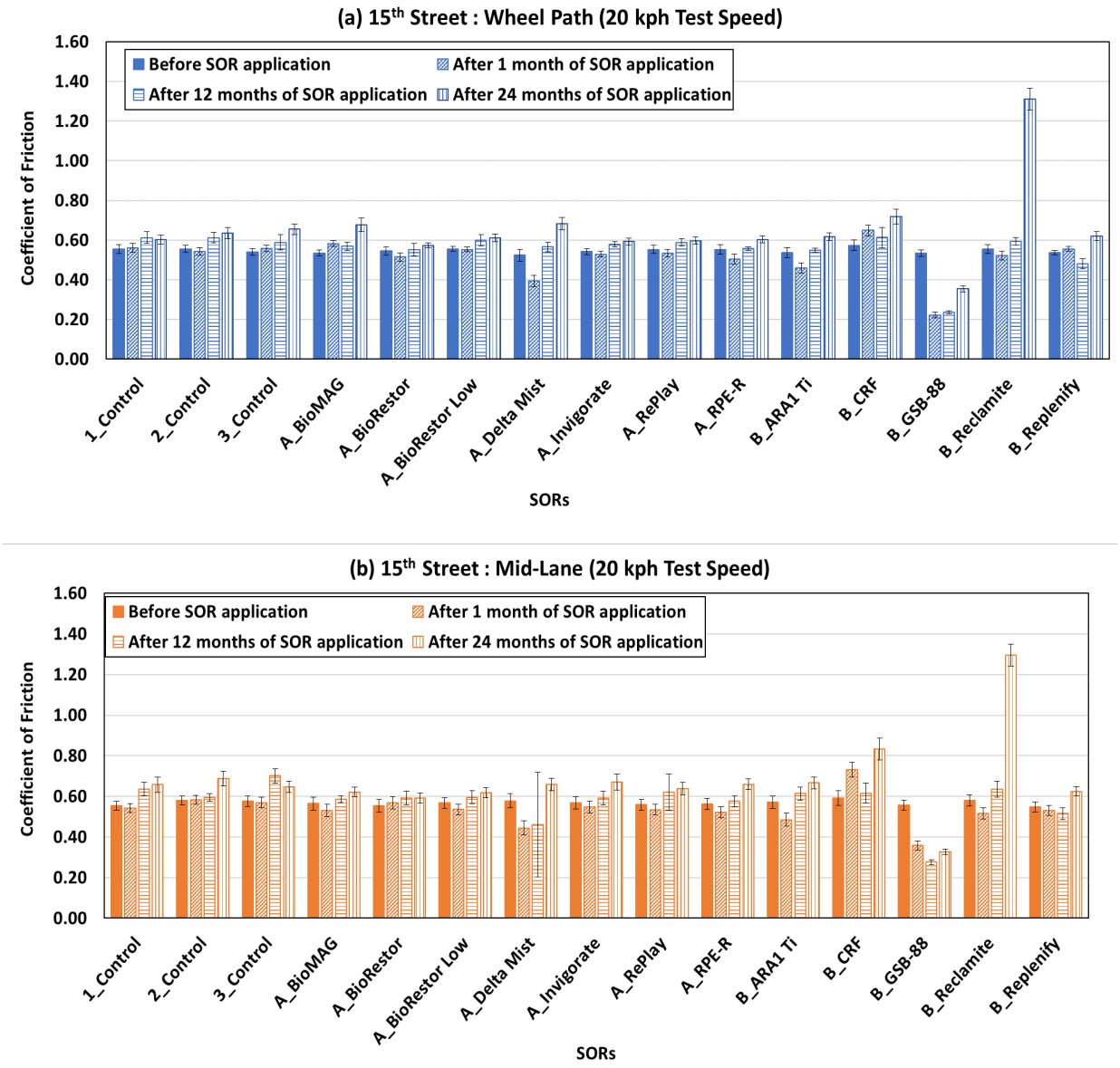

Figure D-1. Pre and post-SOR applied DFT results of the 15th Street test section at a test speed of 20 kph

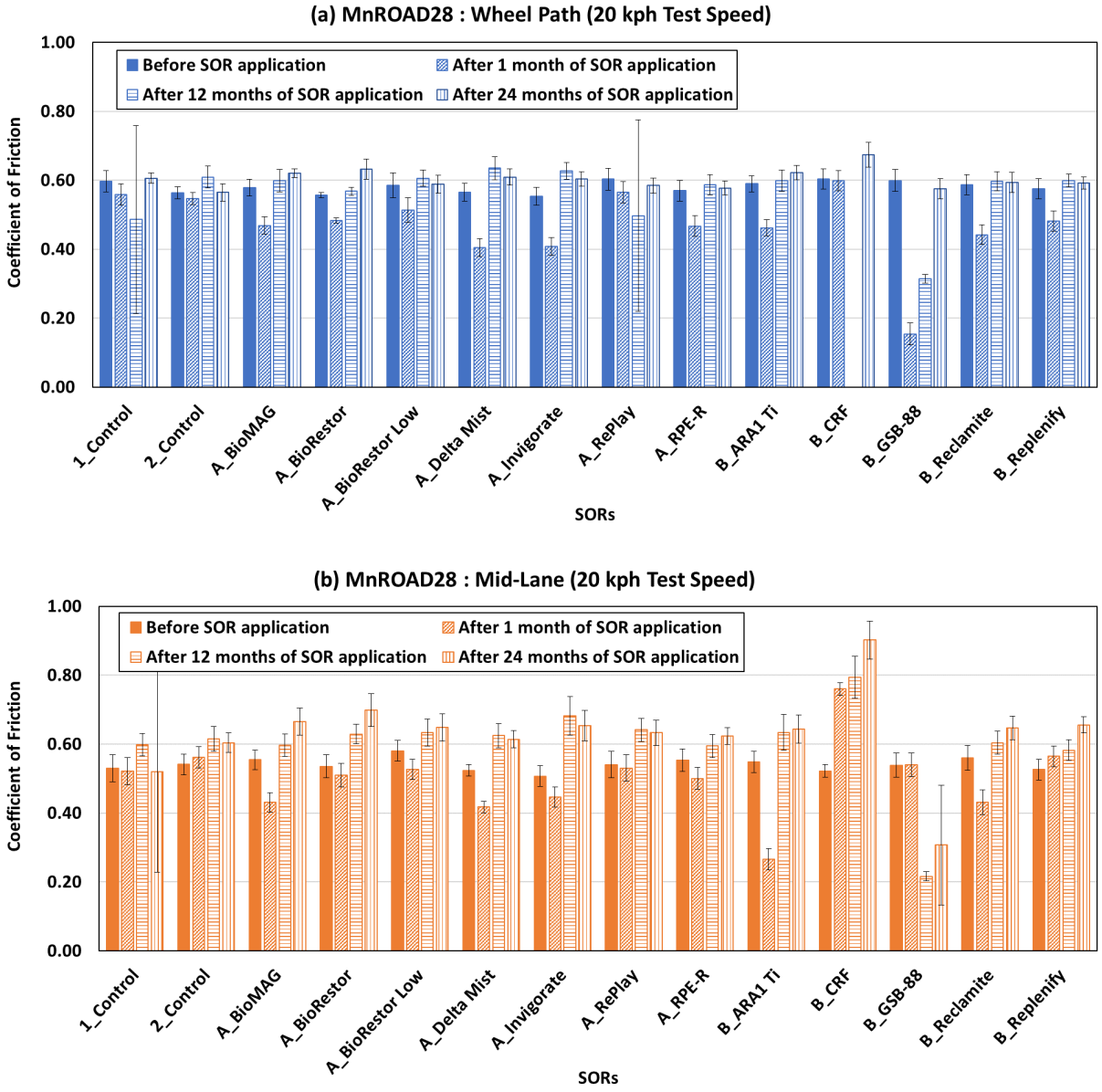

Figure D-2. Pre and post-SOR applied DFT results of MnROAD28 test section at a test speed of 20 kph

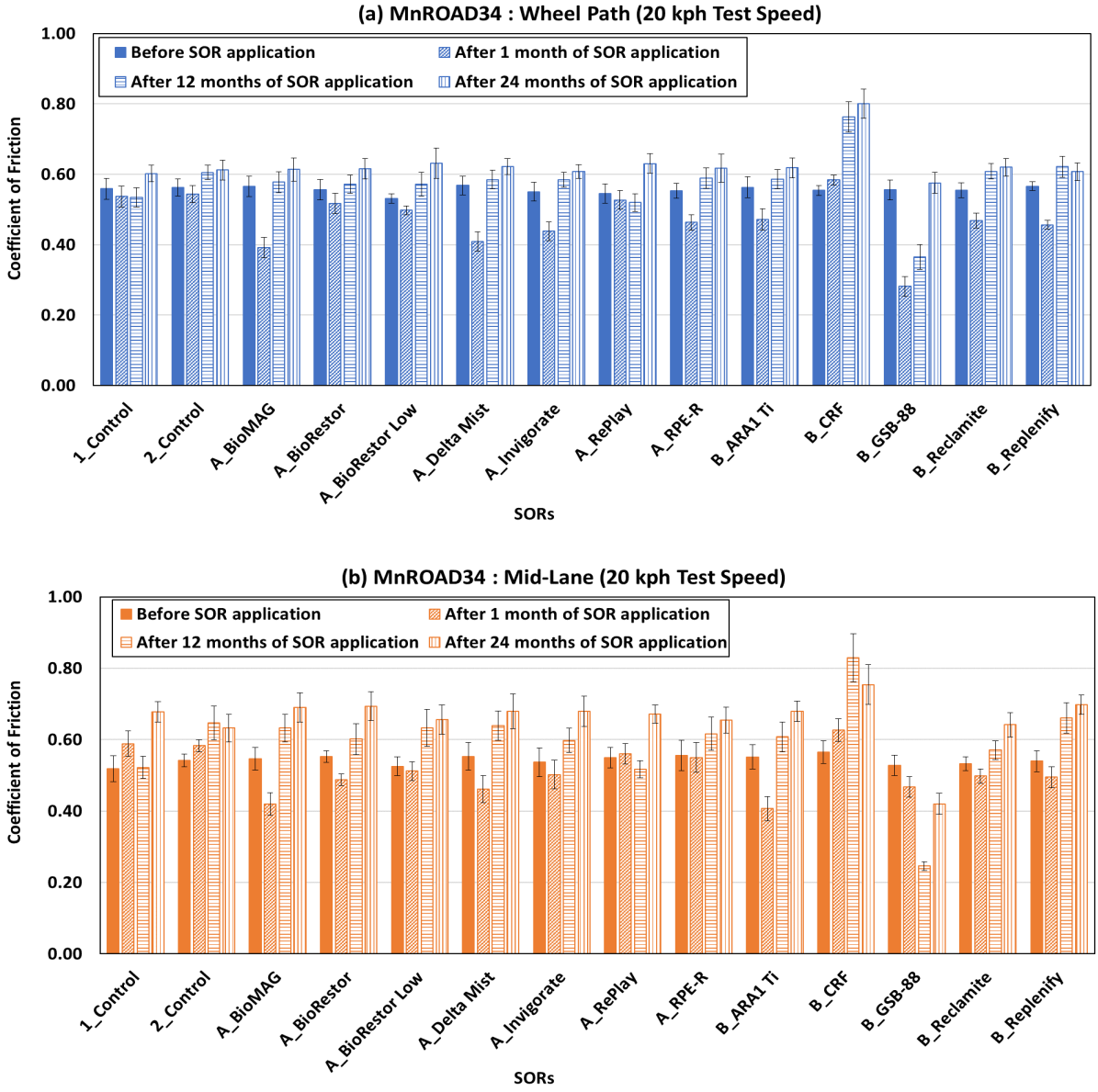

Figure D-3. Pre and post-SOR applied DFT results of MnROAD34 test section at a test speed of 20 kph

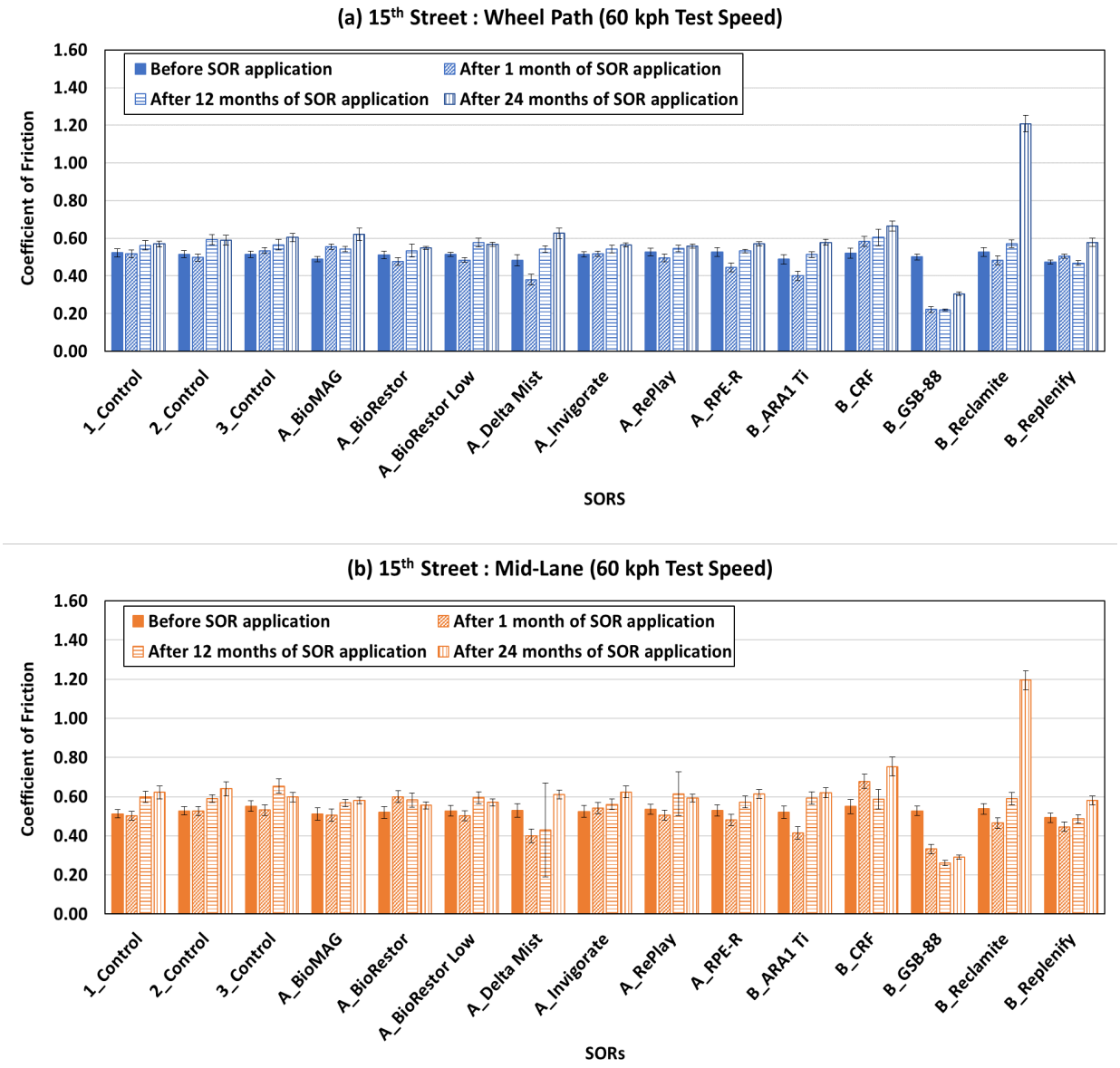

Figure D-4. Pre and post-SOR applied DFT results of the 15th Street test section at a test speed of 60 kph

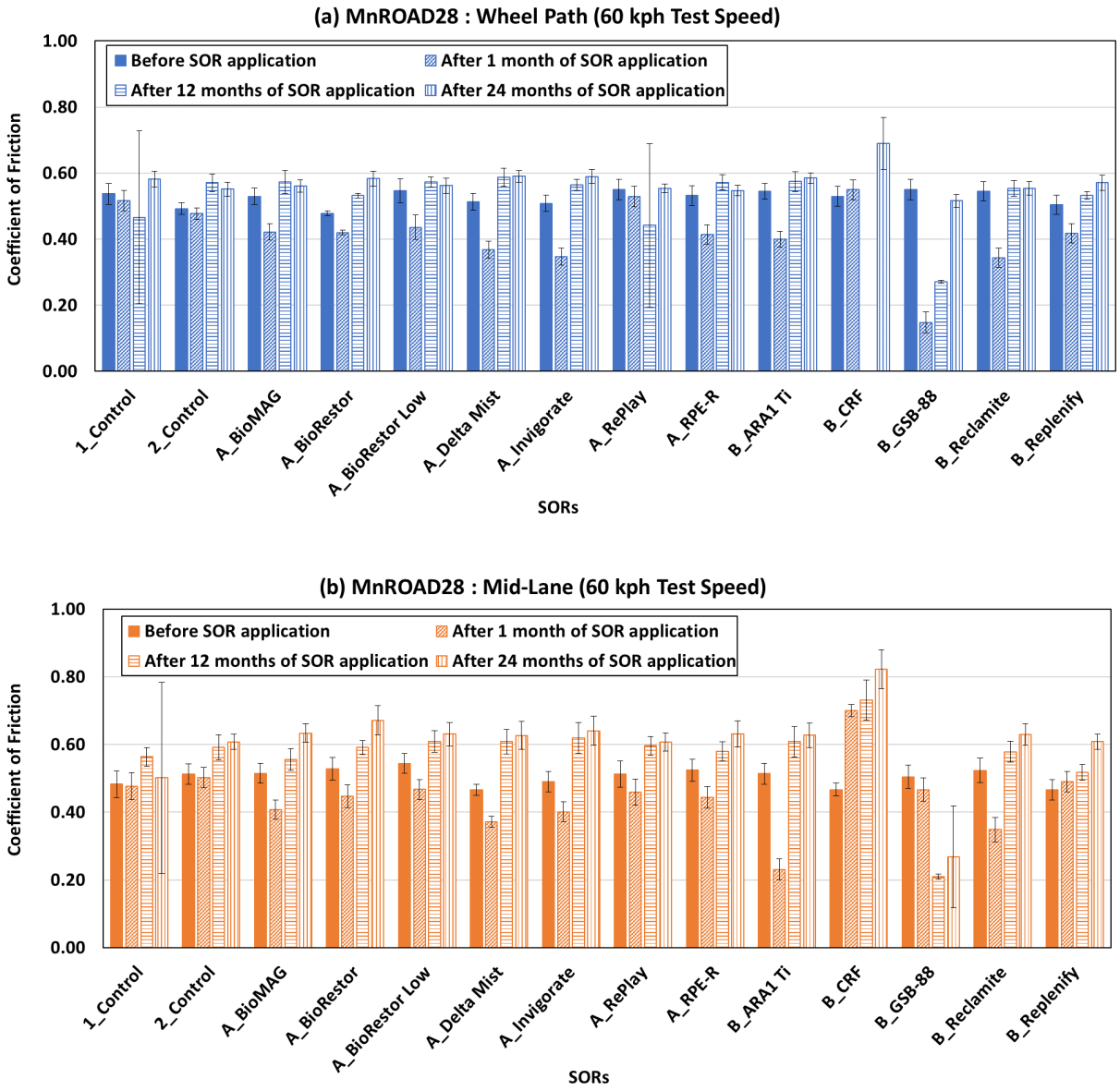

Figure D-5. Pre and post-SOR applied DFT results of MnROAD28 test section at a test speed of 60 kph

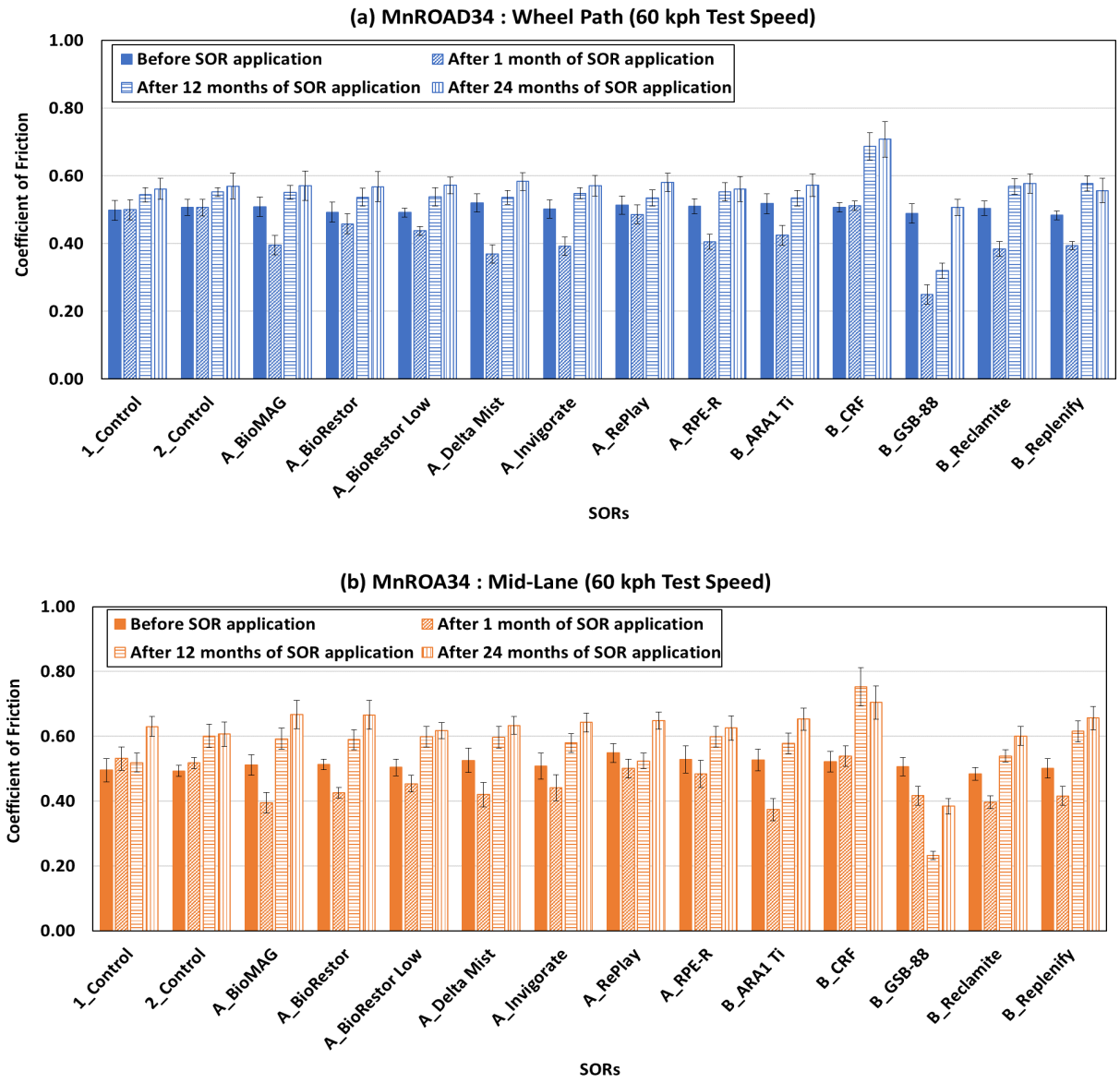

Figure D-6. Pre- and post-SOR applied DFT results of MnROAD34 test section at a test speed of 60 kph